Dissertation

Cardioprotective mechanisms of spermidine in aging and related cardiovascular disease

Submitted by

Mahmoud ABDELLATIF

for the Academic Degree of

Doctor of Philosophy

(PhD)

At the

Medical University of Graz

Clinical Division of Cardiology

Under the supervision of

Assoc. Prof. Dr. Simon SEDEJ

2019

Declaration

I hereby declare that this thesis is my own original work and that I have fully acknowledged by name all of those individuals and organizations that have contributed to the research for this thesis. Due acknowledgement has been made in the text to all other material used. Throughout this thesis and in all related publications I followed the "Standards of Good Scientific Practice and Ombuds Committee at the Medical University of Graz".

Graz, 28th of June, 2019.

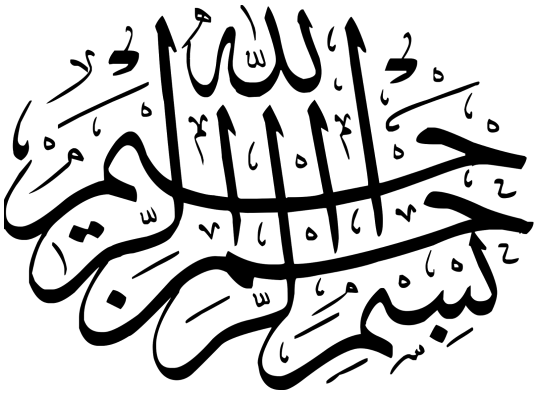

For my dad,

I wish I managed to finish this slightly earlier, then you could have read it.

Acknowledgements

First and foremost, I would like to express my gratitude for the support I received throughout this work from my supervisor Prof. Simon Sedej. It is imperative to mention, before going into details, that acknowledging him is located here at the very beginning not just as a formality typically done by doctoral candidates, but rather because it does stem from my immense feeling of gratitude towards him as the main catalyst for this work. I would like to thank Simon not only for his amazing mentorship, guidance, encouragement and all other valuable roles of a supervisor nurturing a student, but also for having his door open ALL the time, being around and helping in the lab whenever needed. This does not only apply to technically demanding issues, but also if we needed an extra pair of hands. In fact, despite how lucky I feel being supervised by someone of such qualities and calibre, I'd like to thank Simon for something that goes beyond our professional relationship as a doctoral candidate and his supervisor, that is for being my dear friend and older brother in a new country where I had no family, ex-colleagues or anyone I happened to know before joining his lab. Thank you, Simon, for all the times you tapped on my shoulder whenever my experiments did not work and convinced me that I should try again till I succeed, thank you for all the coffees we had (and are yet to have) together, thank you for helping me moving into my apartment, carrying all that stuff and driving the van, let alone all those football matches, barbeques and gins we enjoyed over the past years.

I would also like to deliver my deepest gratitude to my colleague Ms. Viktoria Herbst, MSc. Thank you for all the work you have been (and are) doing in our lab, without you none of the results included in this thesis could have been available in time. Thank you for going through it all with me and Simon till we made it that far with this project and the currently ongoing ones.

In addition, I would like to thank A/Prof. Tobias Eisenberg, my thesis committee members (Prof. Frank Madeo A/Prof. Peter Rainer and A/Prof. Gunther Marsche), and everyone who was actively involved in this work.

I would also like to acknowledge our head of department Prof. Zirlik for his support and belief in basic science and our experimental cardiology group. Thank you for promoting us nationally and internationally, and providing all the necessary facilities for our work.

I would like to thank my friends and colleagues from the PhD program MolMed (Vero, Ila, Franshičič, Ani, Piaš and Natasa) for sharing this path with me, and always providing an outlet for the endless frustrations and (sometimes ☺) celebrations of our successes, for all those homey Christmas parties, joyful trips and ridiculous costume parties, where I get to play my favourite Latin music! I love you all and deeply wish you the best in your lives and careers.

I would like to thank my family; my dad, mom, sisters and brothers, I hope this makes you a bit proud. I am and will always be deeply indebted to you for all the love, support and encouragement I received throughout my life till I got to where I am.

Last but not least, I would like to thank my fiancée and wife-to-be Leen for being there for me all the time and every time. Thank you for helping me believe that I can do this again and again. Thank you for giving me company when I had to work late nights and over the weekends, for our daily dinners, and for reading this thesis line by line picking on what I, and even my supervisor, missed correcting. Thank you for your love, for giving me life outside the lab, for making Graz another home to me and for being now, tomorrow and forever with me. I love you so much!

I (PhD candidate Mahmoud Abdellatif) gratefully acknowledge funding received from the FWF (grant P27637-B28) and training within the frame of the Ph.D. Program Molecular Medicine of the Medical University of Graz.

Disclosures

Parts of this thesis have been published in:

Eisenberg T*, **Abdellatif M***, Schroeder S, Primessnig U, Stekovic S, Pendl T, Harger A, Schipke J, Zimmermann A, Schmidt A, Tong M, Ruckenstuhl C, Dammbrueck C, Gross AS, Herbst V, Magnes C, Trausinger G, Narath S, Meinitzer A, Hu Z, Kirsch A, Eller K, Carmona-Gutierrez D, Büttner S, Pietrocola F, Knittelfelder O, Schrepfer E, Rockenfeller P, Simonini C, Rahn A, Horsch M, Moreth K, Beckers J, Fuchs H, Gailus-Durner V, Neff F, Janik D, Rathkolb B, Rozman J, de Angelis MH, Moustafa T, Haemmerle G, Mayr M, Willeit P, von Frieling-Salewsky M, Pieske B, Scorrano L, Pieber T, Pechlaner R, Willeit J, Sigrist SJ, Linke WA, Mühlfeld C, Sadoshima J, Dengjel J, Kiechl S, Kroemer G, Sedej S, Madeo F. **Cardioprotection and lifespan extension by the natural polyamine spermidine.** *Nat Med*. 2016 Dec;22(12):1428-1438. doi: 10.1038/nm.4222.

Abdellatif M*, Sedej S*, Carmona-Gutierrez D, Madeo F, Kroemer G. **Autophagy in Cardiovascular Aging.** *Circ Res*. 2018 Sep 14;123(7):803-824. doi: 10.1161/CIRCRESAHA.118.312208.

Eisenberg T*; **Abdellatif M***, Zimmermann A, Schroeder S; Pendl T, Harger A, Stekovic S, Schipke J, Magnes C, Schmidt A, Ruckenstuhl C, Dammbrueck C, Gross AS, Herbst V, Carmona-Gutierrez D, Pietrocola F, Pieber TR, Sigrist, SJ, Linke WA, Mühlfeld C, Sadoshima J, Dengjel J, Kiechl S, Kroemer G, Sedej S, Madeo F. **Dietary spermidine for lowering high blood pressure.** *Autophagy*. 2017; 13(4):767-769.

* *denotes equal contribution*

These publications are Open Access and the data were reproduced with permission from the respective publisher (Springer Nature, Wolters Kluwer, or Taylor & Francis, respectively) as indicated where the data appear in the thesis.

All co-authors who contributed to the research in this thesis agreed to the use of their data. These co-authors have actively contributed to the reported results and include the following colleagues:

Dr. Tobias Eisenberg
(Institute of Molecular Biosciences, University of Graz, Graz, Austria)

Dr. Stefan Kiechl
(Department of Neurology, Medical University of Innsbruck, Austria).

Dr. Tobias Pendl
(Institute of Molecular Biosciences, University of Graz, Graz, Austria)

Dr. Mingming Tong
(Rutgers New Jersey Medical School, Rutgers University, New Jersey, USA)

Dr. Alexander Kirsch
(Clinical Division of Nephrology, Medical University of Graz, Graz, Austria)

Dr. Julia Schipke
(Institute of Functional and Applied Anatomy, Hannover Medical School, Hannover, Germany)

Dr. Uwe Primessnig
(Clinical Division of Cardiology, Medical University of Graz, Graz, Austria)

Ms. Marion von Frieling-Salewsky
(Institute of Physiology II, University of Münster, Münster, Germany)

Table of Contents

Abbreviations

ADF	alternate-day fasting
AMPK	adenosine monophosphate-activated kinase
ANCOVA	analysis of co-variance
ANOVA	analysis of variance
ATG	autophagy-related
***Atg*$^{+/+}$**	Autophagy-competent mice (*Atg5*$^{fl/fl}$*MLC2a-Cre*$^{-}$)
***Atg5*$^{-/-}$**	Cardiomyocyte-specific autophagy-deficient mice (*Atg5*$^{fl/fl}$*MLC2a-Cre*$^{+}$)
BMI	body mass index
CVD	cardiovascular disease
***Dahl* SS**	*Dahl* salt-sensitive
EDP	end-diastolic pressure
EDPVR	end-diastolic pressure-volume relationship
EDPVR β	end-diastolic pressure-volume relationship constant
Ees	end-systolic elastance
EF	ejection fraction
eNOS	endothelial NO-synthase
ESPVR	end-systolic pressure-volume relationship
FMD	fasting mimicking diet
GABR	global arginine bioavailability ratio
GFP	green fluorescent protein
HFpEF	heart failure with preserved ejection fraction
HFrEF	heart failure with reduced ejection fraction
HS	high salt
HW	heart weight
IGF-1	insulin/insulin-like growth factor-1
IP	intraperitoneal
IQR	inter-quartile range
LS	low salt
LV	Left ventricle
LVmass	left ventricular mass

mTOR	mechanistic target of rapamycin
NAD^+	Nicotinamide adenine dinucleotide
NMN	nicotinamide mononucleotide
NO	nitric oxide
NT-proBNP	N-terminal pro-B type natriuretic peptide
$ONOO^-$	peroxynitrite
PI3K	phosphoinositide 3-kinase
PV	pressure volume
ROS	reactive oxygen species
SD	standard deviation
SEM	standard error of mean
SIRT	sirtuins
tf-LC3	tandem-fluorescence mRFP-GFP-LC3
TL	tibia length
TRF	time-restricted feeding
ULK-1	Unc-51 like autophagy activating kinase-1
VO_2max	maximal oxygen consumption
VVC	ventricular-vascular coupling

List of Figures

List of Tables

Zusammenfassung

Auf Grund der weltweiten kontinuierlich steigenden Lebenserwartung, erhöht sich unter anderem die Prävalenz von chronischen Erkrankungen, welche vor allem das Herz-Kreislaufsystem betreffen. Die Alterung der Bevölkerung bedeutet daher eine massive medizinische und wirtschaftliche Belastung für die Gesellschaft. Bisher konnten durch die Restriktion der Nahrungsaufnahme vielversprechende anti-aging Effekte nachgewiesen werden, jedoch stellt sich die langfristige und umfassende Umstellung der Ernährung auf Grund der zu geringen Patientencompliance als nicht praktikabel dar. Infolgedessen ergibt sich die Notwendigkeit nach pharmazeutischen Alternativen zu suchen, welche in der Lage sind die Effekte einer Kalorienrestriktion zu mimikrieren.

In dieser Studie konnte nachgewiesen werden, dass durch die Nachahmung dieser Ernährungsumstellung mittels des Polyamins Spermidin eine Vielzahl positiver Effekte ausgelöst wird. Alternde Mäuse, welche in ihrem späteren Leben mit 3 mM Spermidin im Trinkwasser behandelt wurden, wiesen Verbesserungen in den meisten Bereichen von altersabhängiger kardialer Dysfunktion, unter anderem bei der Hypertrophie, diastolischer Dysfunktion und der Koppelung zwischen Ventrikel und Arterien auf. Zusätzlich konnten in einem Hypertension-Rattenmodell mit begleitender Kardiomyopathie, kardioprotektive sowie antihypertensive Effekte, aufgrund der Nahrungszugabe von Spermidin, nachgewiesen werden.

Mechanistisch scheint Spermidin über zwei nicht exklusive Wege zu wirken: (i) Es steigert Autophagie und Mitophagie im Herz und den Nieren, was sich durch eine bessere Kardiomyozyten-Struktur und Funktion und möglicherweise bessere Blutdruckkontrolle bemerkbar macht; (ii) exogen zugeführtes Spermidin reduziert den Verbrauch der Vorläufer-Aminosäure Arginin im Rahmen der Polyamin-Biosynthese und scheint stattdessen die Regeneration der NO Bioverfügbarkeit zu unterstützen. Zusätzlich verfügt Spermidin über einen anti-inflammatorischen Effekt, welcher durch einen reduzierten Verbrauch die NO Bioverfügbarkeit erhöht, was essenziell für die kardiovaskuläre Gesundheit ist.

Im alternden humanen Myokard konnte nachgewiesen werden, dass die Spermidin-Konzentration mit der Zeit konstant abfällt. In Patienten mit Herzinsuffizienz konnte eine kompensatorische Steigerung der herzspezifischen Spermidin Konzentrationen nachgewiesen werden. Jene Patienten, welche eine gesteigerte

Spermidin Zufuhr aufwiesen, hatten auch einen niedrigeren Blutdruck und eine geringere Mortalität und Morbidität betreffend kardiovaskuläre Endpunkte.
Zusammenfassend liefert diese Arbeit ausreichende Beweise für klinische Tests von Spermidin beim Menschen, um die Alterung des Herzens und möglicherweise damit verbundene Komplikationen zu verzögern.

Abstract

Due to an ever-increasing population aging worldwide, the prevalence of cardiovascular diseases is progressively growing and, thus, imposing a massive medical and economic burden on society. In this regard, caloric restriction has shown promising cardiovascular and health-promoting effects. However, caloric restriction cannot be broadly implemented as it does not appeal the majority of people, not to mention its uncertain safety profile in the elderly. Therefore, more feasible alternatives, especially pharmaceutical or natural dietary compounds that mimic caloric restriction, are currently needed.

To this end, we found that supplementing the natural polyamine and caloric restriction mimetic spermidine induces a myriad of cardiovascular health-promoting effects. Specifically, aged mice treated later in their life with 3 mM spermidine showed improvements in most aspects of age-related cardiac decline, including hypertrophy, diastolic function, and ventricular-vascular coupling. Consistently, spermidine feeding to an animal model of hypertension and related cardiomyopathy revealed similar cardioprotective, in addition to, anti-hypertensive effects. Mechanistically, spermidine seemed to act *via* two, not necessarily exclusive, routes; Firstly, spermidine boosted autophagy and mitophagy in the heart and kidneys, which improved cardiomyocyte structure and function and possibly also contributed to better blood pressure control. Secondly, exogenous spermidine administration spared its precursor arginine from being utilized for polyamines biosynthesis and, instead, might have redirected arginine metabolism towards replenishing the nitric oxide (NO) bioavailability, which is indispensable for cardiovascular health. Spermidine also had an anti-inflammatory effect, which might limit NO breakdown and, thus, further improve NO bioavailability. In humans, we found spermidine concentrations in the heart to constantly decline with age. More importantly, we detected a compensatory increase in cardiac spermidine levels in heart failure patients, whereas individuals reporting higher dietary intake of spermidine had reduced blood pressure and lower incidence of cardiovascular disease, and related mortality.

Taken together, the results presented in this thesis provide sufficient evidence for clinical testing of spermidine in humans to delay cardiac aging and, possibly, related late-life disorders.

1. INTRODUCTION

1.1. Is aging entirely inevitable?!

According to Stedman's Medical Dictionary, aging is defined as:

"the gradual deterioration of a mature organism resulting from time-dependent irreversible changes in structure that are intrinsic to the particular species, and eventually lead to decreased ability to cope with the stresses of the environment, thereby increasing the probability of death"

(Stedman's Medical Dictionary, 26th Edition)

Although this definition is largely accepted, it does not seem to be entirely accurate any longer due to the fact that the *irreversibleness* of age-related alterations has been severely challenged in recent years. This, as discussed in more detail later, was only possible thanks to the renaissance of our desire to delay aging – which is finally being supported by science, instead of myths and fantasies.

Aspirations to defeat aging and attain eternal youth have flourished for almost as long as humans existed. In fact, recounts of actual pursuit of anti-aging nostrums date back thousands of years and are spread all over the globe. Still, the quest has been largely disappointing as no one succeeded in finding the fictional fountain of youth. Needless to mention, ancient Greeks and Romans were not successful in suppressing aging by getting covered in crocodile dung, nor did fenugreek oil help my Egyptian ancestors, who lived, on average, around 30-35 years.

That being said, we have been constantly cheating aging with every new born brought to life. During this phenomenal event, age is literally zeroed out before our eyes as a new life is created from two originally older adults. Hence, aging might not be as absolutely formidable as previously thought. If we could completely restart age within our own offspring, then it might be possible to – at least – postpone it within ourselves. In fact, many other organisms manage to do this and even more; one such organism is *Turritopsis dohrnii*, also known as the immortal jellyfish (1). When this jellyfish gets old or is exposed to disease and stress, it can – instead of dying – revert back to an earlier immature stage of its lifecycle and restart its life all over again. This represents a spectacular example of an animal that can actually

reverse, not just delay, the aging process and can escape natural death altogether. Another exceptionally long-lived animal – which comes closer to humans being a vertebrate – is the Greenland shark (*Somniosus microcephalus*), which can reportedly live up to 392 years of age and, also, the warm-blooded bowhead whale (*Balaena mysticetus*), which is considered to be the longest-lived mammal as it exceeds 200 years of age (2,3). Interestingly, these whales also have a reduced incidence and delayed onset of disease compared to humans.

As for humans, nowadays a lot of people around the globe seem to reach exceptionally old ages. According to United Nations reports, there have been more than 300 thousand living centenarians, *i.e.*, individuals surpassing 100 years of age, worldwide in 2011 and currently there are likely even more (4). Interestingly, these centenarians usually enjoy an extended *healthy* life span and, thus, the period they live in disease is relatively shorter than average.

Taken together, aging might be more malleable than previously anticipated. Therefore, if we are to identify the specific factors, processes or mechanisms that lead to health preservation in long-lived organisms, animal and humans, we might be able to extend this knowledge to allow the rest of our aging population to enjoy a healthier life for as long as possible. To this end, the last two decades have witnessed major strides in the field of aging, which have shown great promise in preclinical testing. These include – as discussed in detail later in this chapter – the identification of specific interventions, cellular processes and even single molecular targets that effectively regulate the pace of aging and protect from related diseases.

1.2. Caloric restriction: the holy grail of longevity

Although fasting and caloric restriction, *i.e.*, reduced caloric intake without incurring malnutrition, has been practiced for thousands of years, its impact on aging has been rigorously studied in modern history only. Precisely, around a century ago, Osborne *et al.* – writing in *Science* – reported a higher late-life survival of female rats exposed to growth retardation due to limited food intake (5). Later on, McCay *et al.* confirmed this observation as they showed that calorically-restricted rats exhibit substantial lifespan extension compared to *ad libitum*-fed controls. Hence, reduced energy intake attracted a lot of attention as a potential remedy for aging;

especially that it is more modifiable than other recognized determinants of our biological age, including genetic and socioeconomic factors.

More recently, this interest resulted in a plethora of studies validating the beneficial impact of caloric restriction on lifespan, not only in rats (6), but across species, that ranged from unicellular organisms to flies and mammals – including non-human primates (7). More importantly, caloric restriction has been also shown to delay the onset and progression of late-life disorders as it conferred protection against metabolic abnormalities in glucose and insulin homeostasis, as well as cardiovascular risk factors, including elevated blood pressure and abnormal circulating lipids profile (8). It is believed that dietary restriction exerts these beneficial effects on health and lifespan *via* diverting energy utilization from growth, towards cellular maintenance and quality control through the activation of various cellular adaptive and homeostatic processes, which improve stress resistance and enhance functionality.

Despite such startling benefits, caloric restriction is still not ready to be adopted as a standard medical practice or lifestyle for a fair amount of reasons. Firstly, following strict dietary regimens for extended periods is generally challenging for the majority of people. Secondly, it is still unclear whether the elderly can tolerate chronic caloric restriction without incurring any adverse effects, especially in those suffering from osteoporosis, injuries or infections (9). Thirdly, the outcomes of caloric restriction do not seem to be entirely universal as differences in age, strain and sex seem to affect the magnitude and sometimes, unexpectedly, cause negative health outcomes (10). To this end, it is imperative to define the specific molecular targets through which caloric restriction counteracts aging and exploit them to develop novel therapies that could mimic the effects of caloric restriction, but are more feasible to apply and do not exert potential harm.

1.3. Molecular pathways of aging

Extensive experimentation on the effects and mechanisms of caloric restriction resulted in identifying a subset of signalling pathways, whose activity is regulated by food intake. Interestingly, direct manipulation of these nutrient-sensing pathways – without changing food intake – effectively promotes longevity; hence they were

termed *longevity-associated pathways* and these include insulin-like growth factor-1, mammalian target of rapamycin, sirtuins and AMP-activated kinase.

1.3.1. Insulin/IGF-1

Insulin/insulin-like growth factor-1 (IGF-1) pathway is the first discovered and most studied longevity pathway. This pathway is strongly inhibited by caloric restriction. In fact, calorically-restricted mice exhibit lower levels of circulating IGF-1, and this is suggested to mediate their extended lifespan (11,12). Also in humans, reduced food intake is associated with reduced IGF-1 bioavailability and activity due to increased IGF binding protein-1 (13).

Independent of food intake, deactivation of the insulin/IGF-1 pathway has a substantial lifespan-extending effect in various model organisms (14,15). Although slightly more controversial in mammals, most of the literature supports an inverse relationship between IGF-1 activity and aging (14,15). For instance, a large longevity study including 31 genetically distinct mouse strains showed that lower circulating IGF-1 is associated with longer lifespan (16). This finding was confirmed in three independent human epidemiological studies recruiting extraordinarily long-lived individuals, which showed a higher probability of survival when IGF-1 concentration or activity is reduced (17–19).

Inhibiting this pathway has also been shown to promote healthy aging in different body organs, including the heart and vasculature. For instance, IGF-1 depletion or the knock-out of its receptor specifically in cardiomyocytes delays cardiac signs of aging as it attenuates fibrosis, hypertrophy and inflammatory markers in mice (20,21). Consistently, local IGF-1 overexpression deteriorated cardiac systolic function and augmented cardiac maladaptive hypertrophy and collagen deposition at old age (22). However, these observations have been challenged in another study showing protective effects of IGF-1 overexpression; thus, more efforts are warranted to precisely delineate the accurate outcomes of manipulating cardiac IGF-1 signaling (23). At the vasculature, attenuating IGF-1 signaling might be beneficial as well. For instance, reduced growth hormone and IGF-1 signaling in long-lived *Ames* and *Little* mice is associated with a deceleration of age-related decline in vascular function, despite having worsened endothelial function at a young age (24,25). That said, another study showed improved function and

regenerative capacity of endothelial cells in young mice lacking IGF-1 receptor specifically in the endothelium (26,27). Taken together, inhibiting IGF-1 signaling seems to be beneficial for the cardiovascular system at least in advanced age, but manipulating it during earlier life stages is still controversial and warrants more research.

1.3.2. Mammalian target of rapamycin

One of the down-stream targets of IGF-1 signaling is the mechanistic target of rapamycin (mTOR), also referred to as the mammalian target of rapamycin. This nutrient-sensing protein kinase, which is inhibited by caloric restriction, is a master regulator of cellular metabolism (28). Explicitly, mTOR is implicated in a multitude of cellular functions, including protein synthesis, cellular proliferation, motility, growth, and survival (29). Interestingly, aging is associated with increased mTOR activity (30). Contrarily, mTOR inhibition – genetically or by its FDA-approved antagonist, rapamycin – does not only extend the lifespan of yeast, worms and flies, but also extends the lifespan of mice when administrated at a young or old age (31–33).

Furthermore, rapamycin-mediated mTOR deactivation in the heart reverses age-related cardiac dysfunction (34). Rapamycin also confers protective effects on the aged vessels (35). Although some of these health-promoting effects have been challenged, it encourages more research to further define the specific downstream targets or subunits of the mTOR complex, which underlie the anti-aging effects of rapamycin (36,37).

1.3.3. Sirtuins

Nicotinamide adenine dinucleotide (NAD^+)-dependent deacetylases, known as sirtuins, are considered master regulators of metabolism, especially during conditions of energy deficit such as caloric restriction (38). In mammals, there are seven different sirtuins (SIRT1-7) localized in different subcellular compartments, including cytoplasm, mitochondria, and nucleus. At least, the most studied member of sirtuins, SIRT1, is upregulated in response to caloric restriction (39). More importantly, SIRT1 knock-out in mice deprives caloric restriction from its lifespan-extending effect (40). In addition, sirtuin activation by supplementing the NAD^+

precursor, nicotinamide riboside, promotes longevity in mice (41). However, this does not seem to be consistent as transgenic overexpression of SIRT6 extended lifespan only in male mice (42), whereas neither male nor female SIRT1 transgenic mice live longer, despite being healthier than wild-type controls upon aging (43). Similarly, other sirtuin activators, like resveratrol and SRT172037, prevent premature mortality due to metabolic disease, but do not necessarily extend lifespan in naturally aged mice (44–46).

Regardless of their impact on lifespan, sirtuins are consensually acknowledged to promote health. For instance, moderate cardiac SIRT1 overexpression delays cardiac aging as denoted by reduced fibrotic and hypertrophic remodeling and limited cardiomyocyte senescence and apoptosis (47). Contrarily, abolition of SIRT3 induces premature cardiac aging by 13 months of age (48). Similarly, SIRT1 deactivation in young mice causes vascular function deterioration comparable to that observed in aged mice (49). Finally, SIRT1 levels in the vasculature tend to go down with aging in mice and humans, and the degree of reduction correlates with age-related deficit in vascular function (49). Collectively, available data support the notion that sirtuin activity is a major determinant of cardiovascular health and less so of lifespan.

1.3.4. AMPK

Another key metabolic regulator during nutrient stress is the AMP (adenosine monophosphate)-activated kinase (AMPK). Limited cellular ATP or accumulation of AMP (*i.e.*, higher AMP to ATP ratio) catalyze AMPK activity, which in turn ignites a myriad of cellular changes, whereby energy production is increased and ATP consumption is reduced in a highly coordinated fashion (50). Hence, AMPK is clearly activated by caloric restriction, yet it is still uncertain whether this causally underlies the positive effects of caloric restriction in mammalian aging (51–53).

Irrespectively, aging itself is associated with reduced AMPK activity in different organ systems, including the heart and vessels (54–56). More importantly, activating AMPK by the anti-diabetic drug metformin effectively improves health and life-span of mice (57,58). Specifically at the heart, metformin-mediated AMPK activation improves cardiomyocyte function and attenuates β-adrenergic-induced fibrosis in aged mice (54). Furthermore, metformin administration is associated with

reduced cardiovascular events in aged diabetic patients (59). Along the same lines, other AMPK activators confer protective effects against aging. For instance, AICAR (aminoimidazole carboxamide ribonucleotide) preserves vascular health in aged mice and curcumin improves endothelial function in aged humans and rats in an AMPK-dependent manner (55,56,60). In contrast, genetic reduction of AMPK levels induces a premature cardiac aging phenotype, characterized by impaired cardiac structure and function as well as increased mitochondrial abnormalities and oxidative stress (54,61). Collectively, these reports support an essential role of reduced AMPK activity in the process of aging and, thus, potential exploitation of its activators, such as metformin, to influence health outcomes in the elderly.

1.4. Autophagy: the gateway for longevity promotion

A common demeanour of dietary restriction and longevity-associated pathways is that they modify a multitude of diverse cellular processes. However, all these longevity-promoting regimens seem to converge on a common denominator, namely their ability to induce autophagy (*i.e.*, 'self-eating' in Greek).

Macroautophagy (herein referred to as autophagy) is a fundamental homeostatic and survival mechanism, which is responsible for protein quality control in almost every eukaryotic cell (62). During this evolutionarily-conserved process, damaged, dysfunctional, or simply long-lived organelles and protein aggregates are sequestrated within a double-membraned structure, called autophagosome. In turn, autophagosomal contents undergo enzymatic degradation by acidic hydrolases of lysosomes in the so-called autolysosome (Fig. 1). Eventually, the end-products, generated upon the breakdown of these cytoplasmic components, are either utilized for energy production or serve as building blocks for cellular anabolism and organelle recycling (62).

Astonishingly, autophagy seems to function in a selective manner, meaning that it recognizes a particular target within the cell and degrades it for detoxification purposes. One such highly-specialized form of autophagy is that targeting mitochondria, known as mitophagy (63). Hence, autophagy does not only enable the cell to generate enough energy and, thus, withstand stressful conditions (*e.g.*, starvation, physical exertion, and hypoxia), but also helps preserve cellular homeostasis during physiological conditions by targeting specific organelles that are

potentially toxic if damaged. Accordingly, autophagy is considered to play an essential role in health control, not only during aging, but also in a variety of related diseases (64,65). In fact, aging is associated with a reduced autophagic capacity in different cell types and tissues and this is implicated in the functional decline associated with aging (64–66).

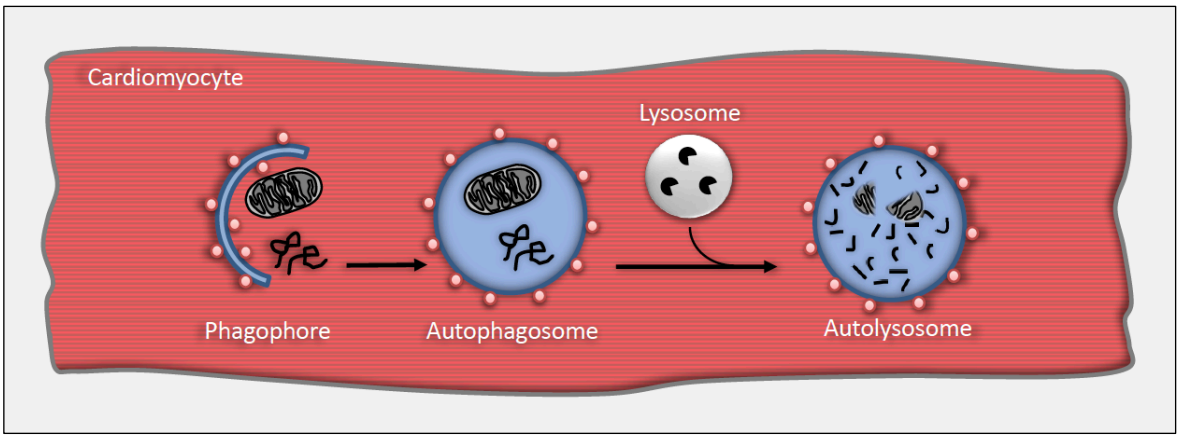

Figure 1. Schematic representation of autophagy in a cardiomyocyte.

During autophagy, damaged, dysfunctional, or long-lived organelles and proteins are sequestrated within a double-membraned structure, called autophagosome. Autophagosomal contents then undergo enzymatic hydrolysis upon contact with the lysosomes in the so-called autolysosome. In addition to detoxification purposes, the resulting end-products of this process are utilized for energy production or alternatively they serve as building blocks for various anabolic processes necessary for cellular recycling.

Among the underlying factors for this characteristic decline in autophagy is age-related changes in longevity pathways (64), including increased IGF-1 and mTOR signalling as well as reduced sirtuins and AMPK activity (Fig. 2).

More interestingly though, all interventions operating through longevity pathways seem to lose their anti- aging effect when deprived from their ability to promote autophagy. For example, deactivating the essential autophagy gene *bec-1* (orthologue of mammalian *beclin-1* in nematodes) almost completely abrogates the lifespan-extending effect of reducing IGF-1 signalling in *daf-2* mutant Caenorhabditis *elegans* (67). Lack of *bec-1* in *C. elegans* seems to also prevent lifespan extension induced by the sirtuin activator resveratrol (68). Similarly, blocking autophagy by abolishing another essential autophagy-related gene, *Atg5*, abolishes the lifespan-prolonging effect of two additional longevity mechanisms, namely mTOR inhibition and AMPK activation (by rapamycin (68) and β-Guanidinopropionic acid (69), respectively) in flies (*Drosophila melanogaster*).

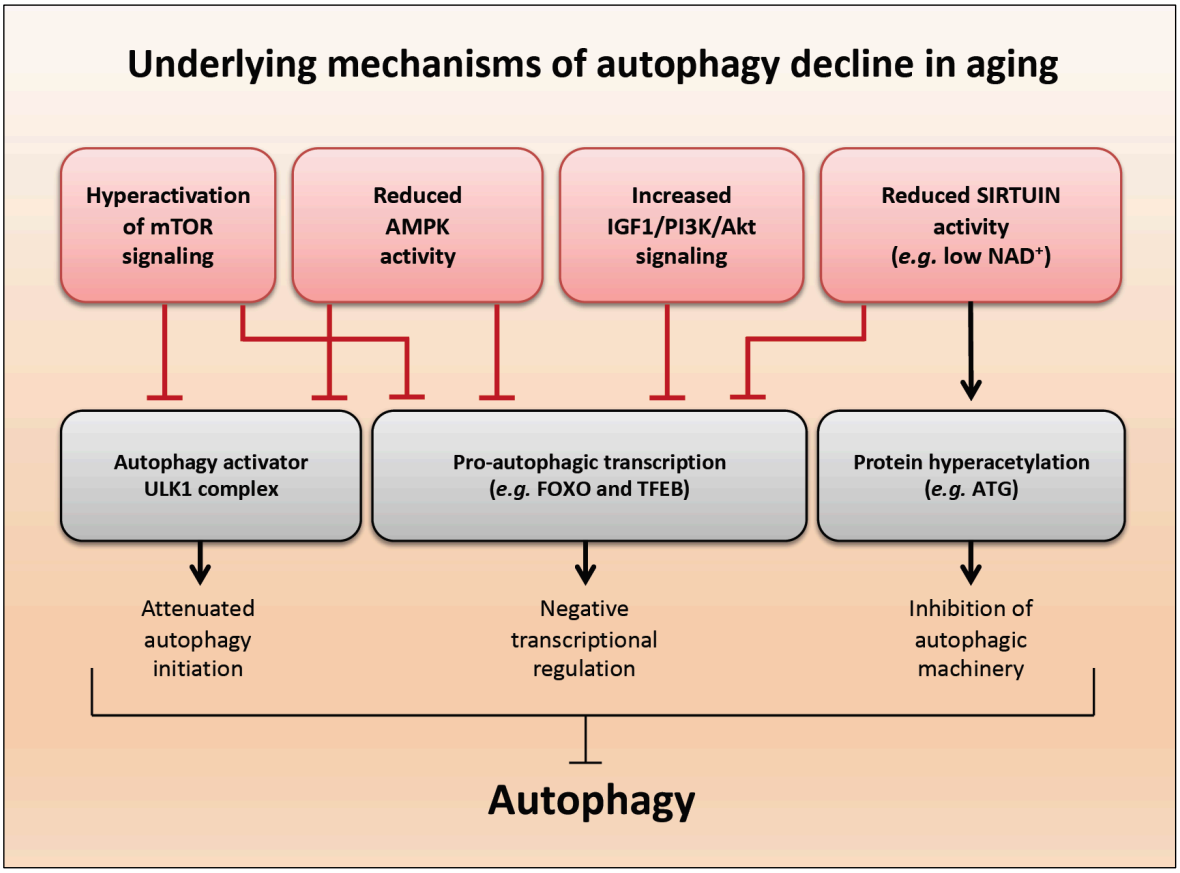

Figure 2. Underlying mechanisms of age-related autophagy decline.

During the course of aging, autophagy is subjected to progressive reduction in its activity due to age-dependent molecular changes in longevity pathways, including increased insulin-like growth factor-1 (IGF-1) and mammalian target of rapamycin (mTOR) signalling and reduced sirtuins and AMP-activated protein kinase (AMPK) activity. Abbreviations: ATG, autophagy-related; NAD^+, nicotinamide adenine dinucleotide; PI3K, phosphoinositide 3-kinase; ULK-1, Unc-51 like autophagy activating kinase-1. *Adapted from Abdellatif et. al. Circulation Research, 2018* (70) *with permission from the publisher (Wolters Kluwer).*

In addition, caloric restriction does not promote longevity without intact autophagy machinery as shown in nematodes (71). In fact, autophagy deactivation in a single organ, like the intestine, is sufficient to stop the lifespan-extending effect of caloric restriction. Altogether, a growing body of evidence suggests that autophagy underlies, at least in part, the positive effects of these interventions on aging and longevity (72). In fact, stimulating autophagy by genetically overexpressing its molecular machinery is sufficient to promote longevity in a wide range of species, including model organisms and mammals, independent of food intake or longevity-related pathways activity (73,74). Hence, emerging molecules that specifically activate autophagy may represent a new avenue for healthy aging and longevity.

1.5. Spermidine: a natural autophagy inducer and caloric restriction mimetic

Despite the astounding benefits of caloric restriction, a minority of people seem to be willing to change their dietary habits and hardly any would do so for extended periods. Therefore, there is a growing interest in developing alternatives that could potentially mimic the metabolic benefits of caloric restriction without necessarily following stringent dietary adjustments. One such alternative is caloric restriction mimetics, which are natural substances or pharmacological agents that boost autophagy (75,76). Given that genetic manipulation of longevity-related molecular targets is not expected to reach humans in the near future due to several safety and ethical concerns, caloric restriction mimetics hold promise as a promising and feasible alternative.

The natural polyamine spermidine, which exists ubiquitously in our cells, is one such caloric restriction mimetic. Spermidine and other polyamines, (*i.e.,* putrescine and spermine) are essential for cellular survival as they serve several fundamental roles, including nucleic acid stabilization, protein synthesis, cell growth, differentiation, apoptosis, oxidative stress resistance and ion channel activity (77). Interestingly, spermidine levels in the bloodstream and different tissues are not only determined by its cellular biosynthesis, catabolism and urinary excretion, but also by its nutritional uptake and production by gut microbiota (78). Therefore, it is conceivable that spermidine levels, which is suggested to decline with aging (79), can be raised by increasing its dietary intake. In this regard, some foods, such as durian fruit and wheat germ, are naturally rich in spermidine. In addition, fermented soy beans and aged cheeses are also very rich in microbially-generated spermidine due to fermentation processes necessary for their production. Other foods that are relatively less spermidine-rich, and less malodorous, include mushrooms, peas, nuts and broccoli (78).

Recently, spermidine emerged as a potential caloric restriction mimetic given a discovered intrinsic ability to induce autophagy (76). By recapitulating such a fundamental trait of caloric restriction, spermidine extends the lifespan of multiple model organisms such as yeast, worms, flies and, additionally, cultured human cells (80). Interestingly, spermidine has also been shown to attenuate age-related memory decline in flies (81).

Taken together, spermidine seems to confer beneficial effects on health and lifespan at least in model organisms. Hence, it appears plausible that spermidine might delay aging in mammals as well, especially given its safety profile being a naturally occurring substance. To this extent, we aimed – within this thesis – to examine the effects of dietary supplementation of spermidine on mammalian aging and related disease, focusing specifically on the cardiovascular system.

1.6. Hypotheses and Objectives of this thesis

The main hypothesis of this work is that the oral supplementation of the natural caloric restriction mimetic spermidine can delay cardiac aging and protect from cardiovascular disease in preclinical testing. In addition, we hypothesized that higher endogenous and dietary levels of spermidine in humans are associated with reduced incidence of cardiovascular disorders. To examine these hypotheses, we set out the following objectives:

1. Examining whether spermidine feeding can attenuate cardiac aging in naturally old mice without concomitant comorbidities.
(*Chapter 3. Spermidine and cardiovascular aging*)

2. Testing the general pro-autophagic capacity of spermidine in the heart and, specifically, that targeting mitochondria (*i.e.*, mitophagy). In addition, we aimed to confirm whether autophagy activation is a prerequisite for the potential cardioprotective effects of spermidine.
(*Chapter 3. Spermidine and cardiovascular aging*)

3. Determine the effect of spermidine on cardiovascular disease, exemplified by hypertension and related cardiomyopathy using *Dahl* salt-sensitive rats.
(*Chapter 4. Spermidine and cardiovascular disease*)

4. Investigating the correlation between endogenous/dietary spermidine levels and the prevalence of cardiovascular disease in humans.
(*Chapter 5. Spermidine in humans*)

2. MATERIALS AND METHODS

2.1. Animal models and spermidine administration

Wild-type C57BL/6 mice were used throughout our cardiac aging studies. Mice were purchased from animal breeding laboratories (male C57BL/6J from Janvier; female C57BL/6J and 6N, from Charles River Laboratories (USA) and Envigo (USA), respectively). Mice were allocated to treatment groups in a random manner, yet systematically taking care that mice derived from a specific strain/provider were evenly assigned to different treatments. As for the treatment, mice received spermidine (3 mM) orally as a supplement in their drinking water, whereas control mice received normal water. The treatment was initiated either at the age of 4 months (*early-in-life regimen*) or later when the mice were aged, specifically at 18 months of age (*late*-in-life regimen). Independent cohorts of mice were used for different experiments, such as echocardiography, hemodynamics, blood pressure measurements, myocardial ultrastructural analysis, mitochondrial respiration, blood chemistry and lifespan analysis. Both food and water intake were regularly monitored (twice a week for at least a month) to exclude any confounding effects of possible differences in energy intake.

Cardiomyocyte-specific *Atg5* (autophagy-related gene 5) knockout mice (*Atg5*$^{-/-}$) were generated by crossing *Atg5*$^{flox/flox}$ mice with cardiomyocyte-specific Cre^{+} recombinase-expressing (*MLC2a-Cre*$^{+}$) mice (obtained from Riken BRC, Japan). Although *Atg5*$^{-/-}$ mice suffer from fulminant heart failure by the age of 9 months, they do not show any signs of structural or functional deterioration till 3 months of age (82). Therefore, male *Atg5*$^{-/-}$ (*Atg5*$^{flox/flox}$*-MLC2a-Cre*$^{+}$) and their wild-type littermates (*Atg*$^{+/+}$*, Atg5*$^{flox/flox}$*-MLC2a-Cre*$^{-}$) were supplemented with spermidine *via* the drinking water soon after weaning (at 4 weeks of age) till 16 weeks of age when final cardiac assessments (echocardiography and hemodynamics) were performed. Lack of ATG5 in *Atg5*$^{-/-}$ mice was confirmed in cardiomyocytes isolated from adult mice by immunoblotting of LC3 (ATG5), whereas genotypes were verified by PCR-based analysis of genomic DNA (isolated from ear biopsies) utilizing commercially-available primers (“exon3-1”, “short 2” and “check 2” for *flox alleles*; “MLC2a-1 (5′-GGATCTATGTGGAGCCCTGTCT-3′)” and “MLC2a-2 (5′-GCACACAAGTCCCTGGCTCTGT-3′)” for *Cre allele*).

Generally, 4-5 littermate mice were housed in single cages (individually ventilated cages, IVC type-III) enriched with paper huts and nesting sheets. The cages were

kept in rooms with controlled 12-hour dark/light cycle. Mice had free access to food (standard chow, *Ssniff* V1534) and water.

***Dahl* salt-sensitive (SS) rats**, an animal model of salt-induced hypertension and heart failure (83), were employed to study cardiovascular disease. 4-week-old *Dahl* SS rats were purchased from Charles River Laboratories (USA) and fed low-salt (LS) diet (0.3% NaCl; #AIN-76A, Research Diets, USA) for a 3-week-long acclimatization period. At the age of 7 weeks, rats received high-salt (HS) diet (8% NaCl-supplemented diet; #AIN-76A, Research Diets, USA) which was either combined with (or without) 3 mM spermidine supplementation in drinking water till the age of 14 or 19 weeks (short-term and long-term *Prevention Cohorts*, respectively). In a third cohort, rats received HS diet only till 12 weeks of age, when they were shifted to a LS diet and received a single intraperitoneal diuretic injection (furosemide, 10 mg/kg body weight) combined with or without 3 mM spermidine supplementation for 5-6 weeks (*Therapy Cohort*). Cardiovascular phenotyping was done in all 3 cohorts.

As for mice, all rats were housed (3 per cage) at the animal facility of the Medical University of Graz under a 12-hour light/dark system with food and water access *ad libitum*.

Researchers involved in any experiments were blinded to the treatment and genotype. All animal studies in this thesis were done following the European ethical regulations (Directive 2010/63/EU) and were approved by the responsible national agencies (BMWFW-66.007/0002-WF/V/3b/2015 - BMWF-66.010/0160-WF/V/3b/2014 - BMWF-66.010/0053-WF/II/3b/2014 - BMWF-66.0070011-lll3bl2013 - BMWF-66.010/0161-II/3b/2012). The 3R principles and ARRIVE guidelines for animal use were followed throughout (84).

2.2. Blood pressure measurements

A tail-cuff method was applied to non-invasively measure blood pressure (systolic, diastolic and mean) together with pulse rate in conscious animals (CODA^{TM} system, Kent Scientific Corporation, USA). The rats were restrained on a previously warmed heating pad to keep their body temperature at 37 °C. Following sufficient acclimatization, at least three independent stable measurements were averaged to get reliable pressure estimates at a normal pulse rate.

2.3. Echocardiography

Cardiac function and dimensions were non-invasively evaluated in lightly anesthetized animals (1-2% or 0.5-1% isoflurane for maintenance in rats or mice, respectively; 4-5% isoflurane for induction) by transthoracic echocardiography (micro-imaging system Vevo770™, VisualSonics Inc., Canada). Animal temperature was kept at 37 °C using a previously warmed heating platform, on which the animals were placed in a supine position with their limbs in direct contact with non-invasive electrocardiogram leads. Pre-warmed ultrasound transmission gel was spread on a shaved chest to obtain cardiac tracings in parasternal long and short axes using high-resolution 30 Mhz or 17.5 MHz linear-array probes for mice or rats, respectively. M-mode tracings were used to evaluate cardiac walls and internal dimensions during systole and diastole, whereas pulsed-wave and tissue Doppler was used to evaluate mitral flow and annulus velocities, respectively. Troy formula was applied to calculate myocardial mass, meanwhile ventricular volumes were estimated based on Teichholtz formula (85). Ejection fraction (%) was determined as 100×([end-diastolic volume-end-systolic volume]/end-diastolic volume). Generally, three steady-state cardiac cycles were averaged to obtain reported measures of cardiac structure and function.

2.4. Hemodynamic evaluation (pressure-volume measurements)

The gold standard for cardiac performance evaluation is real-time intra-cardiac measurement of pressure and volume, *i.e.*, invasive hemodynamics. To perform this procedure, animals were subjected to halogenate anesthesia with isoflurane (induction: 4%; maintenance: 1-2%) before getting intubated for mechanical ventilation (SAR 1000, CWE, Inc. for rats and Harvard Mini-Vent 845 for mice). Animal body temperature was kept at 37 °C by a temperature-controlled warming pad (TC-1000, CWE, Inc.). Three-lead electrocardiogram (Animal Bio Amp, FE136; ADInstruments) was used for continuous monitoring of heart rate. Pressure conductance catheters (1.4F and 2F, #Cat. Nr. SPR-839 and SPR-838, respectively; Millar Instruments) were used for mouse and rat measurements, respectively. Signals were obtained in real-time (MPVS ultra, Millar Instruments) and stored in a digital form at a high sampling frequency (2 kHz) for future offline

analysis (MPVS PL3508 PowerLab 8/35, ADInstruments). The procedure was done in a closed-chest setting. Briefly, after dissecting the right carotid artery from the surrounding neck tissues, the catheter was inserted and advanced into the left ventricle *via* the aorta. Following proper positioning of the catheter (*i.e.*, maximum conductance signal) and animal stabilization, various measures of systolic function (*e.g.*, cardiac output, ejection fraction, end-systolic pressure and maximum rate of systolic pressure change [dP/dt_{max}]) and diastolic function (*e.g.*, end-diastolic pressure, maximum rate of diastolic pressure change [dP/dt_{min}] and isovolumic relaxation constant [τ]) were obtained and averaged from at least 10 cardiac cycles. Transient inferior vena cava occlusions were performed in order to manipulate the loading conditions and derive load-independent indices of cardiac contractility and passive stiffness (end-diastolic and end-systolic pressure-volume relationship, respectively) (86). To minimize the noise introduced by lung filling and motion, analyzed beats were obtained upon temporarily suspended ventilation in end-expiration. Parallel conductance was estimated by intravenous hypertonic saline injection (10% NaCl; 10 µL in mice and 40 µL in rats) for later subtraction during the analysis. To convert measured conductance to volumes, a calibration curve was obtained using standard volume cuvettes for mice and rats (ADInstruments). Due to abnormal geometry and, thus, non-optimal positioning of the catheter in *Atg*$^{-/-}$ mice, conductance-based volumes were corrected by echocardiography-measured volumes (*i.e.*, slope factor α). Whenever a massive difference in the body size of compared animals (*e.g.*, 7 weeks old *vs.* 14 and 19 weeks old *Dahl* rats) was detected, volumes were corrected to body surface area (calculated as [$9.1\times(\text{body weight})^{2/3}$]) to account for differences in cardiac chamber size. Pressure-volume analysis was done offline using LabChart V.8 Pro (ADInstruments). Invasive hemodynamics was performed as a terminal procedure. Animals were then sacrificed and different organs (*e.g.*, heart, lung, kidney, liver and spleen) were collected for gravimetric analysis and processed accordingly for following *in vitro* experiments.

2.5. Maximal effort and oxygen consumption determination

A subset of *Dahl* rats underwent peak effort testing on a motorized treadmill housed in an air-tight closed chamber coupled to a calorimetric unit (TSE Systems, Germany). Ambient air was pushed into the chamber and then extracted for measurement of relative changes in O_2 and CO_2. The flow rates were chosen such that despite sufficient oxygen availability, the difference in O_2 and CO_2 between inflow versus outflow air was within the gas sensors' range of measurement, *i.e.*, 0.3 - 0.7 %. Gas samples were cooled to 5 °C and dried prior to the measurement of O_2 and CO_2. The gas analyzers were calibrated with standardized gas mixtures (Air Liquide, Vienna, Austria) prior to the experimental session following the manufacturer's instructions. Rats were subjected to the ramp exercise protocol with an initial velocity of 0.15 m/s for 3 minutes followed by a constant acceleration of 0.05 m/min at an inclination of 10°. The exercise session ended at maximal exhaustion, which was defined as the rat's inability to maintain running speed despite being in contact with the electrical grid for 5 consecutive seconds. At this point the maximal run distance was recorded. The maximal oxygen consumption (VO_2max) was defined as the point at which oxygen uptake reached a plateau during exhaustive exercise.

2.6. Renal assessment

For renal histology, kidney samples were embedded in paraffin following fixation in 4% neutral-buffered formaldehyde, and then sliced into 4-µm-thick slices. The slices were then stained with periodic acid-Schiff (PAS) stain (Merck, Darmstadt, Germany) for assessment of glomerular injury and arterial hyalinosis according to a PAS-based semi-quantitative scoring system (87) by Dr. Alexander Kirsch (*Department of Nephrology, Medical University of Graz*). For renal fibrosis evaluation, the slides were stained with picrosirus red stain (Sigma-Aldrich, St. Louis, MO, USA). In addition, urinary lipocalin (Lcn)-2 levels were evaluated to assess acute renal injury, using the rat Lcn-2/NGAL DuoSet (R&D Systems, Abingdon, UK) following the manufacturer's recommendations.

2.7. Spermidine quantification

High performance liquid chromatography (HPLC) and mass spectrometry (MS) techniques were generally used for metabolome analysis. Briefly, a mortar and pestle were used to homogenize harvested tissues, which were initially snap-frozen in liquid nitrogen and kept at -80 °C. Around 10-15 mg of tissue were used to prepare an extract, in which the concentration of spermidine and other polyamines was quantified applying an established HPLC-MS/MS protocol in collaboration with Dr. Christoph Magnes (*HEALTH-Institute for Biomedicine and Health Sciences, Joanneum Research, Graz*) (88). Similarly, circulating spermidine levels were quantified in an extract prepared from 10 µl of whole blood (collected in EDTA tubes) or plasma, which was isolated from centrifuged blood at 2500 x *g* for 20 minutes.

2.8. Arginine and citrulline determination

Plasma arginine and citrulline were quantified using chromatography-based techniques in collaboration with Dr. Andreas Meinitzer (*Institute of Medical and Chemical Laboratory Diagnostics, Medical University of Graz*) (89). In detail, after neutralizing the supernatant by sodium carbonate, serum was precipitated with perchloric acid. Amino acids then underwent o-phtalaldehyde-based derivatization and were separated on a reverse-phase column with gradient elution. The ratio of observed fluorescence from pertinent amino acids to norvaline, which served as an internal standard, was used for quantification according to appropriate calibration curves.

2.9. Quantification of cardiac mitochondrial respiration

Mitochondrial respiratory function was determined with high-resolution respirometry in isolated cardiac mitochondria. For mitochondrial isolation, freshly-harvested hearts were subjected to a buffer incorporating bacterial protease (5 mg/ml; Sigma-Aldrich, P8038) and 0.2 % BSA as described (90). Series of dilutions in a TECAN Genios Pro plate reader was used to determine the mitochondrial suspension (excluding bacterial protease) optical density, measured at 600 nm (OD_{600}), which was used later for normalization as a surrogate for mitochondrial mass. Measurement of oxygen consumption was done on 10-20 µg of mitochondria (in OD_{600} equivalents) suspended in 2 mL of measurement medium at 37 °C using a

high-resolution respirometer (Oxygraph-2k, Oroboros Instruments, Austria) according to the manufacturer's instructions.

After measuring leak respiration (*LEAK)* due to residual oxygen consumption (*ROX*), 5 mM pyruvate and 10 mM glutamate were added to measure the activity of complex I. This was followed by consecutive adding of 450 µM ADP (*OXPHOS*) and 10 µM cytochrome c (*OXPHOS + CytC*). Residual respiration (proton leak) was also ascertained by oligomycin (1.25 µM), and maximum respiration was subsequently assessed in an uncoupled state by FCCP titration (in 0.5 µM steps) and ensuing antimycin A-mediated inhibition of respiratory activity. Included recordings had an absolute oxygen concentration of at least 100 nM/mL and experiments were done in pairs of mice (*e.g.*, aged control with old spermidine-treated or with young control mouse). These experiments were done by Tobias Eisenberg (*Institute of Molecular Biosciences, University of Graz*).

2.10. Plasma cytokine measurements

Circulating cytokines were quantified in plasma obtained from fasted 23-month-old mice or non-fasted 21-month-old mice. Briefly, whole blood was collected in EDTA tubes and plasma was extracted by centrifugation at 2500 x *g* for 20 minutes. Plasma cytokines were then measured in 25 µl samples using an electrochemiluminescence-related immunoassay, whereby mouse cytokines were evaluated in MSD V-Plex Plus Proinflammatory Panel 1 kit and rat cytokines in a customized TNFα / IL-10 V-Plex Rat cytokine kit (Meso Scale Diagnostics, USA). To focus our analysis on age-related sterile (subclinical) inflammation, we applied the following approach: mice that had two or more massively increased cytokines were considered to be going through an acute inflammatory process and were excluded from the analysis. A massively increased cytokine was identified by applying a statistical outlier rule, whereby the value had to be more than 2.2 the IQR (inter-quartile range) of the respective group. In case an animal had a high level of a single cytokine, this animal was included, but the cytokine was winsorized to the closest value in the respective group. Notably, comparable numbers of animals had acute inflammatory status in different aged groups. All Meso Scale measurements were done by Dr. Tobias Pendl (*Institute of Molecular Biosciences, University of Graz*) and the analysis was done by myself.

2.11. Immunoblotting and autophagic flux analysis

Tissue homogenates were lysed using a buffer solution (50 mM Tris-HCl, pH 7.4, 1 mM EDTA, 1 mM EGTA, 1 % Triton X-100) complemented with 1x *Complete*® protease inhibitor cocktail (Roche, Austria). Expression of different proteins, such as ATG5, p62/SQSTM1 and LC3-II (lipidated LC3) was then evaluated by standard immunoblotting on a PVDF (polyvinylidenfluorid) membrane using substrate-specific antibodies (Abcam, ab018327 for ATG5; MBL, PM045 for p62/SQSTM1; Cell Signaling Technologies, #2775 for LC3-II, #2118 for GAPDH and #7074 as an HRP-linked anti-rabbit IgG). Eventually, densitometry-based protein quantification was done using ImageLab software (Bio-Rad Laboratories, USA).

For autophagic flux determination, 13-month-old mice were subjected to 4 weeks of 3 mM spermidine supplementation in their drinking water. Mice were then sacrificed and their hearts were collected; LC3-II was then evaluated as detailed above. Fifty minutes earlier, half of the animals received a single intraperitoneal injection of the protease inhibitor leupeptin (40 µg/kg body weight; Sigma-Aldrich, Austria) to block the breakdown of autophagosomes by lysosomal enzymes, allowing for flux evaluation by comparison to the rest of animals that received a vehicle (physiological saline) injection. These experiments were done by Dr. Tobias Eisenberg (*Institute of Molecular Biosciences, University of Graz).*

2.12. Autophagy and mitophagy assessment in transgenic mice

Three-month-old transgenic mice expressing tandem-fluorescent mRFP-GFP-LC3 (Tg-tf-LC3) specifically in the heart were supplemented with 3 mM spermidine for a period of 2 weeks. Four hours prior to euthanasia and cardiac tissue harvesting, the animals either received chloroquine (10 mg/kg) or vehicle (physiological saline). Briefly, fresh cardiac slices were embedded in tissue-TEK OCT compound (Sakura Finetechnical Co., Ltd.) and stored at -80 °C. Frozen cardiac samples were cut into 10-µm-thick slices by a cryostat (CM3050S; Leica, Germany), air-dried for 30 minutes, fixed (10 % formalin for 10 min), mounted with a DAPI-containing reagent, and eventually visualized under a confocal microscope to count fluorescent LC3 puncta, denoting autophagosomes and autolysosomes, as described (91).

As for mitochondrial autophagy (mitophagy) evaluation, Mito-Keima and Lamp1-YFP fluorescence-based method was applied (92). Briefly, aged and young (18 and 6 months old, respectively) mice were injected with AAV-Mito-Keima and AAV9-Lamp1-YFP. One week later, mice were supplemented with or without 3 mM spermidine in their drinking water for 3 weeks. Confocal microscopy was then used to analyze Mito-Keima green (457 nm), Mito-Keima red (561 nm), and Lamp1-YFP fluorescence in the harvested hearts. Mitophagy was denoted by ratiometric images of red to green Mito-Keima (561 nm/457 nm), meanwhile merged Mito-Keima red (561 nm) and Lamp1-YFP images confirmed co-localization of lysosomes with mitochondria at the so-called '*Mito-Keima positive areas'*. These experiments were done by Dr. Mingming Tong (*Rutgers New Jersey Medical School, Rutgers University, New Jersey, USA*).

2.13. Analysis of titin isoforms and phosphorylation

Titin isoforms in cardiac homogenates were separated using SDS–PAGE (1.8%). Different bands were visualized by Coomassie blue staining prior to densitometry-based quantification as described (93). Total and site-specific (phospho-S4080) phosphorylation of titin were probed using anti-phosphoserine/threonine antibodies (from Biotrend Chemicals, Cologne, Germany or custom-made against LFS(PO3H2)EWLRNI; Eurogentec, Brussels, Belgium) and horseradish peroxidase-conjugated IgG (Acris Antibodies, Herford, Germany) served as a secondary antibody. Enhanced Chemoluminescence Western blot detection kit (GE Healthcare, Little Chalfront, UK) amplified the signals, which was visualized by LAS-4000 Image Reader (Fuji Science Imaging Systems) and quantified by Quantity One 1-D Analysis software (Bio-Rad Laboratories, USA). Human cardiac and diaphragmatic extracts were used as *standards* (*i.e.*, size markers for N2B/N2BA and N2A isoforms, respectively). Generally, equally distributed samples from different groups (at least 2 samples per group) were analyzed on the same blot. These experiments were done by Marion von Frieling-Salewsky *(University of Münster, Germany).*

2.14. Cardiomyocyte ultra-structural analysis

Electron microscopy (EM) and design-based stereology techniques were applied to study the ultra-structure of mouse cardiomyocytes (94). Briefly, whole hearts were

fixed by aortic cannulation and coronary artery perfusion with 4% formaldehyde. After 24 hours of submerging the hearts in the same fixative, different cardiac chambers were separated, maintaining intact left ventricle (including the posterior wall and interventricular septum; LV), which was subsequently weighed and randomly sampled for EM. LV samples were incubated again in a fixative comprising 1.5% paraformaldehyde and 1.5% glutaraldehyde in 0.15 M HEPES buffer. Samples were then treated with 1% osmium tetroxide, stained with uranyl acetate (50% saturation, in water) and finally embedded in epoxy resin after serial dehydrating acetone concentrations. Samples were then cut into ultra-thin slides, which were analysed by a Morgagni transmission electron microscope (FEI, Eindhoven, Netherlands) following additional lead citrate and uranyl acetate staining. Morphometric test fields were assessed according to a systematic uniform scheme for random sampling using a camera (95). Volume estimation of a specific structure (*e.g.*, mitochondria, myofibrils, nucleus, interstitium or a whole cardiomyocyte) was performed using projected point grids on to the field. According to the ratio between the amount of points hitting the structure of interested *versus* those hitting the reference volume, the volume could be calculated by multiplying this ratio with the known reference volume, taking in consideration muscle tissue density (defined as 1.06 g/cm^3). These experiments were done by Dr. Julia Schipke (*Institute of Functional and Applied Anatomy, Hannover Medical School, Hannover, Germany*).

2.15. Human myocardial samples

Human donor hearts were collected according to the University regulations on human tissue handling and were approved by its ethics review committee. All hearts were explanted either before cardiac transplantation surgery in case of heart failure with reduced ejection fraction patients (HFrEF), or post-mortem together with other organs in case of non-failing and HF with preserved ejection fraction (HFpEF) donors. Upon ice-cold cardioplegia, cardiac biopsies were harvested from the left ventricular free wall, quickly frozen in liquid nitrogen and stored at -80° C for future analysis. All three groups (non-failing, HFpEF, and HFrEF) had comparable average age (±SEM); (58±3.5, 59±2.5 and 53±3.9 years, respectively; P=0.462) and gender distribution; (5 females and 6 males, 3 females and 7 males, 3 females and 6m, respectively). HFrEF patients suffered from non-ischemic dilated cardiomyopathy

with severe contractile dysfunction (EF<40%) and underwent cardiac transplantation surgery. HFpEF patients had echocardiographic evidence of diastolic dysfunction (E/e'>13) or clear structural remodelling in the form of hypertrophy or dilated left atrium, with elevated NT-proBNP levels (>125 pg/ml), but preserved EF (>50%). As for the non-failing hearts, they belonged to deceased donors who had normal NT-proBNP levels and no clinical history of any cardiac abnormalities.

2.16. Statistical analysis of preclinical data

Normally-distributed data are presented as mean ± SEM or SD, as indicated. Data that are non-normally distributed are presented as median [interquartile range]. As for the graphical representation, various kinds of charts were used, including bar charts with error bars, dot plots with mean lines or box plots showing mean, median, interquartile range, minimum and maximum within 1.5-fold IQR (whiskers) and outliers (more or less than 1.5-fold IQR; separately-plotted). Sample size is always indicated within the figure legend and represents biological replicates (*i.e.*, independent animals).

Paired or independent Student's *t*-test was used to compare two groups, whereas multiple groups were compared with one-way or factorial analysis of variance (ANOVA) with Tukey's post-hoc, as appropriate. In case of repeated measures (or mixed) factorial ANOVA, Greenhouse-Geisser correction was applied if sphericity was violated (as tested by Mauchly's test). Whenever factorial ANOVAs showed a significant main factor or significant interaction between different factors, they were followed by pairwise comparisons of different levels of each factor (*i.e.*, simple main effects) – these were corrected by Bonferroni if more than 2 groups were being compared. Multi-beat load-independent hemodynamic measures (*e.g.*, end-diastolic and end-systolic pressure-volume relationships) were analyzed applying analysis of covariance, whereby myocardial chamber stiffness constant (β) and end-systolic elastance (Ees) were compared including other parameters in the fitting equation (*i.e.*, α or V_0 when β or Ees were compared, respectively) as co-variates to correct for their potential influence.(86) Of note, ANCOVA was conducted after confirming homogeneity of regression slopes between included groups.

Generally, normality of data residuals distribution was checked by Shapiro-Wilk's test and homogeneity of variances was confirmed by Levene's test. If these

assumptions were not met, data were either transformed (*e.g*, log transformed) or compared using nonparametric statistics as follows: (i) if data were non-normally distributed: after confirming ranks variances equality (by non-parametric Levene's test), Kruskal-Wallis was used to compare the data and following pairwise multiple comparisons were done by Mann-Whitney *U* test adjusting the significance level (α) according to the number of multiple comparisons (*n*) to α=0.05/*n*, to control for inflated family-wise error rate. (ii) in case of homogeneity of variance violation, we used Welch's *t*-test (to compare two groups) or Welch's test followed by *Games-Howell* post-hoc (for multiple groups comparison).
Inflammatory cytokines statistical analysis is detailed in Methods section 2.10. Generally, statistics were carried out using IBM SPSS statistics software (Version 23) and significance was always set to two-sided type-I error (α) of 0.05.

2.17. Human epidemiological data analysis

Subjects: human data included in our study belong to the participants of the Bruneck cohort, which is a prospective, population-based survey on the epidemiology and pathogenesis of atherosclerosis and cardiovascular disease (96). Patient recruitment and baseline examination was done in 1990, including exclusively the inhabitants of Bruneck, Italy (*n*=829). Follow-up was done in 5-year intervals *(i.e.,* on 1995, 2000, 2005 and 2010) and was obtained from almost all participants. This was only feasible because a single local hospital received all medical referrals and due to the generally very low mobility rates in the region. A total of 345 mortalities were encountered throughout the study period (until 2010).

Dietary intake: ascertainment of nutrients intake was done by a dietitian employing a 118-item food frequency questionnaire (FFQ), which was based on gold standard FFQ (97), but taking into consideration the particularities of the survey region. Participants needed to describe their daily intake of a specific food on a scale (ranging from 'never' to 'more than six times') of common units or portions. When needed, food pictures were provided to the participants or their nurses, such as in cases of aphasia. In addition, a whole section in the survey was dedicated to foods that were not included in the questionnaire and were consumed at least once per week. Complex recipes were broken down to their basic components. Dietary spermidine intake was calculated based on a compilation of published nutrient data

(Table 1). Of note, the correlation of spermidine intake between different visits was at 0.54, which supports stability of food intake over the study period. This validates that surveyed intake well represents long-term food intakes. Throughout the study, a total of 2450 diet records were collected from the 829 participants, of these 815 were collected in 1995 and 484 in 2010.

Clinical outcomes: as for mortality, data on timing and cause of death were available for every participant who succumbed throughout the study. This was accessible thanks to thorough medical records and even autopsy data in non-expected mortality cases. Heart failure-related mortality was defined according to ICD-10 diagnosis codes I50.x, I13.0, I13.2, I11.00, I11.01 (hypertensive heart disease with (congestive) heart failure, with and without hypertensive crisis), and I97.1 (heart failure due to presence of cardiac prosthesis or following cardiac surgery). As for heart failure diagnosis, Framingham diagnostic criteria (*i.e.*, presence of at least 2 major criteria or 1 major criterion combined with 2 minor criteria) were adopted (98). Finally, incident cardiovascular disease (CVD) comprised acute coronary artery disease (*i.e.*, nonfatal myocardial infarction [MI], new-onset unstable angina, and acute coronary interventions) and vascular death (due to MI, ischemic stroke, or sudden cardiac death).

Statistical analysis: dietary intake at a given follow-up visit was calculated as the cumulative average of the records obtained during the respective and preceding visits. This provides a more robust representation of long-term dietary habits and also reduces within-subject variance. Spermidine intake was transformed (log function) and corrected for total caloric intake by the residual method (99), whereby a log-log simple linear model was applied. Spermidine intake was then stratified into units of standard deviation (SD) variance, in a way that the risk of a given outcome was tested for every SD unit increment in spermidine dietary intake. Cox or Fine and Gray proportional hazard models were used to analyse time-to-event outcomes (*i.e.*, incident CVD and mortality, respectively) during 15 years of follow-up (1995 until 2010) employing 1995 dietary record of spermidine intake as baseline exposure. Blood pressure and overt heart failure were examined cross-sectionally using cumulative average of spermidine intake in a mixed linear model or logistic regression, respectively. Generally, the effects were tested in single- and multi-

variate models, adjusting for potential confounding factors, such as age, sex, total caloric intake, diabetes mellitus, diastolic pressure, current smoker or alcohol consumption, as indicated. Normality of residuals distribution was confirmed in quantile-quantile plots. Two-sided type-1 error (α) at 0.05 was considered significant. Data were analysed in R 3.1.1.

The results obtained from the Bruneck study in this thesis were generated by Dr. Stefan Kiechl (*Department of Neurology, Medical University of Innsbruck, Austria*).

Table 1. Spermidine content in different foods.

Food Category	Spermidine content (nmoL/g)
1. Milk and Dairy Products	
Full cream milk	2
Skim milk	3
Yoghurt	2
Curd	0
Cheese	47
2. Fruits	
Grapes	87
Apples	193
Peaches or apricots	42
Oranges	35
Citrons	34
Water melon	8
Sugar melon	81
Strawberries	41
Blackberries	35
Prune (dried)	11
Pineapple	30
Mango	199
Cherry	19
Banana	60
3. Vegetables	
Tomato	20

Tomato sauce	58
Cucumber	44
Salad	150
Cabbage	82
Broccoli	309
Cauliflower	207
Carrots	46
Turnips	92
Peas	449
Kidney beans	134
Lentils	60
Spinach, uncooked	185
Spinach, cooked	50
Celeriac	184
Garlic	181
Mushrooms	651
Wheat germs	2440
4. Protein	
Eggs	0
Poultry	37
Beef or veal	45
Pork	22
Game	106
Lamb, mutton and fawn-meat	34
Sausages (mortadella, wiener, chorizo)	26
Innards (chicken, pork, beef)	218
Tuna	23
Freshwater fish	54
Saltwater fish	25
Soybean	854
Nuts	252
5. Sweets	
Chocolate	0
Confection of pastry	0
Ice cream	0

Goodies and candies	0
Honey	0
Cookies	0
6. Carbohydrate	
White bread/ Pizza dough	35
Whole-grain bread	129
Noodles	49
Dumplings	0
Cereals mixed	167
Potatoes	97
Rice	16
Polenta	298
Omelet	48
Chips	171
Potato chips	259
7. Butter, Oils and Cooking Fats	
Butter	0
Lard	0
Margarine	0
Olive oil	0
Seed oil	0
Mayonnaise	0
8. Drinks	
Cola	0
Lemonade	0
Apple juice	0
Lemon juice	0
Orange juice	13
Mineral water	0
Red wine	2
White wine	0
Beer	3
Liquor, Schnapps	0
Coffee	0
Black tea	4

Green tea	23
Tea, general	1

Zero values refer to spermidine concentrations below detection limit. This table is adapted from Eisenberg and Abdellatif et. al. Nature Medicine, 2016; Ref. (100) *with permission from the publisher (Springer Nature).*

3. Spermidine and Cardiovascular Aging

(RESULTS & DISCUSSION)

The results presented in this chapter have been published in Eisenberg and Abdellatif et. al. Nature Medicine, 2016; Ref. (100) *and were reproduced with permission from the publisher (Springer Nature).*

3.1. Introduction to cardiovascular aging

Through a far-reaching circulatory tree, the cardiovascular system is responsible for the delivery of oxygen and nutrients to virtually every cell in the body and the disposal of their harmful waste. Given such fundamental role, a satisfactory performance of the circulatory system is a major determinant of whole organismal health. That being said, aging insinuates detrimental structural and functional alterations to the heart and vasculature, which undermine their homeostasis and impair their functionality. Hence, aging is the main risk factor for several life-threatening cardiovascular diseases, such as hypertension, atherosclerosis, ischemic heart disease, stroke and heart failure.

3.1.1. Structural and functional decline of the aged heart

The heart of an aged individual tends to be stiffer than it used to be at a younger age and this is largely due to a slow progressive increase in fibrosis (101,102) and wall thickening (103,104) during the course of age even in absence of comorbidities (Fig. 3). Although such remodelling helps the heart preserve its pumping ability in face of aged rigid vessels, it does cost dearly. Specifically, cardiac stiffening causes a characteristic age-related functional decline in the form of diastolic dysfunction. This, in turn, leads to impaired filling properties where most of the filling has to be actively carried out by the atria, unlike the normal setting where most of the work is passively carried out during ventricular diastole. As a result, the atria become enlarged and remodelled. Furthermore, cardiac reserve capacity gets impaired, which manifest as reduced maximal heart rate, ejection fraction and cardiac output (103,105,106). Altogether, this culminates in compromised effort tolerance – due to limited oxygen consumption capacity – and, thus, frailty and diminished quality of life in late-life (107,108).

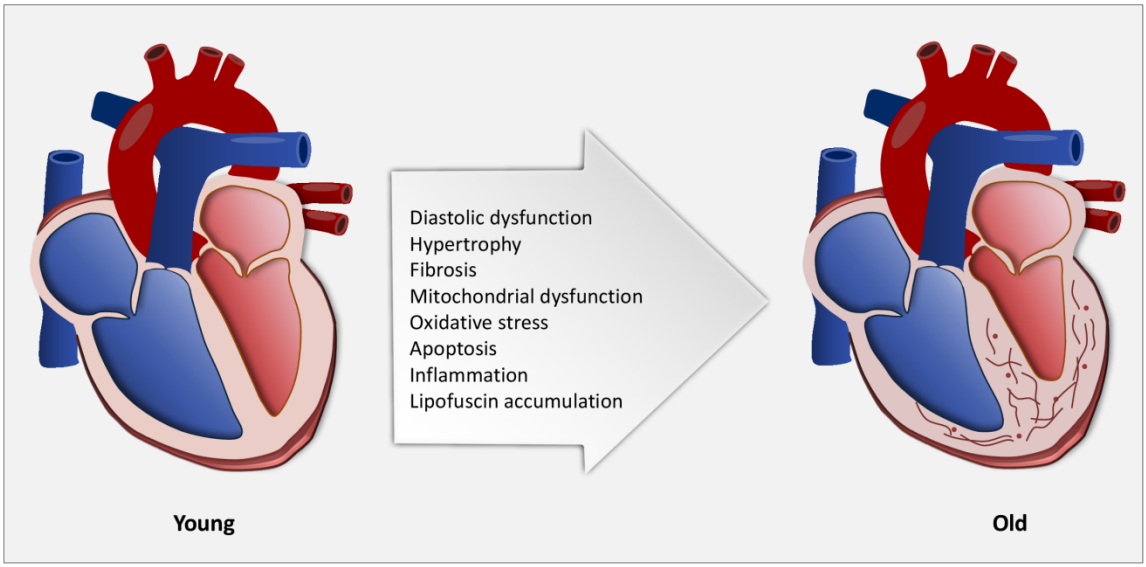

Figure 3. Cardiac signs of aging.

Shown are the detrimental alterations and ensuing functional decline of the heart upon aging. Note in the right panel how the aged heart exhibits atrial remodelling and ventricular hypertrophy, fibrosis, and apoptosis. *Adapted from Abdellatif et. al. Circulation Research, 2018; Ref.* (70) *with permission from the publisher (Wolters Kluwer).*

3.1.2 Structural and functional decline of the aged vessels

Given their elastic structure, the aorta and other large conduit arteries expand and recoil with every heartbeat. This allows for sufficient blood delivery to distal organs throughout the cardiac cycle (*i.e.*, during both systole and diastole) meanwhile dampening the pulse wave to the lowest possible degree. However, with aging large elastic arteries become stiffer (109), mainly due to increased elastin fractures and collagen deposition (110) (Fig. 4). In addition, aging is associated with vascular endothelial dysfunction and reduced endothelial NO synthase (eNOS) expression; both of which lead to impaired nitric oxide (NO)-dependent vasorelaxation (111). Aged endothelial cells also have compromised proliferation capacity and disrupted barriers, allowing vascular smooth muscle cell migration to sub-endothelial compartments, which in turn foster extracellular matrix deposition and intimal thickening (112). Therefore, the aged, now less elastic, vessels fail to provide sufficient buffer against age-related increases in pulse wave, which promote peripheral tissue damage, especially at highly-perfused organs such as the brain and kidneys.

3.1.3 Ventricular-vascular uncoupling in aging

Age-related arterial remodelling accelerates concurrent cardiac alterations by imposing additional afterload (*i.e.,* resistance), a vicious cycle that progressively aggravates age-related cardiovascular decline in the form of a mismatch between ventricular and vascular counterparts of the cardiovascular system. A fundamental prerequisite for normal cardiovascular performance is efficient coordination or coupling between the ventricular and arterial systems. Age-related ventricular-vascular uncoupling is typically exposed during exercise (or similar stress) when an acute rise in vascular stiffness cannot be further compensated for by the aged heart, which has already exhausted its reserve (107). Worth mentioning, such uncoupling between the heart and vessels underlies a major part of the compromised functional capacity of the whole cardiovascular system in the elderly.

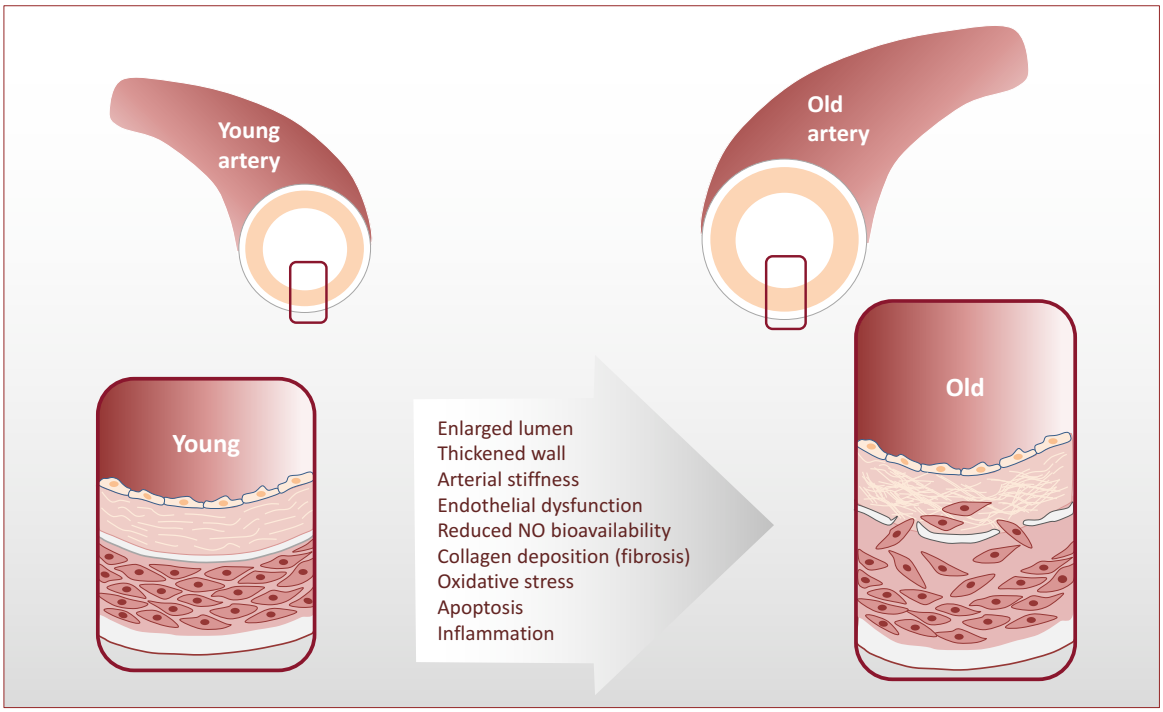

Figure 4. Vascular signs of aging.

Shown are the detrimental processes involved in late-life structural and functional decline of vessels. Note in the right panel how aged vessels show subendothelial migration of vascular smooth muscle cells, which in turn stimulate extracellular matrix disarray in the form of higher elastin fractures and collagen deposition. All together lead to intimal thickening and vascular stiffening. Abbreviations: NO, nitric oxide. *Adapted from Abdellatif et. al. Circulation Research, 2018; Ref.* (70) *with permission from the publisher (Wolters Kluwer).*

3.1.4 Molecular mechanisms of cardiovascular aging

In the aged heart, cardiomyocytes display mitochondrial inefficiency and, thus, reduced ATP production. In addition to the functional deficit, aged cardiac mitochondria are structurally impaired as they are typically more swollen and display less cristae and a generally deformed matrix (113). In addition, they generate higher levels of reactive oxygen species (ROS), which can instigate cardiomyocyte death (114). Therefore, aged cardiomyocytes do not only suffer from insufficient energy supply, but they also have to deal with an exceptional burden of oxidative stress. This is particularly challenging for cardiomyocytes as they predominantly reside in a post-mitotic state and so defective mitochondria and other toxic cellular cargo cannot be diluted into daughter cells (115). When added to the fact that aging is associated with a global decline in autophagy – the alternative defensive mechanism by which cardiomyocytes deal with toxic cargo (82,116), this makes aging especially challenging for the heart. Similarly, aged cardiomyocytes accumulate large amounts of lipofuscin (117), which has been reported to induce cell death and aggravate mitochondrial abnormalities (118). Other mechanisms that have been suggested to contribute to cardiac aging include; deranged calcium homeostasis (119), sodium mishandling (120), exaggerated apoptosis (121), activation of sterile (low-grade) inflammatory processes (122,123) and telomere dysfunction (124).

As for age-related vascular remodelling, it is also believed that increased oxidative stress is a major culprit (125). On one hand, increased ROS consumes NO to generate peroxynitrite ($ONOO^-$) (126), thus limiting NO bioavailability and NO-dependent vasorelaxation. On the other hand, ROS jeopardize mitochondrial DNA stability (127) and activate NF-κB, which in turn, stimulates pro-inflammatory cytokine secretion causing vascular inflammation (123).

3.1.5. Murine models of human cardiovascular aging

Many experimental studies on cardiac aging typically employ aged rodents as models because aged mice and rats exhibit an aged cardiac phenotype that closely mimics humans (128). Mice, for instance, experience a progressive increase in myocardial mass and fibrosis with aging and show clear evidence of diastolic dysfunction similar to humans (128). Aged mice also exhibit vascular stiffness and

endothelial dysfunction (129). Consequently, cardiovascular death accounts for a major proportion of overall mortality in mice (130). From a mechanistic point of view, recognized subcellular changes in aged cardiomyocytes (see Chapter 1) have been either discovered or, at least, confirmed in aged murine hearts. Taken together, these characteristics make mice a very suitable model to study human cardiac aging.

That said, aged mice do not show common cardiovascular disease risk factors of humans, such as hypertension and diabetes mellitus. While this might sound like a disadvantage in the sense that mice do not fully recapitulate the clinical context where aged individuals suffer from multiple comorbidities in conjunction with aging, it makes mice a unique preclinical model to examine the specific mechanisms and potential therapies for cardiac aging itself without the influence of any confounding factors, which could indirectly affect the pace of aging. To this end, we employed aged mice to test whether autophagy induction by spermidine can attenuate, delay or maybe even prevent cardiac aging.

3.2. Results: Cardiac anti-aging effects of spermidine

18-month-old C57BL6 mice were supplemented with 3 mM spermidine in their drinking water for 5-6 months (Fig. 5A) and were then subjected to a comprehensive cardiac investigation at the organismal, cellular and molecular levels.

3.2.1. Spermidine attenuates cardiac signs of aging in vivo

At the age of 24 months, mice are considered to be as old as a 70-year-old human. By then, they show all the cardinal signs of cardiac aging. Indeed, when compared to young (5-month-old) mice, aged (23- to 24-month-old) mice showed hypertrophy, increased myocardial stiffness, delayed relaxation and lower slope of end-systolic pressure-volume relationship, a load-independent contractility index, despite having a normal ejection fraction (Supplementary Tables 1 and 2; Fig. 7B). Nevertheless, spermidine supplementation attenuated many of these characteristic age-related abnormalities. Firstly, increased circulating spermidine levels upon spermidine feeding was associated with a significant reduction in echocardiographic measures of myocardial hypertrophy, including myocardial mass index and posterior wall thickness (Fig. 5B and C and Supplementary Table 1), to levels matching 18-month-old mice (*i.e.,* the age at which spermidine supplementation was initiated).

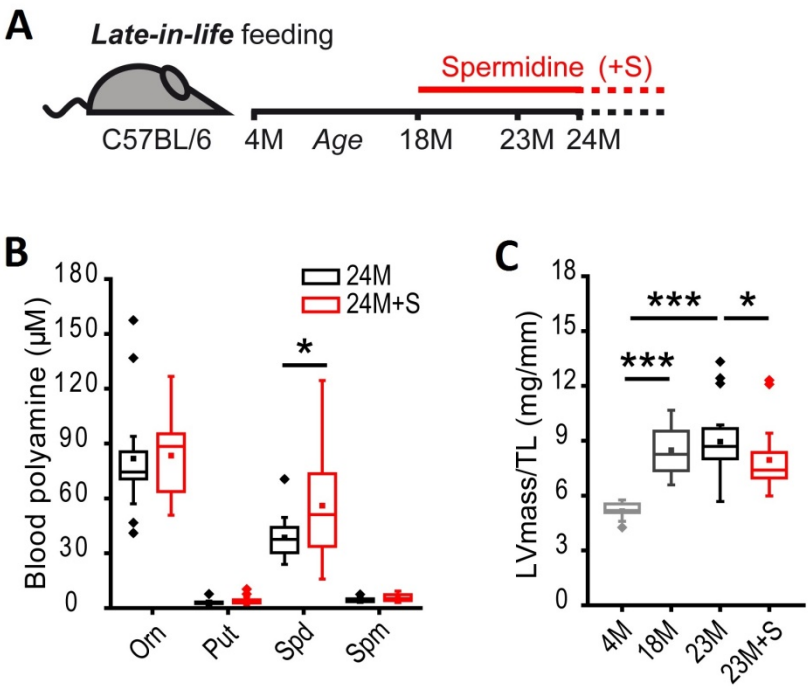

Figure 5. Late-life spermidine feeding attenuates age-related hypertrophy

(A) Schematic presentation of spermidine feeding regimen to aged 18 months old C57BL6 mice.

(B) Circulating polyamines in whole blood obtained from spermidine-fed (24M+S) and control (24M) aged mice (*n*=18 and 15, respectively).

(C) Echocardiography-measured left ventricular mass (LVmass) to tibia length (TL) ratio, a measure of hypertrophy (*n*=10, 14 and 20 for 4 months, 18 months, and 23 months (±S) old mice, respectively). ***P< 0.001, **P < 0.01, *P < 0.05, by Welch's *t*-test in (B) and by analysis of variance (ANOVA) with Tukey post-hoc test in (C). Abbreviations: Orn, ornithine; Put, putrescine; Spd, spermidine; Spm or S, spermine; M, month.

Secondly, spermidine attenuated age-related diastolic impairment – the hallmark of cardiac aging as evaluated *in vivo* by invasive intra-cardiac hemodynamics. Specifically, spermidine reduced end-diastolic pressures, myocardial passive stiffness constant and shifted the end-diastolic pressure-volume relationship downwards (Fig. 6A-C and Fig. 7A). Spermidine-fed mice also tended to have a faster relaxation than control aged mice as evaluated by ventricular pressure decay constant τ (Supplementary Table 2). In line with these findings, unlike aged controls, spermidine-fed mice were protected from lung congestion as measured by post-mortem lung weight to body weight ratio (Supplementary Table 3). Thirdly, spermidine restored ventricular-vascular coupling in aged mice to levels comparable to young mice, denoting improved coordination between the cardiac and vascular systems, thus, improving overall cardiovascular efficiency and performance (Fig. 6D).

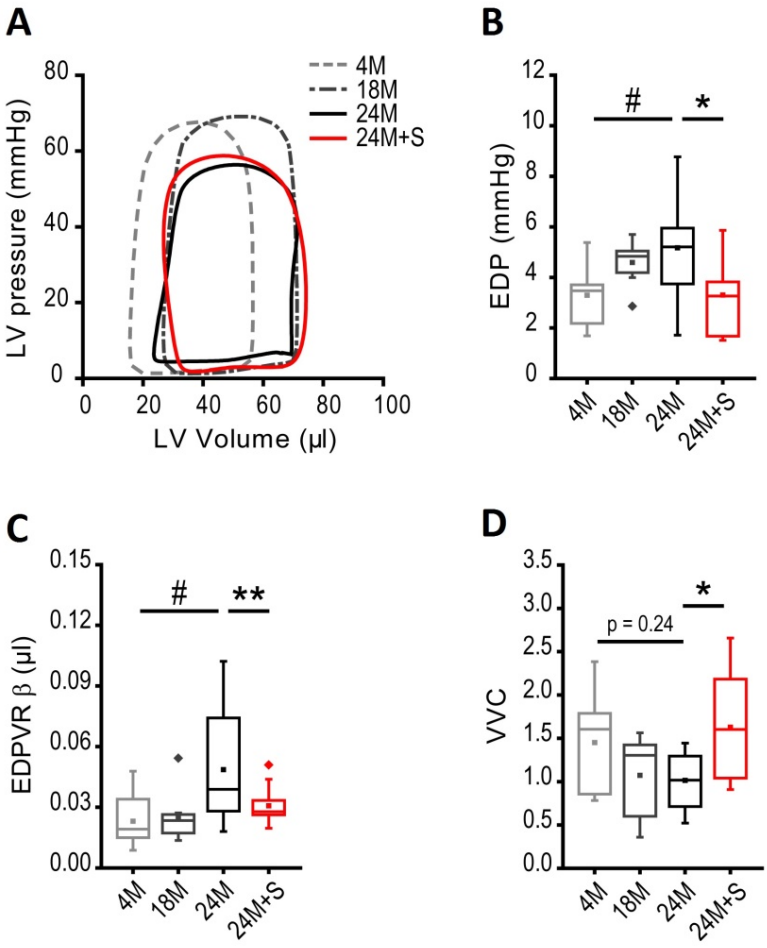

Figure 6. Spermidine improves both diastolic dysfunction and ventricular vascular coupling in aged wild-type mice

(A) Representative left ventricular (LV) pressure-volume (PV) loops.

(B) End-diastolic pressure (EDP).

(C) End-diastolic pressure-volume relationship constant (EDPVR β), a measure of myocardial stiffness.

(D) Ventricular-vascular coupling (VVC), a measure of cardiac- vascular interaction and overall system efficiency. (*n*=8-10 mice/ group).

$^{**}P < 0.01$, $^{*}P < 0.05$, $^{\#}P < 0.06$ by analysis of variance (ANOVA) with Tukey post-hoc test in (B and D) or by analysis of covariance (ANCOVA) with Bonferroni post-hoc test in (C). *Abbreviations*: M, month; S, spermidine-treated.

Collectively, spermidine delays structural and functional aspects of cardiac aging at the organ level and these benefits seem to be cardiac-specific as spermidine-fed mice did not differ from aged controls in afterload as measured by arterial elastance, end-systolic pressure (Supplementary Table 2 and Fig. 7B).

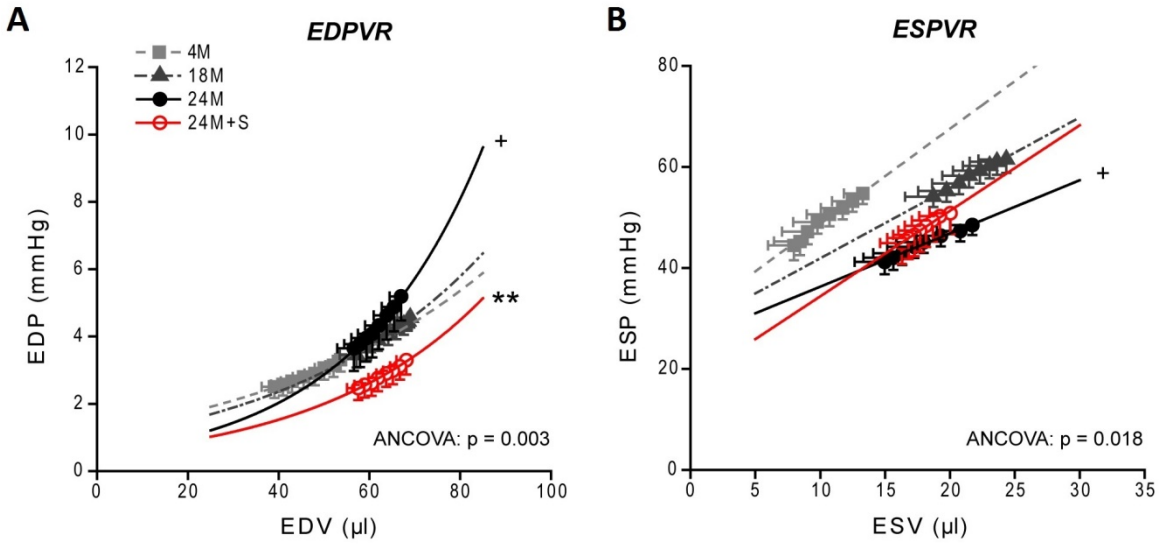

Figure 7. Spermidine improves left ventricular passive stiffness in aged mice

(A) Exponential left ventricular end-diastolic pressure-volume relationship (EDPVR). *Note the downward shift, indicating reduced stiffness, in spermidine-fed old mice (24M+S) as compared to aged controls (24M).*

(B) Linear left ventricular end-systolic pressure-volume relationship (ESPVR).

(*n*=8-10 mice/group). $^{**}P < 0.01$ *vs.* 24M control, $^{+}P < 0.05$ *vs.* 4M, $^{\#}P < 0.06$ by analysis of covariance (ANCOVA) with Bonferroni post-hoc test.

3.2.2. Spermidine improves aged cardiomyocytes composition

To elucidate the underlying mechanisms of spermidine effects on cardiac aging, we examined the structure and function of aged cardiomyocytes at the cellular, sub-cellular and molecular levels. Using design-based stereology analysis, we found aged mice to have reduced relative cardiomyocyte content (*i.e.*, organelle-to-cardiomyocyte size ratio) of myofibrils (contractile apparatus) and mitochondria (the cellular power house) and, thus, increased organelle-free sarcoplasmic volume compared to young mice (Fig. 8A-B). Contrarily, cardiomyocytes of aged spermidine-fed mice had similar composition to young mice as denoted by restored myofibrillar and mitochondrial relative volumes (Fig. 8A-B). In fact, not only relative mitochondrial volume, but also the absolute volume was higher in spermidine-fed mice compared to aged controls (Fig. 8C).

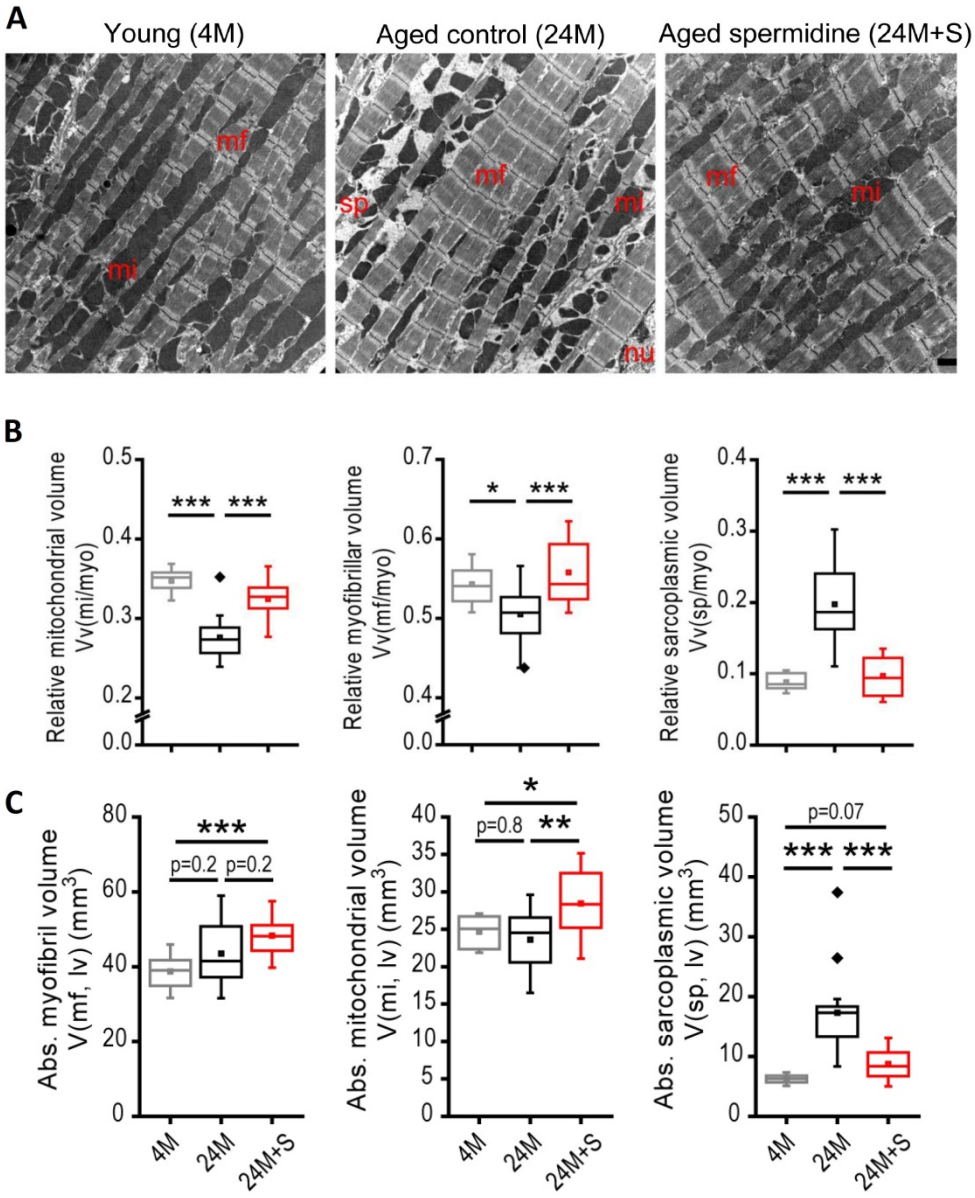

Figure 8. Spermidine improves the (ultra)structure of aged cardiomyocytes

(A) Representative transmission electron micrographs. Scale bar, 2 µm.

(B) Relative volume of left ventricular cardiomyocyte mitochondria Vv(mi/myo), myofibrils Vv(mf/myo) and organelle-free sarcoplasm Vv(sp/myo) normalized to cardiomyocyte volume.

(C) Absolute myofibril volume, V(mf, lv), mitochondrial volume, V(mi, lv) and organelle-free sarcoplasmic volume, V(sp, lv) in the whole left ventricle.

In B and C, *n*=10 for 4M; *n*=15 for 24M; *n*=14 for 24M+S. ****P*< 0.001, **P*< 0.05 by analysis of variance (ANOVA) with Tukey post-hoc, Welch's test with Games–Howell post-hoc or Kruskal-Wallis with Mann-Whitney U-test.

Abbreviations: mi, mitochondria; mf, myofibrils; myo, cardiomyocyte; nu, nucleus; sp, sarcoplasm; M, month; S, spermidine.

(Cardiomyocyte ultra-structural analysis was performed by Dr. Julia Schipke, Hannover Medical School, Germany)

To test whether such increase in myocardial content of mitochondria was associated with improved function, we evaluated mitochondrial respiration in isolated cardiac mitochondria. Indeed, we found aged spermidine-fed mice to have improved mitochondrial oxygen consumption as compared to aged controls, which had impaired mitochondrial respiratory capacity when compared to young controls (Fig. 9). Therefore, spermidine feeding was not only associated with ameliorated cardiomyocyte composition, but also function.

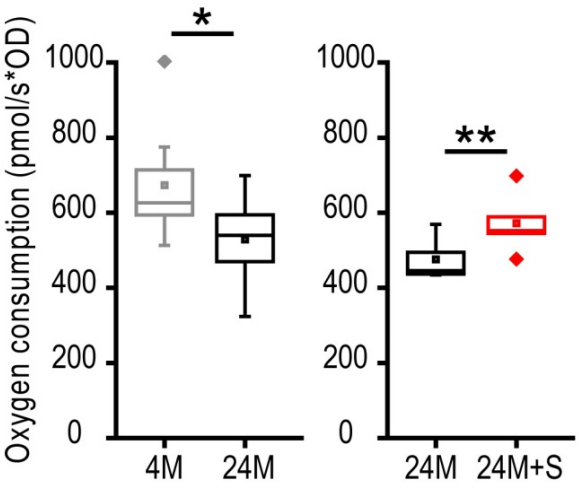

Figure 9. Spermidine restores cardiac mitochondrial function in aged wild-type mice

High-resolution respirometry-measured oxygen consumption (complex-I respiration) in isolated mitochondria from the hearts of young (4 months, 4M), control aged (24 months, 24M) and spermidine-fed aged mice (24M+S). *n*=8 mice/group (left) and *n*=5 mice/group (right). ***P*< 0.01, **P*< 0.05 by paired Student's *t*-test. (Mitochondrial respiration was assessed by Tobias Eisenberg, University of Graz, Austria)

At the molecular level, we examined the composition and post-translational modification of titin, a giant spiral-like molecule, which largely determines single cardiomyocyte passive stiffness. Although spermidine feeding was not associated with any changes in titin isoform composition as assessed by the ratio between its large (elastic) and short (stiffer) isoforms (N2BA and N2B, respectively), it increased titin phosphorylation (Fig 10). This could, at least in part, underlie the attenuated cardiac stiffness and, thus, diastolic dysfunction in aged mice fed spermidine as titin phosphorylation is known to improve cardiomyocyte elasticity. Of note, systemic inflammatory status regulates titin phosphorylation. Therefore, we evaluated markers of inflammation, where we found circulating levels of TNF-α to be significantly reduced in spermidine-fed mice, indicating attenuated sterile (subclinical) inflammation typically associated with aging (Fig. 11).

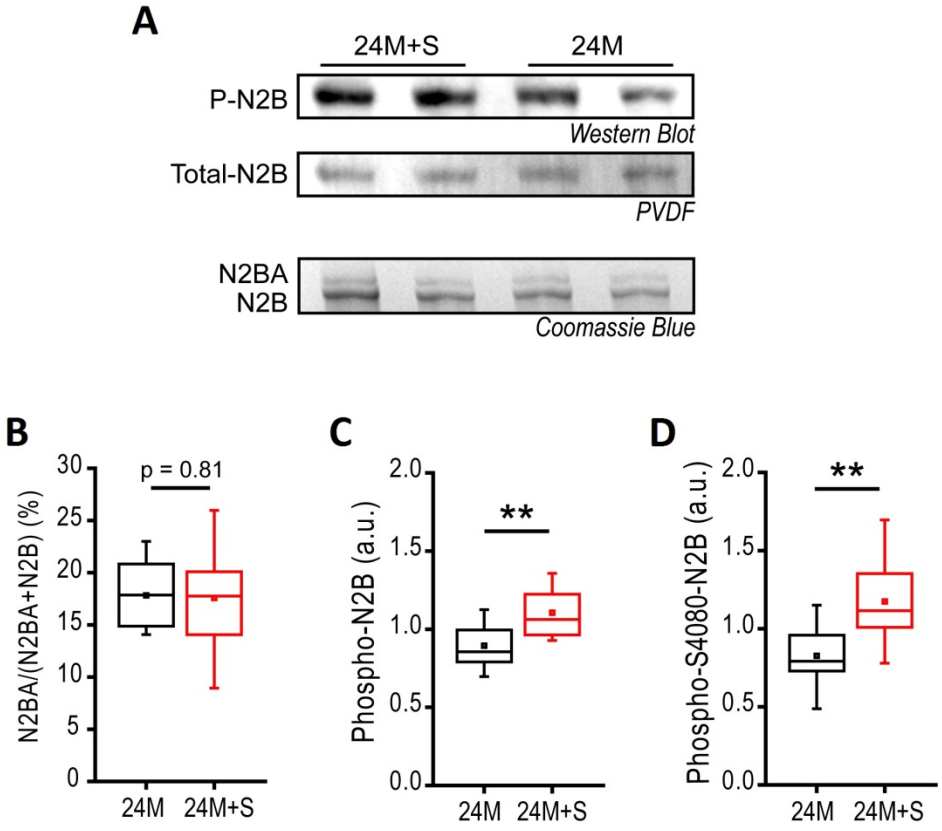

Figure 10. Spermidine supplementation enhances titin phosphorylation, known to improve cardiomyocyte elasticity, in aged wild-type mice

(A) Representative blots of titin isoforms expression and phosphorylation.

(B) The ratio between different titin isoforms expression N2BA/(N2BA+N2B).

(C) Total titin N2B isoform phosphorylation.

(D) Ser4080 (S4080)-site specific titin N2B isoform phosphorylation.

(*n*=12 mice/group). ***P*< 0.01, by independent Student's *t*-test. Abbreviations: a.u., arbitrary units; M, month; S, spermidine. *(These blots were done by Marion von Frieling-Salewsky, University of Münster, Germany)*

3.2.3. Spermidine protects the heart by stimulating autophagy

Higher abundance of spermidine in the circulation upon its oral administration (Fig. 5B) effectively increased its myocardial levels, thus, confirming successful delivery to the heart (Fig. 12A). To validate whether higher spermidine concentration in the heart boosts cardiac autophagy, we evaluated cardiac autophagic flux *in vivo*. For this purpose, 13-month-old mice were treated with spermidine for 4 weeks and markers of autophagy were blotted after injecting the mice with either saline or the protease inhibitor leupeptin.

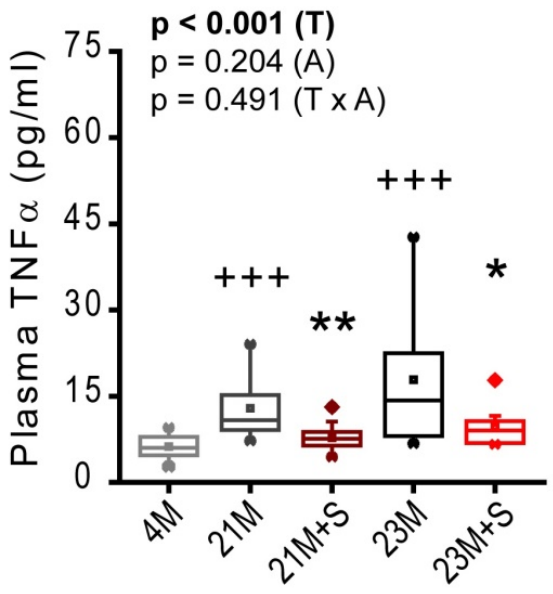

Figure 11. Spermidine attenuates age-related subclinical inflammation

Shown are the circulating levels of the pro-inflammatory cytokine TNF-α following spermidine (S) supplementation for 3 or 5 months in 21 months old (21M) and 23 months old mice (23M), respectively. (*n*=12 mice for 5M; *n*=12 mice for 21M; *n*=13 mice for 21M+S; *n*=9 mice for 23M; *n*=10 mice for 23M+S). $^{+++}P < 0.001$ by ANOVA and Tukey post-hoc test *vs.* 4M; $^{**}P < 0.01$, $^{*}P < 0.05$ by Student's *t*-test *vs.* age-matched control; Shown *P* values are for factor comparisons (T, treatment; A, age) by two-way ANOVA including 21M±S and 23M±S groups. (*These measurements were performed by Dr. Tobias Pendl, University of Graz, and then analysed by the candidate)*

Here, we found that in the absence of protease inhibition by leupeptin, *i.e.*, under baseline conditions, the amount of autophagosomes, as measured by LC3-II, was comparable in spermidine-fed and control mice. However, autophagosomal accumulation in response to protease inhibition by leupeptin was higher in spermidine-fed mice than in the controls, indicating a cardiac pro-autophagic action of spermidine *in vivo* (Fig. 12B).

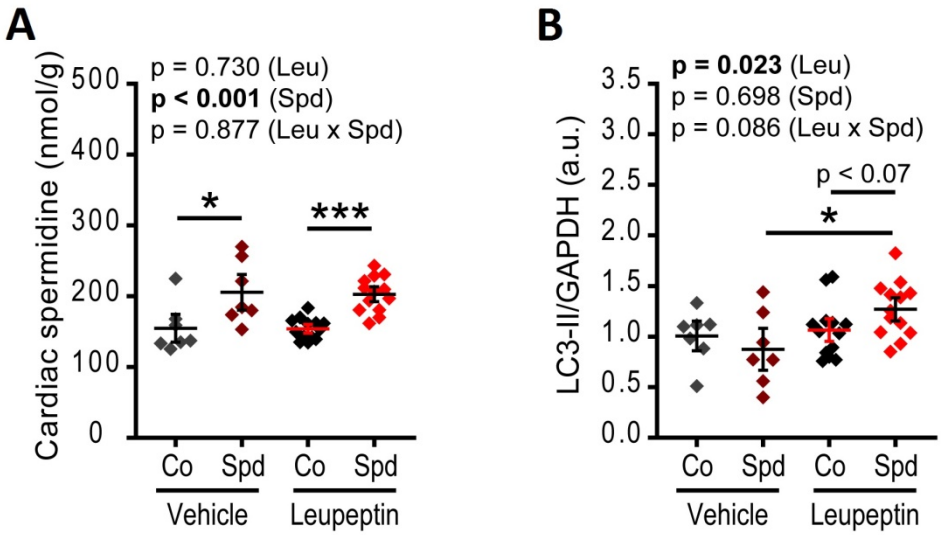

Figure 12. Spermidine supplementation activates autophagy in middle-aged mice

(A) Cardiac spermidine levels and **(B)** LC3-II/GAPDH ratio in 13-month-old mice treated with or without spermidine for 4 weeks and injected or not with the protease inhibitor leupeptin 50 min before tissue collection. Shown are the means±SEM of *n*=7 in vehicle and *n*=13 in leupeptin. Shown *P* values are two-way ANOVA factors (Spd, spermidine; Leu, leupeptin); $^{***}P<0.001$; $^{*}P<0.05$ for the pairwise comparisons. *(These measurements were done by Dr. Tobias Eisenberg, University of Graz, Austria)*

To substantiate the evidence that cardiac autophagic flux is induced by spermidine, we employed an autophagy reporter mouse strain: transgenic cardiac-specific tandem-fluorescence mRFP-GFP-LC3 mice (tf-LC3). These mice express labelled autophagosomes (in red and green; mRFP and GFP, respectively) and autolysosomes (only in red; mRFP). After 2 weeks of spermidine supplementation to young tf-LC3 mice, cardiomyocytes were harvested and subjected to confocal microscopy evaluation of autophagosomes and autolysosomes in the presence or absence of the protease inhibitor chloroquine. Here we also found spermidine-supplemented tf-LC3 mice to have higher numbers of autophagosomes and autolysosomes both at baseline and under conditions of inhibited autophagosomal turnover (Fig 13).

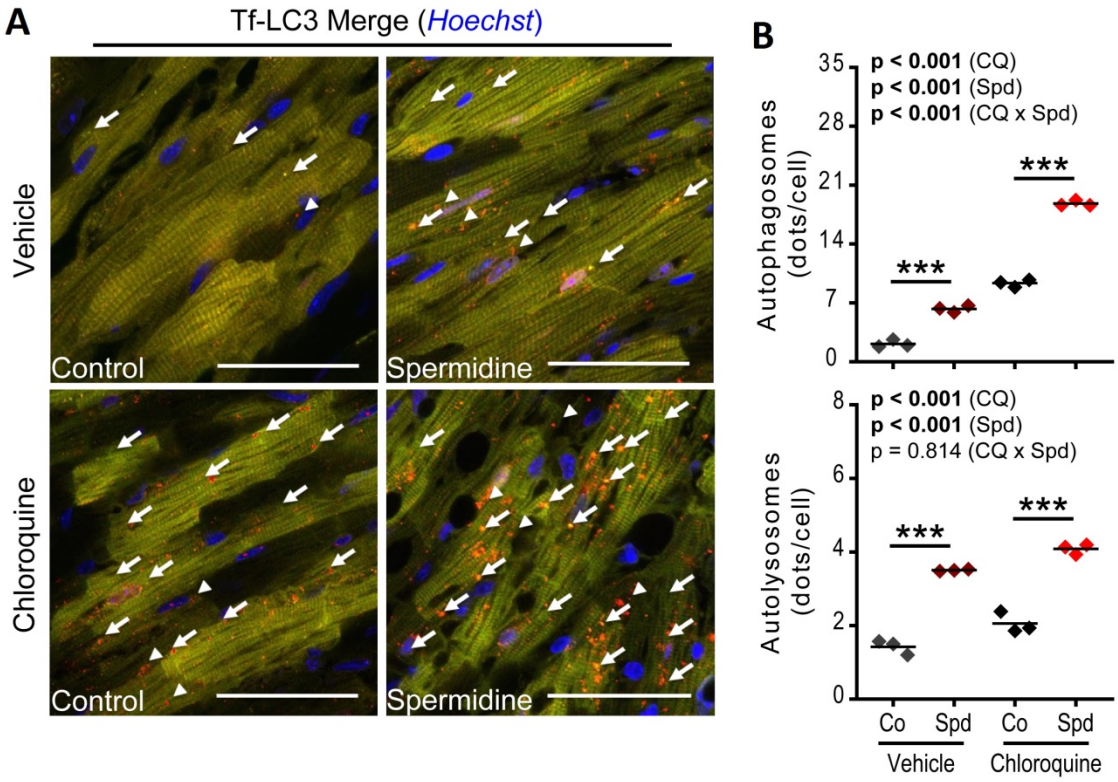

Figure 13. Spermidine boosts cardiac autophagic flux *in vivo* in transgenic mice

See next page for figure legend

(A) Representative overlays of RFP, GFP and Hoechst. Orange puncta marked by arrows indicate autophagosomes; red puncta marked by arrowheads indicate autolysosomes. Scale bars, 50 μm.

(B) Autophagosomes and autolysosomes quantified following 2 weeks of spermidine feeding to young transgenic mice in the presence or absence of the protease inhibitor chloroquine.

Shown are the means of *n*=3 mice/group. Indicated *P* values are for two-way ANOVA factors (Spd, spermidine; CQ, chloroquine); ***$P<0.001$ for the following pairwise comparisons. Abbreviations: Co, control. (*These measurements were done by Dr. Mingming Tong, Rutgers–New Jersey Medical School, Newark, USA)*

Next, we evaluated a highly-specialized form of autophagy, called mitophagy, whereby defective mitochondria are targeted for autophagic breakdown. To do so, young (3-month-old) and old (18-month-old) mice were injected with adenovirus-associated virus expressing the mitochondrial-targeted fluorescent biosensor (Mito-Keima). Mito-Keima fluorescence changes its excitation characteristics in a pH-dependent manner allowing for the detection of Keima-labelled mitochondria coming in contact with the acidic lysosomal milieu during mitophagy. Both aged and young mice had higher Mito-Keima positive area, indicative of activated mitophagy, after 2 weeks of spermidine supplementation (Fig. 14).

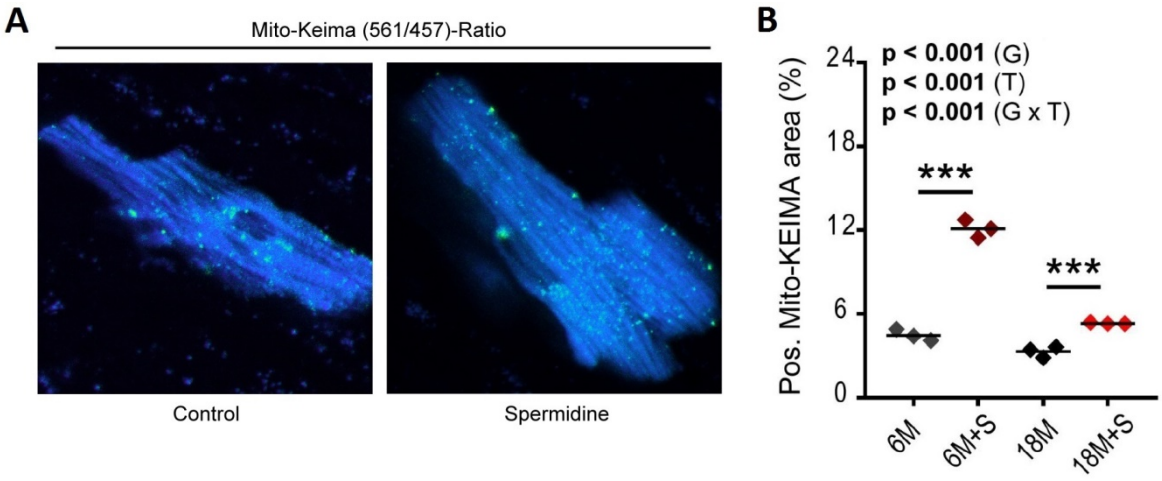

Figure 14. Spermidine induces mitophagy *in vivo* in young and aged wild-type mice

(A) Representative scans showing *Mito-Keima positive area* signals (ratiometric images; 561 nm/457 nm).

(B) Quantification of Mito-Keima positive areas following 2 weeks of spermidine supplementation or normal drinking water to young (6 months) and old (18 months) wild-type mice injected with the adenovirus-associated virus expressing Mito-Keima.

Shown are the means of *n*=3 mice/group. *P* values indicate two-way ANOVA factor comparisons (G, age; T, treatment); ***$P<0.001$ for the following pairwise comparisons. Abbreviations: S, spermidine; M, month. (*These measurements were done by Dr. Mingming Tong, Rutgers–New Jersey Medical School, Newark, USA)*

These results clearly indicate that spermidine effectively induces cardiac autophagic flux, yet still do not necessarily imply that autophagy underlies spermidine cardioprotective effects. To this end, we employed cardiomyocyte-specific autophagy-deficient mice (*Atg5*$^{fl/fl}$*MLC2a-Cre*$^{+}$; herein referred to as *Atg5*$^{-/-}$) to determine whether cardiac autophagy induction is a prerequisite for the beneficial effects of spermidine. As *Atg5*$^{-/-}$ mice suffer from reduced lifespan, it is not possible to study them at old age. Instead, we studied them at a young age when they show no apparent abnormalities under baseline conditions compared to their autophagy-competent littermates (*Atg5*$^{fl/fl}$*MLC2a-Cre*$^{-}$; herein referred to as *Atg*$^{+/+}$). *Atg5*$^{-/-}$ and *Atg*$^{+/+}$ mice were supplemented with spermidine in their drinking water soon after weaning (at 4 weeks of age) and later, at the age of 16 weeks, they underwent a comprehensive cardiac investigation (Fig. 15A). In detail, echocardiographic evaluation revealed reduced left ventricular mass index (LVmass/tibia length) in *Atg*$^{+/+}$ mice in response to spermidine treatment (Fig. 15B and Supplementary Table 4). Spermidine-fed *Atg*$^{+/+}$ mice also had superior contractility, indicated by a higher ESPVR slope, and also improved ventricular-vascular coupling upon invasive haemodynamic assessment (Fig. 16A-C, Fig. 17A and Supplementary Table 5).

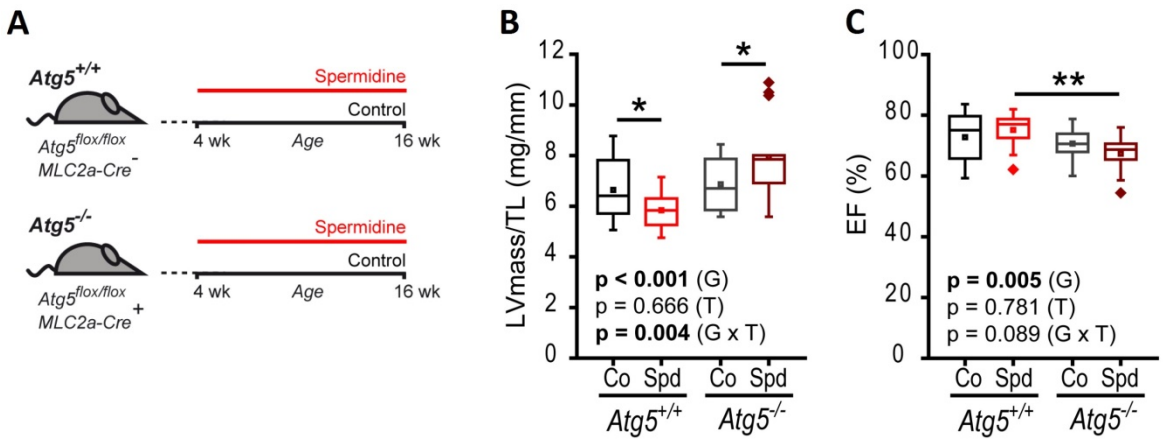

Figure 15. Spermidine deteriorates cardiac fitness in autophagy-deficient mice

(A) Spermidine feeding scheme to autophagy-deficient (*Atg5*$^{-/-}$) and autophagy-competent (*Atg*$^{+/+}$) mice.

(B) Tibia length (TL)-normalized left ventricular mass (LVmass), echocardiographic measure of hypertrophy.

(C) Ejection fraction (EF) measured by echocardiography.

(*n*=12-16/group). Shown *P* values indicate two-way ANOVA factor comparisons (G, genotype; T, treatment); ***P*<0.01, **P*<0.05 for the following pairwise comparisons. Abbreviations: Co, control; Spd, spermidine; wk, week.

Contrarily, *Atg*$^{-/-}$ mice did not benefit from spermidine feeding. In fact, spermidine had unexpected negative effects on *Atg*$^{-/-}$ mice as they showed hypertrophy and reduced ejection fraction (Fig. 15B-C and Supplementary Table 4). Furthermore, *Atg*$^{-/-}$ mice suffered from worsened diastolic function upon spermidine feeding as denoted by a higher myocardial stiffness constant and an upward shift of the EDPVR (Fig. 16D, Fig. 17B and Supplementary Table 5). Taken together, these findings support an essential role of autophagy in mediating the cardioprotective effects of spermidine.

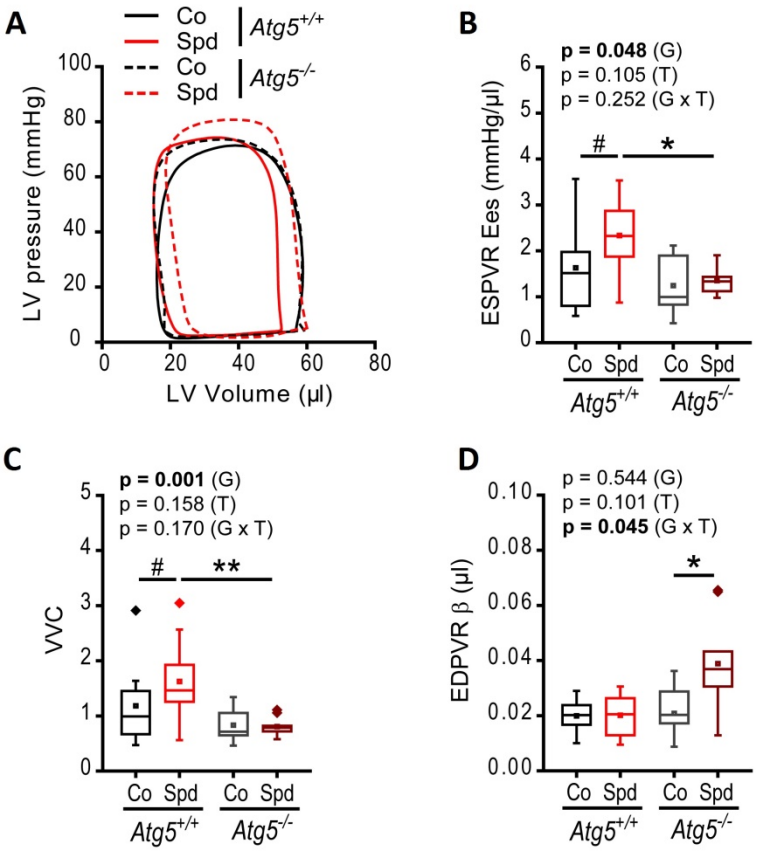

Figure 16. Spermidine improves contractility and ventricular- vascular coupling in autophagy-competent mice only.

(A) Representative left ventricular (LV) pressure-volume (PV) loops of spermidine-treated (Spd) or control (Co) cardiomyocyte-specific autophagy-deficient (*Atg5*$^{-/-}$) and autophagy-competent (*Atg*$^{+/+}$) mice. **(B)** End-systolic pressure-volume relationship slope (ESPVR Ees), a contractility measure. **(C)** Ventricular-vascular coupling (VVC), a measure of cardiovascular efficiency. **(D)** End-diastolic pressure-volume relationship constant (EDPVR β), a measure of myocardial stiffness. (*n*=9-11 mice/group). Shown *P* values indicate two-way ANOVA (ANCOVA in B and D) factor comparisons (G, genotype; T, treatment); ***P*<0.01, **P*<0.05, $^{\#}$*P*<0.06 for the following pairwise comparisons.

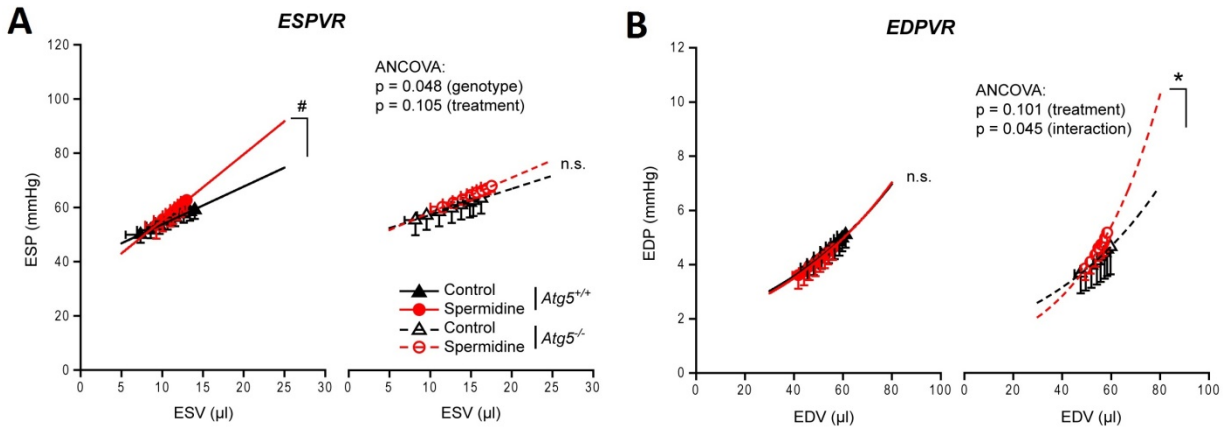

Figure 17. Intra-cardiac pressure-volume relationships of cardiomyocyte-specific autophagy-deficient mice upon spermidine feeding.

(A) Linear left ventricular end-systolic pressure-volume relationship (ESPVR). *Note the upward shift, indicating improved contractility, only in autophagy-competent mice* (*Atg5*$^{+/+}$) treated with spermidine.

(B) Exponential left ventricular end-diastolic pressure-volume relationship (EDPVR). *Note the upward shift, indicating increased stiffness, only in autophagy-deficient mice* (*Atg5*$^{-/-}$) treated with spermidine.

(*n*=9-11 mice/group). **P*<0.05, $^{\#}$*P*<0.06 *vs.* respective control by analysis of covariance (ANCOVA) and Bonferroni post-hoc test.

3.3. Discussion

In this chapter, we have shown that spermidine reduces, or occasionally prevents, cardinal signs of cardiac aging in mice, including maladaptive hypertrophy, myocardial stiffness, diastolic dysfunction and ventricular-vascular mismatch. These improvements were driven by effects at the (sub-)cellular and molecular levels, culminating in the overall rejuvenation of cardiomyocyte structure and function. We have also extended the evidence that spermidine is an effective autophagy inducer in model organisms by reporting clear *in vivo* activation of cardiac autophagy and mitophagy in mice upon oral supplementation.

In addition to cardiac autophagy, spermidine had other effects that could contribute to the resulting cardioprotection. Specifically, spermidine had an intriguing anti-inflammatory effect, which might directly, regardless of autophagy status, benefit the heart. In fact, age-related cardiac stiffening and diastolic dysfunction are largely attributed to the progressive increase in subclinical inflammation induced by aging and associated comorbidities (122). Specifically, exaggerated inflammation causes titin dephosphorylation and, thus, increases cardiomyocyte stiffness. Interestingly, spermidine upregulated titin phosphorylation, coinciding with improved myocardial elasticity and diastolic function in treated mice. Furthermore, increased titin phosphorylation may originate from a direct inhibitory effect of spermidine on serine/threonine protein phosphatase 5, which is known to dephosphorylate titin (131). That said, whether these mechanisms are completely uncoupled from autophagy is still to be confirmed in future studies.

Irrespective of these, seemingly, autophagy-independent mechanisms, we have found autophagy to be causally implicated in the cardioprotective effects of spermidine as inferred from cardiac autophagy-deficient mice, which not only failed to benefit, but instead suffered from an exacerbated cardiac phenotype in response to spermidine feeding. Hence, the findings reported in this chapter strongly support a growing body of evidence that strongly suggests an intimate relationship between the maintenance of autophagy and cardiovascular health in aging (132). Indeed, as detailed below, several genetic, nutritional and pharmaceutical interventions that boost autophagy have been shown to effectively delay signs of aging in the heart (Fig. 18 and Table 2).

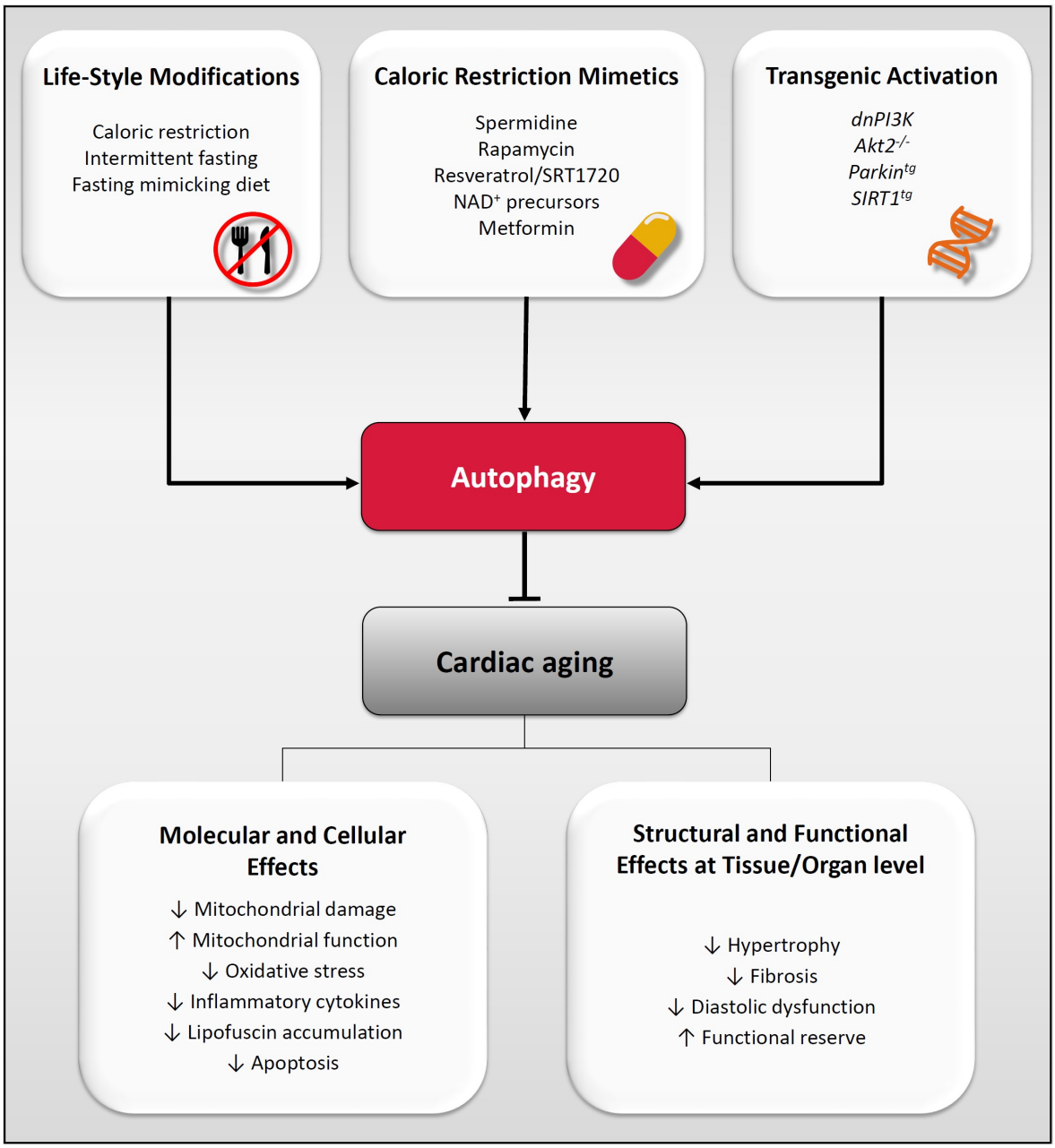

Figure 18. Autophagy-promoting interventions that delay cardiac aging.

Abbreviations: Akt2, serine/threonine-specific protein kinase 2; dnPI3K, dominant negative phosphoinositide 3-kinase; NAD^+, nicotinamide adenine dinucleotide; SIRT1, Sirtuin 1; *tg*, transgenic overexpression. *Adapted from Abdellatif et. al. Circulation Research, 2018; Ref.* (70) *with permission from the publisher (Wolters Kluwer).*

3.3.1. Dietary activation of autophagy

3.3.1.1. Caloric restriction

Caloric restriction, defined as reduced total daily intake of calories without incurring malnutrition, is considered the gold standard and by far the most powerful autophagy inducer in almost every tested organism (133,134). Experimental testing of caloric restriction, ranging from 15% to 40% reduction in caloric intake, proved efficient in attenuating almost every aspect of cardiac aging, including hypertrophic and fibrotic remodelling and both diastolic and systolic impairments (28,135,136). Caloric restriction does so by conferring multiple improvements on the cardiomyocyte itself, including enhanced mitochondrial fitness and limited oxidative stress, apoptotic cell death, telomere dysfunction and markers of senescence and inflammation (135). Interestingly, such cardioprotective effects of caloric restriction are reproducible whether it is applied throughout life (28,136) or only for a short duration at a later life stage (135,137,138). That said, the ability of caloric restriction to exert beneficial effects on the heart are limited, abolished or even reversed if caloric restriction is applied during the early thriving phases of life. In fact, young mice exposed to caloric restriction unexpectedly show restrained autophagy activation and abnormal cardiac performance (135), which further deteriorates if autophagy is additionally deactivated by AMPK deletion (139,140). This strongly suggests that induction of autophagy is essential for any cardioprotective effects of caloric restriction, which seem to be restricted to late-life periods.

3.3.1.2. Intermittent fasting

Intermittent fasting, which consists of cycles of normal food intake interrupted with periods of reduced or no feeding, is another dietary regimen known to promote autophagy and exert beneficial health and longevity effects. Among the known forms of intermittent fasting is alternate-day fasting (ADF), *i.e.*, fasting on alternate days separated by normal feeding days, and time-restricted feeding (TRF), whereby food intake is restricted to a short window (4-8 hours) during the day. While TRF has so far been shown to preserve cardiac function in aged fruit flies only (141), ADF is known to delay cardiac aging in mammals as it reduces age-related cardiac hypertrophy and fibrosis (142,143) and also extends lifespan (144) of rats. At the molecular level, ADF attenuates cardiac oxidative stress, inflammation and collagen accumulation (142,143). These effects were attributed to phosphoinositide 3-kinase

(PI3K) inhibition (142), which is known to induce autophagy (145). Although direct evidence is still lacking for causal involvement of autophagy in intermittent fasting effects on cardiac aging, it does exist for other cardiac disease settings. Specifically, the cardioprotective effects of intermittent fasting against ischemia-reperfusion injury were absent in mice deficient in autophagy due to a LAMP2 knockout mutation (146). This is highly suggestive of an essential role of autophagy in underlying the benefits of intermittent fasting on the aged heart.

3.3.1.3. Metabolic shifting diets

As extended periods of reduced caloric intake or fasting are especially challenging, other dietary regimens that do not necessarily involve food abstinence are much needed. Therefore, other regiments, which primarily focus on diet composition to induce similar metabolic shifts to caloric restriction, have been proposed. For instance, increased circulating ketone bodies observed in caloric restriction are recapitulated by the ketogenic diet, which consists of increased fat intake with slight, if any, carbohydrate consumption. Controlled intake of the ketogenic diet, whereby avoiding any increase in body weight known to occur upon *ad libitum* feeding of such high-caloric diet, was associated with extended healthy lifespan (147,148). At the heart level, cyclic ketogenic diet improved age-related cardiac phenotype, as assessed by a composite score incorporating myocardial mass, fractional shortening, heart rate and arterial pressure gradient (147). Although the specific mechanism by which ketone bodies exert their effects are still largely elusive, it is conceivable that autophagy might play a role given that a higher level of ketone bodies is known to inhibit a major negative regulator of autophagy, namely mTORC1 (147). That said, further testing is warranted to delineate the exact role played by autophagy in the context of controlled ketogenic diet. Another example for metabolism-shifting diets is the fasting mimicking diet (FMD), which features reduced caloric content from proteins and sugars while remaining high in unsaturated fats (149). Short-term administration of FMD reduces various cardiovascular disease risk factors in humans, including lower fasting glucose, body mass index and inflammatory markers as well as improved blood pressure and lipid profile (150). Similarly, FMD extends lifespan and promotes health in aged mice as denoted by reduced tumorigenesis and improved cognitive and immune functions (149). Although autophagy can be induced by FMD due to reduced total caloric

intake and inhibited IGF-1 signalling, which are associated with FMD, it is still to be elucidated whether autophagy causally contributes to the effects of this diet.

3.3.2. Genetic activation of autophagy

By genetic reinforcement of the molecular alterations observed in caloric restriction, various mouse models of activated autophagy have been generated to identify the therapeutic potential of this process. On such animal model is the cardiomyocyte-specific dominant negative PI3K (dnPI3K) mouse. These mice have a healthier aged cardiac phenotype characterized by improved cardiac functional reserve and reduced hypertrophy and fibrosis (145). Increased autophagy in dnPI3K cardiomyocytes is also associated with reduced lipofuscin deposition, oxidative stress, inflammatory and senescence biomarkers (145). Similarly, stimulation of autophagy by global abrogation of Akt2 in *Akt2*$^{-/-}$ mice enhances mitochondrial integrity, calcium handling and contractile function in aged cardiomyocytes (151). Interestingly, autophagy inhibition by 3-methyladenine abolishes these benefits which highly supports the hypothesis that autophagy underlies, at least in part, enhanced cardiac health in aged *Akt2*$^{-/-}$ mice (151).

Furthermore, cardiomyocyte-specific overexpression of the mitophagy protein Parkin leads to enhanced mitochondrial integrity and respiration in aged mice (152). Activated mitophagy in aged *Parkin*^{tg} mice is also associated with reduced senescence, inflammation and oxidative damage, which all culminate in enhanced cardiac functional reserve (152). However, it is still to be tested whether inhibition of mitophagy in these mice would abrogate the observed benefits. Similarly, it is still not clear to what extent autophagy contributes to improved cardiac structure and function observed in transgenic mice overexpressing SIRT1, known to induce autophagy. These *Sirt1*^{tg} mice also have reduced hypertrophy, fibrosis and contractile dysfunction upon aging (47,153).

Taken together, transgenic animal models of activated autophagy fairly reproduced many of the cardiac benefits associated with caloric restriction. However, for human translational purposes, pharmaceutical agents or natural substances, like spermidine, which can be orally administrated and have an acceptable safety profile hold promise as more feasible alternatives.

3.3.3. Pharmacological activation of autophagy

In line with the cardioprotective effects of spermidine feeding, other natural and pharmacological autophagy inducers showed promising results in the context of cardiac aging. One such autophagy inducer and caloric restriction mimetic is rapamycin, which activates autophagy by inhibiting mTOR. Rapamycin feeding for 3 months attenuated age-related hypertrophy and decline in cardiac function. It also limited local (at the heart) and systemic pro-inflammatory cytokines (34). More recently, it has been shown that a decline in cardiac hypertrophy is noticeable as soon as 2 weeks after the administration of rapamycin to aged mice. Within these 2 weeks rapamycin induces autophagy, which is then followed by enhanced fatty acid oxidation, energy homeostasis and mitochondrial biogenesis, but no more pro-autophagic effect (154). The lack of any additional reduction in myocardial remodelling following these first 2 weeks of autophagy activation in rapamycin-fed mice strongly suggests a direct link between autophagy and rapamycin anti-aging impact on the heart (154).

Other autophagy inducers, such as resveratrol and SRT1720, which induce autophagy by activating SIRT1, have been shown to delay the functional and molecular signatures of cardiac aging (136,151). In addition, metformin (155) and caffeine (156,157), which also possess autophagy-activating capacities, have been shown to decelerate cardiac aging (54,158,159). Nevertheless, further research is warranted to establish the extent to which autophagy contributes to their benefits on cardiomyocyte aging, whereas other candidate autophagy promoting molecules, such as trehalose, still await testing in the setting of cardiac aging (160).

In conclusion, autophagy activators, including spermidine, hold great promise at least in preclinical testing to substitute caloric restriction as a more feasible and safe strategy to attenuate, retard or even avert cardiac aging and related diseases. To this end, we continued with spermidine testing by applying it to an evident cardiovascular disease condition, namely hypertensive cardiomyopathy, which is discussed in detail in the next chapter.

Table 2. List of interventions that induce autophagy and delay cardiac aging

Intervention; Specificity	Mechanism of autophagy regulation	Effect on cardiac aging phenotype	Age; Model	Cardiac effect abolished by	Ref.
Caloric restriction	SIRT1 activation mTOR inhibition AMPK activation	- Attenuated hypertrophy and fibrosis; ameliorated systolic and diastolic functions as well as cardiac reserve - Reduced mitochondrial damage, lipid accumulation, oxidative stress, apoptosis, telomere shortening, senescence and inflammatory markers	22-28 months; Mice 24-30 months; Rats 52.7±11.9 years [M±SD]; Humans	*Prkaa* ablation (139,140)	(28) (135 – 138) (161, 162)
Intermittent fasting	SIRT1 activation mTOR inhibition AMPK activation	- Reduced hypertrophy and fibrosis; prolonged lifespan - Decreased myocardial collagen deposition, oxidative stress, inflammatory markers and B-type natriuretic peptide levels	24 months; Rats	Not reported	(142 – 144)
Cardiac-specific *dnPI3K*	mTOR activation	- Reduced hypertrophy and fibrosis; enhanced cardiac functional reserve; improved survival - Reduced oxidative stress, lipofuscin accumulation, senescence and inflammatory biomarkers as well as rejuvenated genetic profile.	20-24 months; Mice	Not reported	(145)
Global *Akt2*$^{-/-}$	mTOR activation FOXO inhibition	- Enhanced contractile function despite accentuated hypertrophy; prolonged lifespan - Improved cardiomyocyte mechanical properties, calcium handling and mitochondrial integrity	24 months; Mice	Autophagy inhibitor 3-methyladenine	(151)
Cardiac-specific *Parkin*^{tg}	Enhanced Parkin-mediated mitophagy	- Increased cardiac functional reserve - Enhanced mitochondrial structure and function; reduced oxidative stress, senescence and inflammatory markers	20 months; Mice	Not reported	(152)
moderate cardiac-specific *Sirt1*^{tg}	SIRT1 activation	- Reduced hypertrophy, fibrosis; Enhanced contractility - Reduced apoptosis and aging markers	18 months; Mice	Not reported	(47) (153)
Rapamycin	mTOR inhibition	- Reduced hypertrophy; enhanced contractile function; - Promoted mitochondrial biogenesis and restored fatty acid oxidation; reduced systemic and cardiac inflammation	24-27 months; Mice	Not reported	(34) (154)
Resveratrol	SIRT1 and AMPK activation	- Restored myocardial performance index - Rejuvenated genetic signature	25 months; Mice	Not reported	(136)
SRT1720	SIRT1 activation	- Rescued cardiomyocyte contractility *in vitro*	24 months; Mice	Parkin deficiency or co-incubation with insulin	(151)

Abbreviations: Akt2, serine/threonine-specific protein kinase 2; dnPI3K, dominant negative phosphoinositide 3-kinase; mTOR, mechanistic target of rapamycin; SIRT, Sirtuin; tg, transgenic overexpression; M±SD, mean±standard deviation. *This table is adapted from Abdellatif et. al. Circulation Research, 2018; Ref.* (70) *with permission of the publisher (Wolters Kluwer).*

4. Spermidine and Cardiovascular Disease

(RESULTS & DISCUSSION)

Parts of the results presented in this chapter have been published in Eisenberg and Abdellatif et. al. Nature Medicine, 2016; Ref. (100) *and were reproduced with permission from the publisher (Springer Nature).*

4.1. Introduction to hypertension

Age is the primary determinant of cardiovascular and general health of an individual. Therefore, extended life expectancies and population aging worldwide led to an ever-increasing prevalence of chronic disorders, especially those affecting the cardiovascular system. This public health problem is further exacerbated by hypercaloric diets, obesity, sedentariness and other features of modern-day life which cause premature onset of cardiovascular ailments. Indeed, cardiovascular diseases are currently the leading cause of sickness and death worldwide representing a massive global medical burden.

4.1.1. Aging lays down the foundation of cardiovascular disease

Several aspects of aging predispose the elderly to distinctive forms of cardiovascular ailments. For instance, age-related vascular stiffness and endothelial dysfunction underlie the development of hypertension, especially in its isolated systolic form, which is the most common variant of hypertension in aged individuals (163). Furthermore, atherosclerosis develops in aging vessels under the influence of intimal thickening and inflammation. Atherosclerotic lesions, in turn, predispose the aged heart to coronary artery disease, which itself is further aggravated in the presence of hypertrophy (103,164,165). Additionally, age-related myocardial stiffness, diastolic dysfunction and hypertension are major risk factors for the development of heart failure with preserved ejection fraction (HFpEF) (166,167). HFpEF, which affects half of all heart failure patients, still lacks evidence-based or life-saving therapies, despite being the leading cause of hospitalization in those above 65 years of age (168). Last but not least, dilation and structural remodelling of the aged atria as a consequence of augmented ventricular filling pressures is largely involved in yet another disease limited to the elderly, namely atrial fibrillation (AF). AF is considered the most common cardiac arrhythmia of clinical significance and represents a major risk factor for life-threatening thromboembolisms (169).

It is clearly noticeable that elevated blood pressure or hypertension is a common risk factor for almost every form of age-related cardiovascular disorder. In fact, hypertension is not just implicated, but even underlies some of these diseases. Therefore, I will focus in this chapter on hypertension as a reasonable example and a highly-relevant clinical entity of late-life cardiovascular disease.

4.1.2. Hypertension: a major risk for fatal cardiovascular events

Hypertension, *i.e.*, systolic blood pressure (SBP) ≥ 140 mmHg, in quantitative terms, is the most important risk factor of premature cardiovascular disease as it is more frequent than any other major risk factor, including diabetes mellitus, dyslipidemia and smoking. In fact, current prevalence of hypertension is devastating as the count of hypertensive patients has almost doubled during the last 25 years and currently affects 874 million persons (170). That said, non-optimal systolic blood pressure is the foremost contributing risk factor to morbidity and all-cause mortality worldwide, causing 212 million lost healthy life years and 9.4 million deaths every year (171).

Elevated blood pressure causes a multiple fold increase in the likelihood of cardiovascular disease development. For instance, hypertensive patients, depending on their gender, are three-to-four times more likely to suffer heart failure than non-hypertensives (172). Contrarily, reducing high blood pressure by 10-12 mmHg systolic blood pressure (or 5-6 mmHg diastolic blood pressure) lowers the risk of stroke and ischaemic heart disease by 38% and 16%, respectively (173). Despite such benefits of reducing elevated blood pressure, hypertension is still the leading risk factor of many life-threatening cardiovascular diseases, including cardio-renal failure (170,174). Thus, hypertension constitutes a massive challenge for public health and causes extravagant economic expenditure, currently being the costliest cardiovascular disease (175).

As mentioned previously, extended life expectancy and aging of the world population are major culprits in such unprecedented prevalence of hypertension. Similarly, habitual risk factors, such as higher caloric and salt intake combined with a sedentary lifestyle, have facilitated the age-related surge in blood pressures. That said, limited interventions have proven successful in achieving extended and long-lasting control in blood pressure. While intensive search for more successful interventions has been ongoing for decades, anti-hypertensive pharmacotherapy remains the only remedy to reduce high blood pressures. However, anti-hypertensive drugs, albeit fairly effective and accessible at an affordable price almost everywhere, are far from ideal. In fact, although a great majority (87.5%) of individuals diagnosed with hypertension receive regular pharmacological therapies, only a minority (32.5%) show controlled blood pressures (systolic BP < 140 mmHg), despite the fact that nearly one third of them already receive two or more drugs

(176). Therefore, more efforts are warranted to achieve better management of hypertension and its subsequent complications.

4.1.3. Dahl salt-sensitive rats: a model of hypertensive cardiomyopathy

Dahl salt-sensitive (SS) rats are a selected Sprague-Dawley strain, which due to a spontaneous mutation in the renin gene, are more prone to salt-induced hypertension (177). In fact, *Dahl* SS rats exhibit many traits of hypertensive disease observed in humans. When fed a high-salt diet, they develop a rapid surge in blood pressure, which in turn causes concentric cardiac hypertrophy and diastolic or systolic dysfunction depending on the extent, duration and age at which salt intake is initiated (83). Specifically, when *Dahl* SS rats are exposed to a high-salt diet at the age of 7 weeks, they develop diastolic dysfunction between 14 and 19 weeks of age, meanwhile high-salt administration at a younger age or extending it beyond the age of 19 weeks causes systolic dysfunction. Consequently, according to the salt feeding regimen, these rats suffer from heart failure in its diastolic or in its systolic form and this is evident from several manifestations, including tachypnea, labored respiration and obvious gravimetric lung congestion (83). Furthermore, hypertensive *Dahl* SS rats, like hypertensive patients, suffer from extra-cardiac complications, such as renal dysfunction (178). Therefore, *Dahl* SS rats on a high-salt diet represent a clinically relevant model of hypertension and related complications, including diastolic heart failure.

To this end, we decided to examine the impact of spermidine supplementation on the development of salt-induced hypertension and diastolic heart failure in *Dahl* SS rats. This allowed us to extend our results from the context of functional decline and increased risk of cardiovascular disease in aged mice to a full picture of cardiovascular disease. In addition, supplementing spermidine to *Dahl* SS rats before and after the development of hypertension allowed us to determine whether spermidine acts in a preventative manner (*i.e.*, in primary prevention) only or it can also reverse existing cardiovascular demise (*i.e.*, in secondary prevention or therapy).

4.2. Results: Cardioprotective effects of Spermidine in hypertension and related cardiomyopathy

Dahl SS rats were fed a high-salt diet (8%) starting from 7 weeks of age and their blood pressure was measured biweekly; then at the age of 14 or 19 weeks, they were subjected to a thorough cardiac examination. A subset of rats received 3 mM spermidine in their drinking water, which was either initiated with the high-salt diet (*prevention cohort*) or later at the age of 12 weeks after the development of hypertension (*therapy cohort*).

4.2.1. Spermidine improves blood pressure control and attenuates hypertensive heart failure

High salt feeding to *Dahl* SS rats causes a rapid increase in mean, systolic and diastolic blood pressures, which we observed within a mere 2 weeks (Fig. 19). However, co-administration of spermidine with high salt-diet restrained the increase in blood pressure and, thus, delayed hypertension to a significantly older age (by 4 weeks as measured along the progression line of mean blood pressure; Fig. 19).

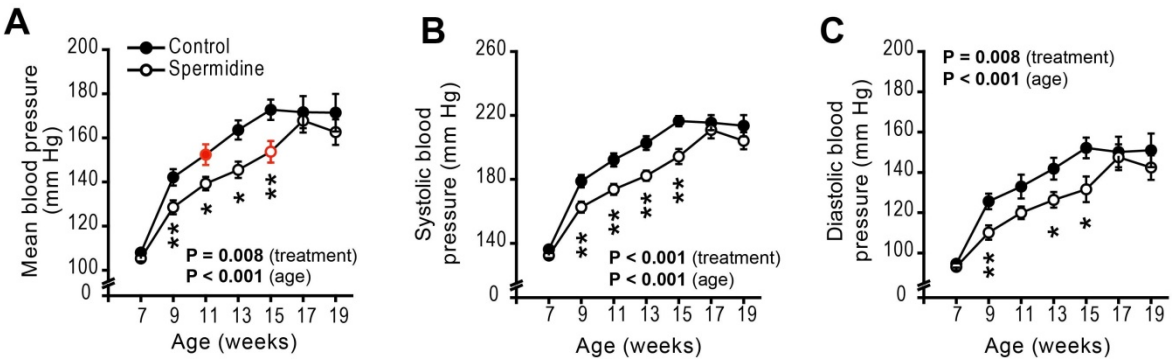

Figure 19. Spermidine delays salt-induced hypertension onset and progression.

(A) Mean arterial blood pressure non-invasively measured by a tail-cuff technique.

(B) Systolic arterial blood pressure.

(C) Diastolic arterial blood pressure.

The red symbols indicate the first time point at which mean blood pressure did not show a significant difference from the peak pressure reached by the respective group. (n=10 rats/group); shown P values indicate factor comparisons (age and treatment) by two-way mixed-design ANOVA and $^{**}P<0.01$, $^{*}P<0.05$ represent the following pairwise comparisons (*i.e.*, simple main effects).

We hypothesized that the anti-hypertensive action of exogenous spermidine is mediated by inhibiting *de novo* synthesis of polyamines and, thus, their precursor L-arginine can be instead re-directed towards increasing the production of the vasodilator nitric oxide (NO). Indeed, we found increased circulating levels of spermidine in the treated rats to be associated with reduced plasma concentrations of ornithine (Fig. 20A-B), indicating spermidine-mediated inhibition of *de novo* polyamine synthesis. More importantly, treated rats had a higher level of plasma arginine, as measured by the global arginine bioavailability ratio (GABR, arginine/[citrulline+ornithine]), already within 2 weeks of spermidine administration (Fig. 20C).

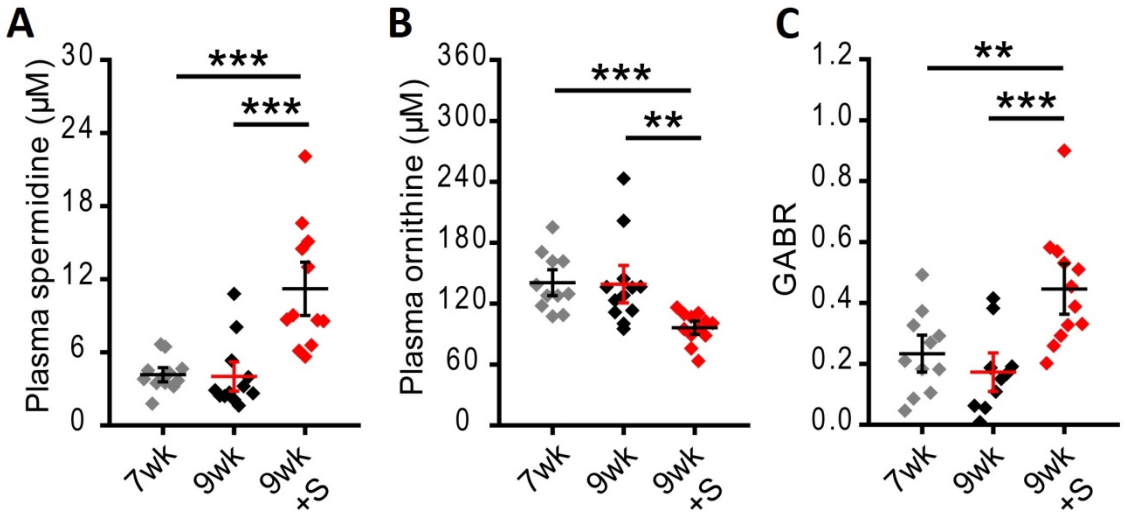

Figure 20. Exogenous spermidine spares the NO precursor arginine by diverting it from *de novo* synthesis of polyamines.

(A) Plasma spermidine levels in *Dahl* SS rats at baseline and after 2 weeks of high-salt diet combined (or not) with spermidine supplementation in the drinking water.

(B) Circulating ornithine levels.

(C) Global arginine bioavailability ratio (GABR), calculated as arginine/(citrulline+ornithine).

(*n*=11-12/group); ***P<0.001, **P<0.01 by ANOVA and Tukey post-hoc test. Abbreviations: S, spermidine, wk, week

As for the heart, spermidine feeding attenuated hypertension-associated cardiac hypertrophy as assessed by echocardiography-measured left ventricular mass and posterior wall dimension (Fig. 21 and Supplementary Table 6) and post-mortem whole heart weight (Supplementary Table 7). Not only cardiac remodelling, but also left ventricular dysfunction was attenuated by spermidine feeding. In this regard,

diastolic function was improved in spermidine-treated rats as denoted by lower E/e', an echocardiographic surrogate of end-diastolic pressure and diastolic function (Fig. 21 and Supplementary Table 6).

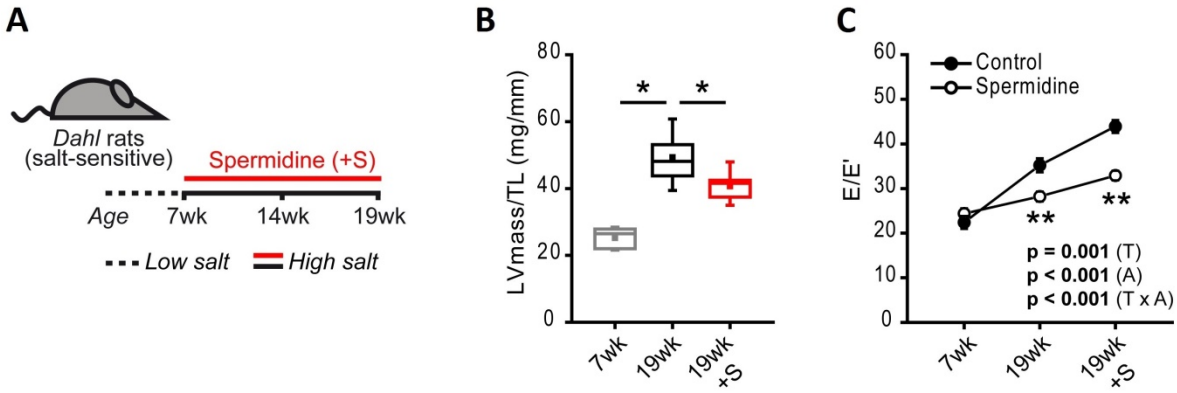

Figure 21. Spermidine ameliorates cardiac hypertrophy in hypertensive *Dahl* SS rats

(A) Schematic representation of spermidine feeding to *Dahl* SS rats on a high-salt diet.

(B) Tibia length (TL)-normalized left ventricular mass (LVmass), an echocardiographic index of hypertrophy.

(C) Peak early Doppler trans-mitral blood flow velocity (E) to the corresponding myocardial tissue Doppler velocity (e'), a measure of diastolic dysfunction.

(*n*=10 rats/group); in (B), **P*<0.05 by Kruskal–Wallis and corrected multiple-comparisons by Mann-Whitney U test; in (C), shown *P* values indicate factor comparisons (A, age; T, treatment) by two-way mixed-design ANOVA and ***P*<0.01 represent the following pairwise comparisons (*i.e.*, simple main effects). (Parts of these results were generated by Dr. Uwe Primessnig, Medical University of Graz)

More importantly, when we evaluated cardiac performance by intra-cardiac pressure-volume measurements, we found spermidine-fed *Dahl* SS rats to have reduced left ventricular filling pressures, lower myocardial stiffness and a downward-shifted pressure-volume relationship, all indicative of improved diastole (Fig. 22 and 23). This was further corroborated by ameliorated cardiomyocyte elasticity, as denoted by an increase in total and S4080 site-specific phosphorylation of titin (Fig. 24). In addition, spermidine reduced circulating TNFα, a pro-inflammatory cytokine known to increase in heart failure (Fig. 24). This corroborates the anti-inflammatory effect we initially observed in aged mice and may contribute, at least in part, to the increased phosphorylation of titin.

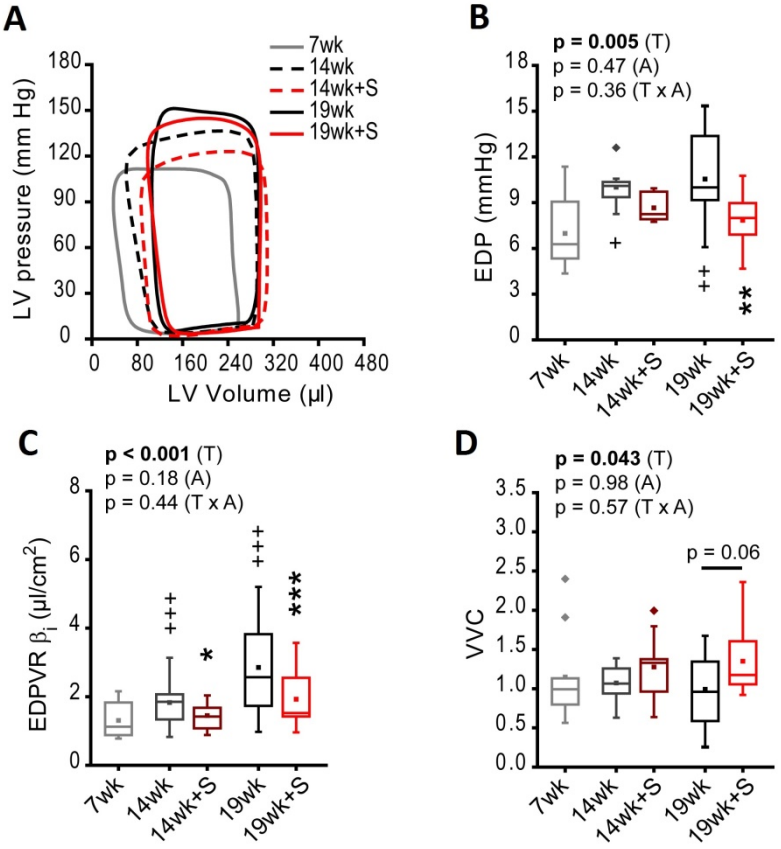

Figure 22. Spermidine improves diastolic function and ventricular-vascular coupling in hypertensive *Dahl* SS rats.

(A) Representative left ventricular (LV) pressure-volume (PV) loops. **(B)** End-diastolic pressure (EDP). **(C)** End-diastolic pressure-volume relationship constant (EDPVR β), a measure of myocardial stiffness. **(D)** Ventricular-vascular coupling (VVC), a measure of cardiac-vascular interaction and overall system efficiency. (*n*=9-10 rats/group); Shown *P* values indicate factor comparisons (A, age; T, treatment) by two-way ANOVA (ANCOVA in C) including 14 weeks and 19 weeks groups treated (or not) with spermidine (+S) and the following pairwise comparisons are indicated by ***P<0.001, **P<0.01, *P<0.05; ^{+++}P<0.001, ^{++}P<0.01, ^{+}P<0.05 by ANOVA (ANCOVA in C) and Tukey post-hoc comparing the 3 control groups (7wk, 14wk and 19wk) only.

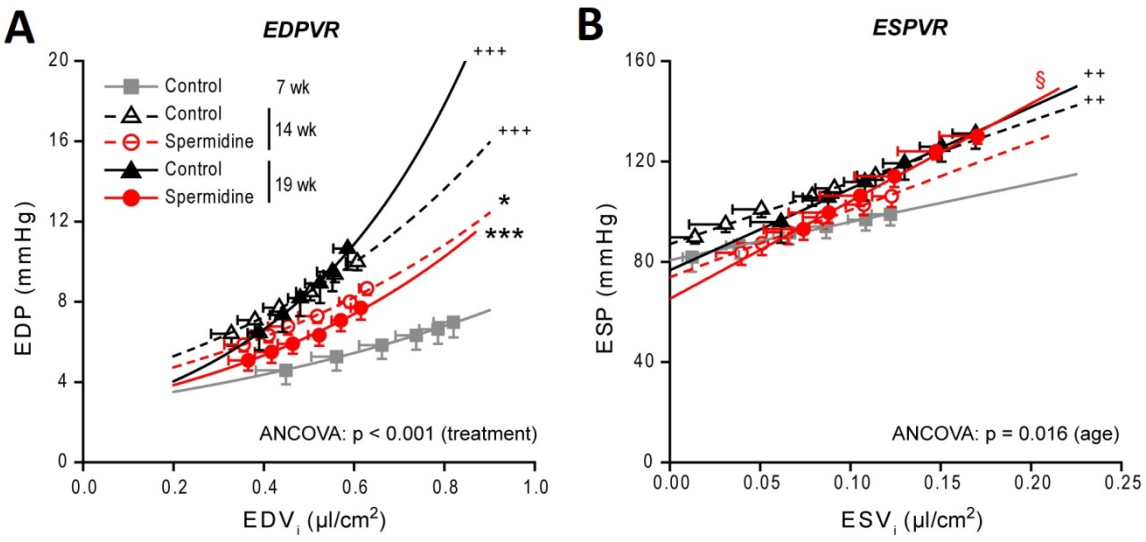

Figure 23. Spermidine attenuates passive myocardial stiffness in hypertensive *Dahl* SS rats

See next page for figure legend

(A) Exponential left ventricular end-diastolic pressure-volume relationship (EDPVR). *Note the downward shift, indicating reduced stiffness,* in spermidine-fed 14 weeks old and 19 weeks old rats as compared to their respective controls, which both had increased stiffness compared to 7-week-old non-hypertensive controls.
(B) Linear left ventricular end-systolic pressure-volume relationship (ESPVR). *Note the upward shift, indicating increased contractility, in all high-salt diet-fed rats (14wk and 19wk) whether treated or not, as compared to the 7-week-old non-hypertensive controls.*
(*n*=9-10 rats/group); ^{+++}P<0.001, ^{++}P<0.01 by ANCOVA and Bonferroni post-hoc test comparing the 3 control groups (7wk, 14wk and 19wk) only; shown *P* values indicate factor comparisons (age, 14wk and 19wk; treatment, control and spermidine) by two-way ANCOVA and following pairwise comparisons are indicated by ***P<0.001, *P<0.05 (*vs.* age-matched control) or $^{§}P$<0.05 (*vs.* treatment-matched group).

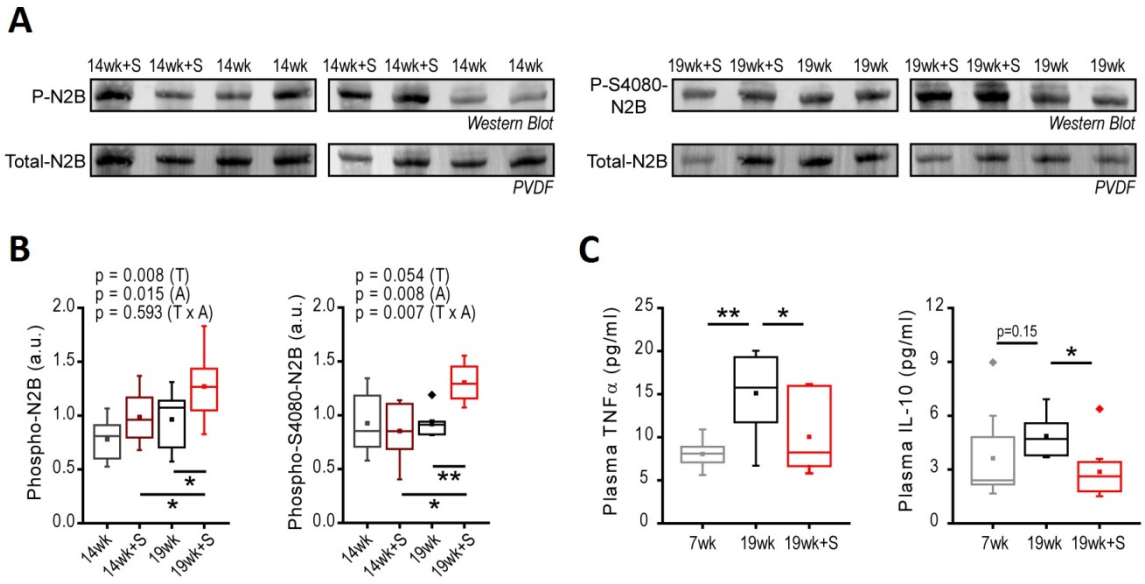

Figure 24. Spermidine promotes titin phosphorylation and limits the pro-inflammatory cytokine TNFα levels in hypertensive *Dahl* SS rats.

(A) Representative blots of titin N2B isoform expression and phosphorylation.
(B) Total (left) and Ser4080 (S4080)-specific (right) titin N2B isoform phosphorylation. (*n*=8 rats/group); shown *P* values are for factor comparisons (T, treatment; A, age) by two-way ANOVA and the following pairwise comparisons are represented by **P<0.01, *P<0.05.
(C) Plasma levels of the pro-inflammatory cytokine TNF-α. (*n*=7-12 rats/group); **P<0.01, *P<0.05 by ANOVA and Tukey post-hoc test. Abbreviations: S, spermidine; wk, week. *(Western blots were done by Ms. Marion von Frieling-Salewsky, University of Münster, Germany)*

Of note, contractility as measured invasively by the end-systolic pressure volume relationship (ESPVR) slope, was preserved in both treated and non-treated rats (Fig. 22 and Supplementary Table 8), yet ventricular-vascular coupling was still significantly improved upon spermidine feeding essentially due to reduced arterial stiffness (Supplementary Table 8). Last but not least, spermidine reduced pulmonary and hepatic congestion, as evaluated in a post-mortem gravimetric

analysis (Fig. 25 and Supplementary Table 7). Taken together, these results indicate that supplementation of *Dahl* SS rats with spermidine slows the progression of salt-induced hypertension, meanwhile it successfully mitigates the development of diastolic heart failure at least in the setting of 'primary prevention'.

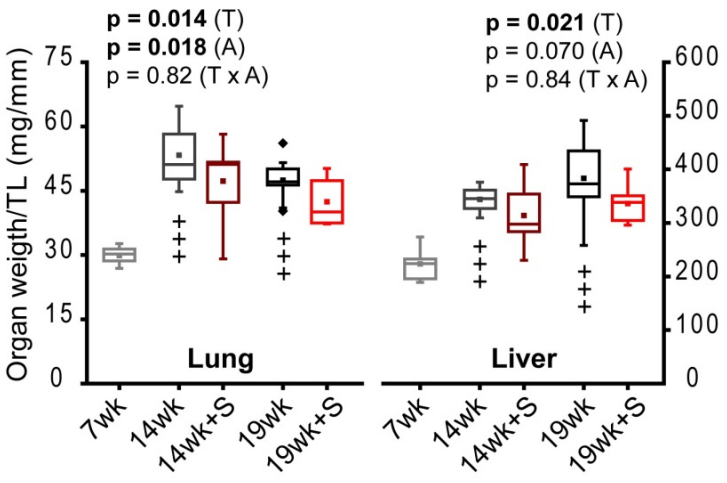

Figure 25. Spermidine suppresses pulmonary and systemic congestion in hypertensive heart failure

Depicted are the post-mortem lung and liver weights normalized to tibia length (TL) in 14 weeks and 19 weeks old *Dahl* hypertensive rats (treated or not with spermidine) and their non-hypertensive 7-week-old controls. (*n*=9-10 rats/group); $^{+++}P<0.001$ by ANOVA and Tukey post-hoc tests comparing the 3 control groups (7wk, 14wk and 19wk) only; shown *P* values indicate factor comparisons (A, age; T, treatment) by two-way ANOVA including 14 weeks and 19 weeks groups treated or not with spermidine and the following pairwise comparisons are indicated by $^{*}P<0.05$. Abbreviations: S, spermidine; wk, week.

4.2.2. Spermidine protects from renal complications of hypertension

As a result of increased salt intake, hypertensive *Dahl* SS rats suffer from multiple renal abnormalities. In fact, we found non-treated *Dahl* SS rats to show histological signs of arterial hyalinosis, fibrosis, glomerulosclerosis and thrombotic microangiopathy, all of which were improved in spermidine-treated rats (Fig. 26). Furthermore, increased kidney content of spermidine was associated with reduced acute renal injury as reflected by a lower level of lipocalin-2 (Fig. 27A-B). Such renal protective effects of spermidine are mediated, at least partly, through autophagy induction as denoted by the reduction of p62, a specific autophagy substrate, which is depleted upon activation of autophagic flux (Fig. 27C).

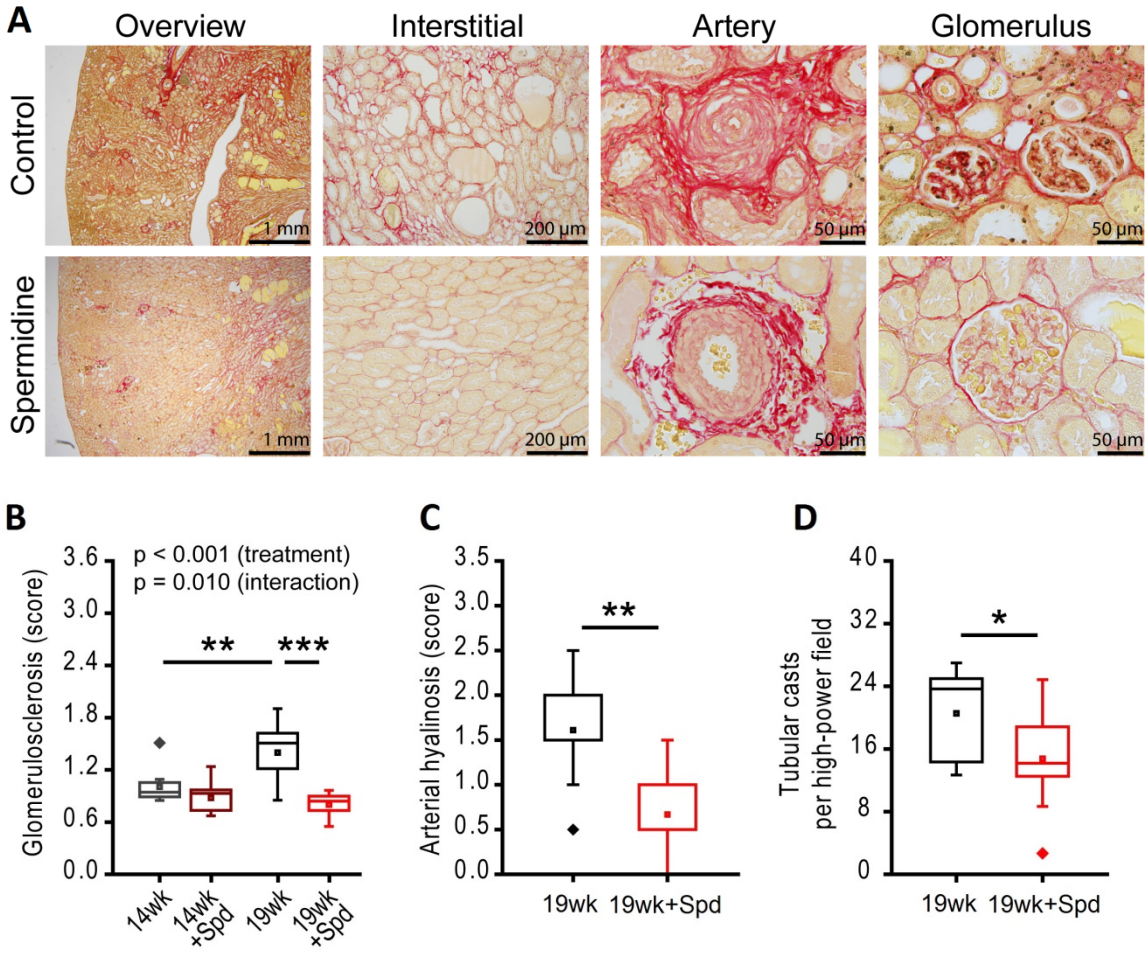

Figure 26. Spermidine alleviates hypertensive nephropathy in *Dahl* SS rats

(A) Representative picrosirius red-stained renal fibrosis slides of 19-week-old hypertensive rats treated with or without spermidine in the drinking water.

(B) Glomerulosclerosis and **(C)** Arterial hyalinosis semi-quantitative score, as evaluated on PAS-stained renal tissue at the indicated ages.

(D) Renal tubular casts count as averaged from 6 high-power fields.

(*n*=9 rats/group); shown *P* values in (B) indicate factor comparisons (A, age; T, treatment) by two-way ANOVA including 14 weeks and 19 weeks groups treated or not with spermidine (+Spd); **P*<0.05, ***P*<0.01 by unpaired Student's *t*-test. *(This analysis was performed by Dr. Alexander Kirsch, Medical University of Graz)*

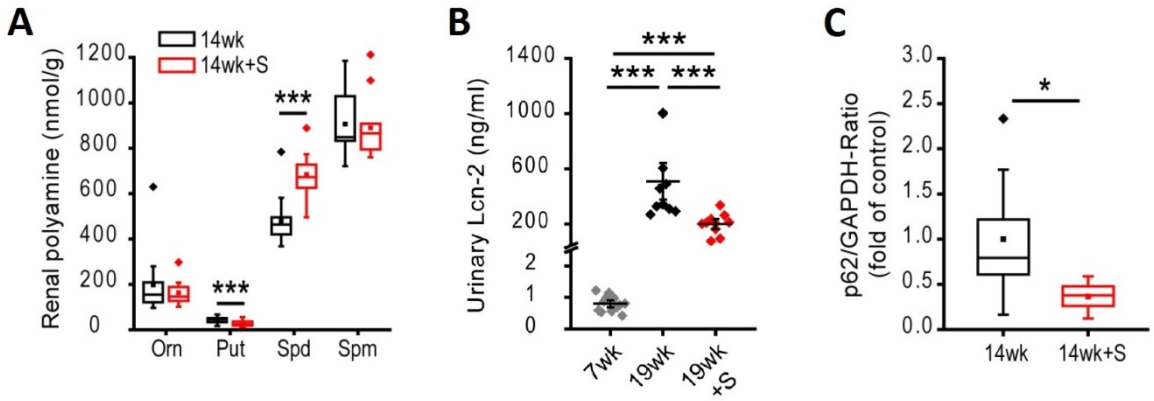

Figure 27. Spermidine-induced autophagy is renoprotective in hypertensive rats

(A) Renal concentration of different polyamines in control and spermidine-treated hypertensive *Dahl* rats (*n*=11-13 rats/group). Abbreviations: Orn, ornithine; Put, putrescine; Spd, spermidine; Spm, spermine.

(B) Urinary lipocalin (Lcn)-2 content in non-hypertensive (7wk) and hypertensive (19wk) rats treated (or not) with spermidine (+S). (*n*=10-12 rats/group).

(C) GAPDH-normalized quantification of p62 immunoblot signal in renal tissue extracts of control and spermidine-treated (+S) hypertensive rats (*n*=9-12 rats/group).

**P*<0.05, ****P*<0.001 by unpaired Student's *t*-test (A and C) or by ANOVA and Tukey post-hoc test (B).

(These measurements were done by Dr. Tobias Eisenberg, University of Graz and Dr. Alexander Kirsch, Medical University of Graz)

4.2.3. Spermidine therapeutically attenuates hypertension and related cardiac dysfunction

To examine the effect of spermidine supplementation on established hypertension, we administrated spermidine to *Dahl* SS rats that have been already on a high-salt diet for 5 weeks (Fig. 28A). At this point, the rats have already developed severe arterial hypertension and cardiac hypertrophy. Then, they received a standard anti-hypertensive treatment in the form of (i) a diuretic (furosemide, 10 mg/kg body weight) as a single intraperitoneal injection combined with (ii) a dietary shift to a low-salt diet. The reduction in salt intake combined with adjuvant diuresis resulted in a transient and relatively small reduction in blood pressure (Fig. 28B-D). However, co-administration of spermidine with this therapy resulted in a stronger and long-lasting reduction in blood pressure (Fig. 28B-D). Spermidine also restored vascular elasticity to the levels of healthy control rats that received a low-salt diet throughout the experiment (Fig. 29A).

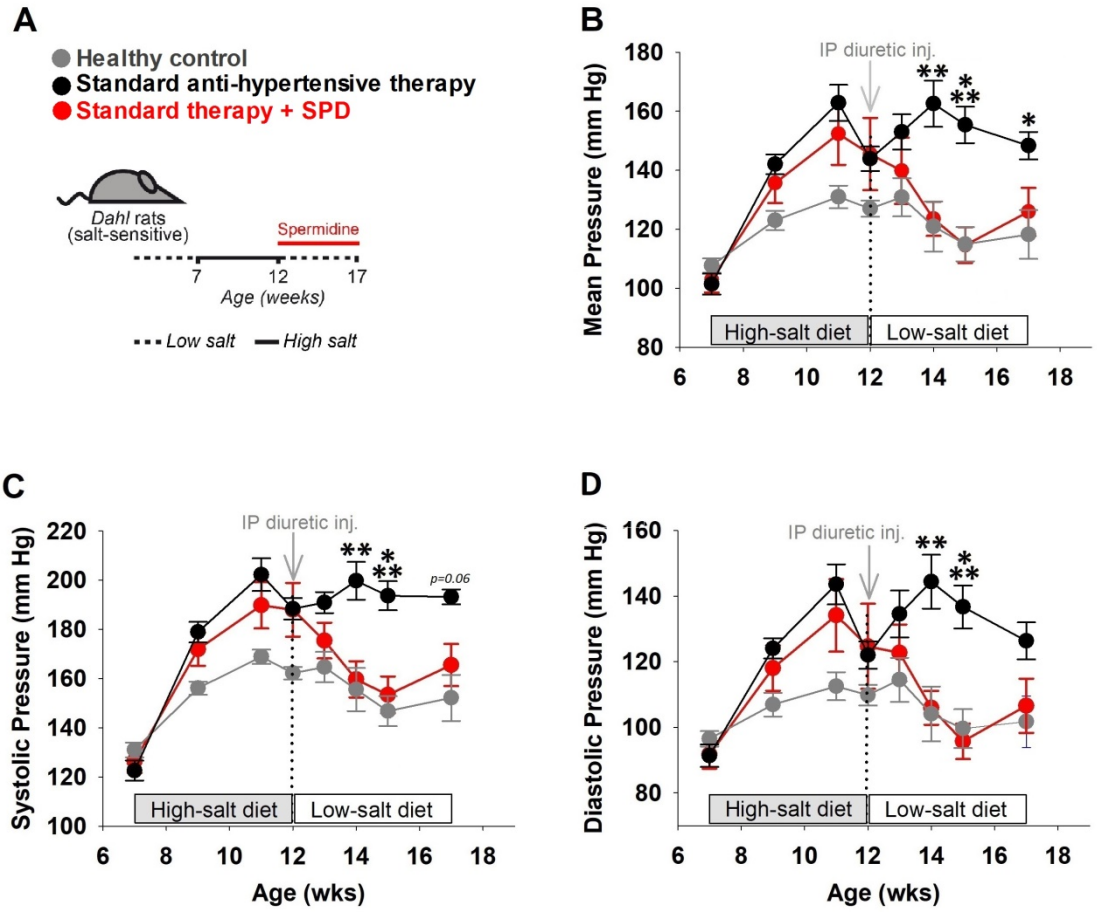

Figure 28. Spermidine synergistically improves standard anti-hypertensive therapy

(**A)** Schematic representation of spermidine therapeutic feeding to *Dahl* SS rats with established hypertension. **(B)** Mean, **(C)** systolic and **(D)** diastolic arterial blood pressure that was non-invasively measured by the tail cuff method in *Dahl* SS rats that either never received high-salt diet (*healthy control*) or received high-salt diet till 12 weeks and then were fed a low-salt diet combined with a single intraperitoneal (IP) diuretic injection alone (*standard anti-hypertensive therapy*) or additionally supplemented with spermidine in the drinking water (*standard anti-hypertensive therapy+SPD*). *Note the relatively small and transient reduction in the blood pressures of the standard therapy group. Contrarily, co-administration of spermidine in standard therapy+SPD group synergistically improved the blood-pressure lowering effect to reach levels comparable to the healthy control group, which received a low-salt diet throughout the experiment.*

(*n*=6 rats/group); **P*<0.05, ***P*<0.01, ****P*<0.001 *vs. standard therapy+SPD* group by pairwise comparisons (simple main effects) following 2-way mixed-design ANOVA.

At the heart, therapeutic application of spermidine reduced cardiac hypertrophy as evaluated by tibia length-normalized postmortem heart weight (Fig. 29B) and improved diastolic function as indicated by restoring normal left ventricular filling pressure and minimum rate of pressure change (dPdt_{min}) (Fig. 29 C-D). These cardiac improvements in spermidine-fed rats translated to improved exercise tolerance, indicating enhanced cardiopulmonary functional capacity. Indeed, spermidine restored maximal treadmill running distance and oxygen consumption (VO_2max) of hypertensive *Dahl* SS rats (Fig. 30). Altogether, these results indicate a therapeutic potential of spermidine application against salt-induced hypertension and associated cardiomyopathy.

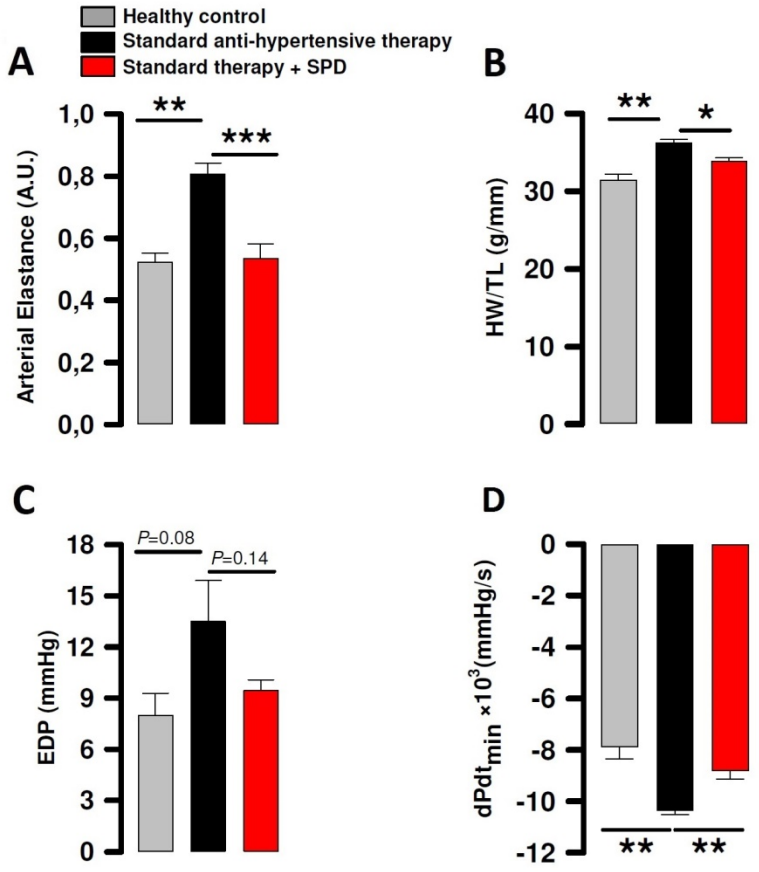

Figure 29. Therapeutic application of spermidine reverses established cardiomyopathy induced by hypertension in *Dahl* SS rats.

(A) Arterial elastance measured as the ratio between intra-cardiac end-systolic pressure and stroke volume.

(B) Post-mortem heart weight (HW) normalized to Tibia length (TL), a measure of hypertrophy.

(C) End-diastolic pressure (EDP).

(D) Minimum change rate in left ventricular pressure (dPdt_{min}), a measure of diastolic function.

(n=5-6 rats/group); **P<0.01, *P<0.05 by ANOVA and Tukey post-hoc test.

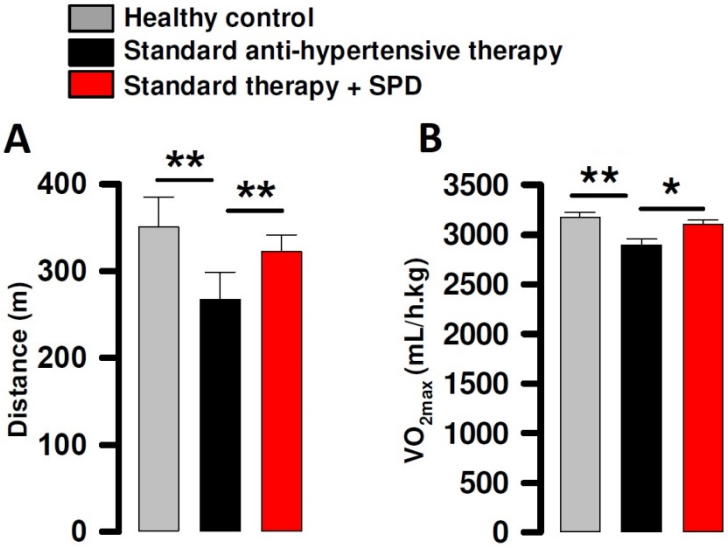

Figure 30. Spermidine restores exercise tolerance and maximum oxygen consumption in hypertensive *Dahl* SS rats

(A) Maximal treadmill run distance by *Dahl* SS rats that received an anti-hypertensive therapeutic strategy combined with (or without) spermidine in the drinking water.

(B) Maximal oxygen consumption (VO_2max) during treadmill exercise testing in the same rats.

(*n*=6 rats/group); ***P*<0.01, **P*<0.05 by ANOVA and Tukey post-hoc test.

4.3. Discussion

In this chapter, we could identify numerous beneficial effects of spermidine administration in the context of cardiovascular disease, exemplified by hypertension and related cardiomyopathy. Spermidine supplementation to *Dahl* SS rats fed a high-salt diet led to improved blood pressure regulation, thereby delaying the onset and progression of hypertension. Furthermore, spermidine diminished hypertension-induced hypertrophy, preserved cardiac function and protected the rats from imminent heart failure.

Even when co-administrated after full development of hypertension, spermidine improved the efficacy of standard therapy, thereby synergistically strengthening the anti-hypertensive effect and restoring cardiac structure, function and overall cardiopulmonary performance. Collectively, the data presented in this chapter denote potential therapeutic applications of spermidine alone or in conjunction with standard pharmacotherapies to prevent or even reverse hypertension and subsequent cardiac dysfunction and heart failure.

In a considerable proportion of the general population, increased salt intake causes significant fluctuations in disease burden (179). These individuals – regarded 'salt-sensitive' – are closely mimicked by *Dahl* SS rats. In fact, when fed a high-salt diet, *Dahl* SS rats exhibit several structural and functional abnormalities common to hypertensive patients. Therefore, from a translational perspective, these rats represent a highly clinically relevant model of hypertension. Similar to humans, reduced bioavailability of the vasodilator nitric oxide (NO) contribute to the development of hypertension in *Dahl* SS rats upon increased salt intake (180). In fact, hypertension can be mitigated in these rats by supplementing the NO precursor L-arginine (180). Interestingly, L-arginine serves also as a precursor for polyamines, including spermidine. Accordingly, increased circulating and tissue levels of spermidine, upon exogenous supply, spared *de novo* synthesis of polyamines from L-arginine, which instead became readily available for the production of NO (Fig. 31). Indeed, lower blood pressure in spermidine-fed *Dahl* SS rats coincided with higher levels of arginine and reduced *de novo* synthesis of polyamines.

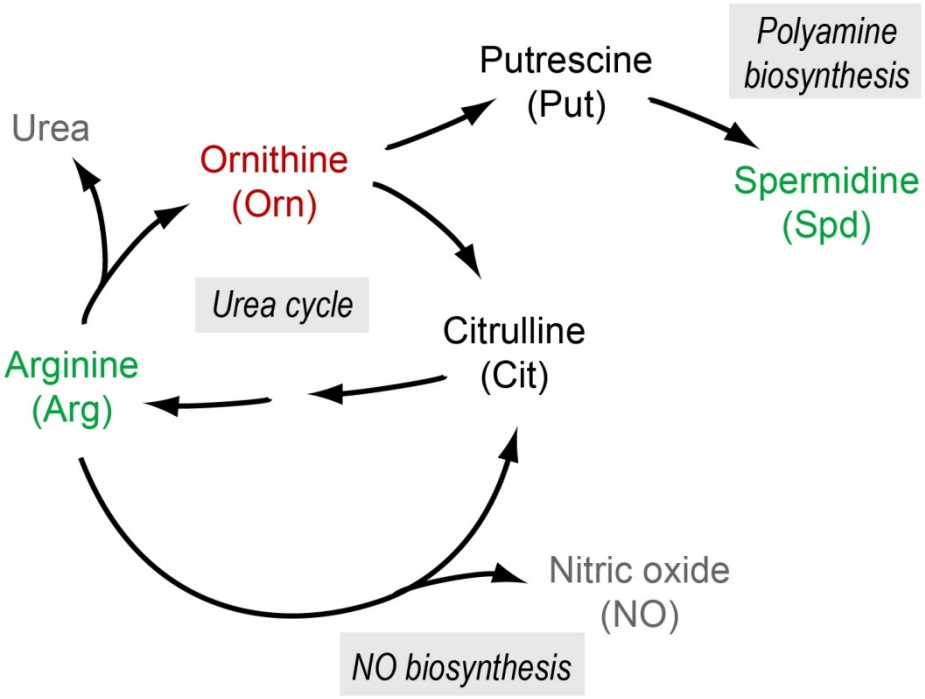

Figure 31. Arginine is a common precursor for NO and polyamines

Schematic depiction of the relationship between arginine metabolism (urea cycle) and biosynthesis of polyamine *vs.* nitric oxide (NO). *Adapted from Eisenberg and Abdellatif et. al. Nature Medicine, 2016; Ref.* (100) *with permission from the publisher (Springer Nature).*

Another potential mechanism by which spermidine feeding may increase NO levels is the suppression of vascular inflammation. A chronic inflammatory status is usually associated with increased oxidative stress and reactive oxygen species production, which in turn limits NO bioavailability by converting it to peroxynitrite. In this regard, spermidine had an anti-inflammatory effect as it reduced plasma levels of the pro-inflammatory cytokine TNF-α. Suppressed systemic inflammation did not only benefit the vasculature, but also the heart as increased titin phosphorylation, which consequently improved diastolic function (122).

Collectively, increased L-arginine bioavailability and reduced inflammation contribute to spermidine-mediated protection in the settings of hypertension and heart failure likely *via* enhancing NO production, availability and likely utilization.

In addition to these apparently autophagy-independent mechanisms, spermidine-induced autophagy might play an anti-hypertensive role as well. In fact, we found autophagy activation in the kidneys of treated rats to be associated with protection from hypertensive nephropathy. Although we have not performed direct testing

within this thesis, it is conceivable to hypothesize that preserved renal structure and function by autophagy activation in the kidneys plays an indispensable role in spermidine's antihypertensive effect. More importantly, spermidine-induced autophagy in the vasculature itself might be implicated as well. In fact, spermidine has been previously shown to restore normal aortic pulse velocity and NO-dependent vasodilation in aged mice, indicating reversed age-related arterial stiffening and endothelial dysfunction, respectively (129). In addition, spermidine-fed aged mice showed lower levels of vascular collagen accumulation, oxidative stress and advanced glycation end-products, all of which are common complications of aging (129). Importantly, these vascular anti-aging effects have been shown to be autophagy-dependent as when incubated with the autophagy inhibitor chloroquine, aortic rings from aged spermidine-fed mice had no advantage over age-matched controls (129).

In addition to spermidine, other autophagy-promoting interventions have been shown to confer similar beneficial effects on vascular health at least in the context of aging (Table 3). For instance, the natural autophagy inducer trehalose restores vascular function and NO bioavailability in aged mice by increasing eNOS expression. Trehalose also reduces vascular oxidative stress levels and pro-inflammatory cytokines (181). Furthermore, trehalose has been shown to exert similar beneficial effects in humans. When supplemented to the elderly, trehalose improved vascular function in resistance arteries as denoted by increasing both bioavailability and smooth muscles sensitivity of NO (182). Of note, trehalose loses its beneficial effects, in cultured endothelial cells, when co-incubated with the autophagy inhibitor 3-MA. This supports the notion that trehalose-mediated vascular protection is essentially mediated by autophagy (181).

Consistently, resveratrol, SRT1720 and nicotinamide mononucleotide (NMN), all of which induce autophagy *via* sirtuin activation, have been shown to improve vascular health. Resveratrol improves vascular function in aged mice as it improves NO-dependent vasodilation and reduces endothelial apoptosis, oxidative stress and inflammation. Consistently, resveratrol preserved vascular health in Rhesus monkeys fed a diet that was abnormally high in fat and sucrose. Specifically, dietary resveratrol reduced pulse wave velocity-measured vascular stiffness as well as arterial wall inflammation (183). Similar to non-human primates, resveratrol has

shown promising vascular effects in overweight and obese individuals as it improved flow-mediated vasodilation (184).

Also, SIRT1 activation by SRT1720 has been shown to confer vascular protection in the form of preserved endothelial function and attenuated pro-inflammatory cytokines and oxidative stress (185). Finally, replenishing cellular NAD^+ levels by NMN supplementation activates SIRT1 and reverses age-related arterial stiffening as measured *in vivo* by aortic pulse wave velocity and *in vitro* by elastic modulus. In addition, NMN improves endothelial function and attenuates collagen deposition and elastin fractures in aged mice aortae (186). That said, although SIRT1 activation is known to induce autophagy (187), it is still to be elucidated to what extent the beneficial effects of SIRT1 activators rely on autophagy.

The benefit of autophagy activation on vascular health is further substantiated by autophagy-boosting dietary regimens. One such regimen is caloric restriction, which exerts a multitude of health-promoting effects on vasculature when initiated early or later in life. Caloric restriction enhances NO bioavailability and also reduces vascular thickening and stiffness in aged mice. These effects are mediated by a reduction in vascular oxidative stress and inflammation, collagen deposition as well as elastin fragmentation (188). Even when applied for a short period during a late-life stage, caloric restriction still improves endothelial function and reduces inflammatory and oxidative damage (189,190). In fact, incubating endothelial cells in a serum obtained from calorically-restricted animals is sufficient to reduce inflammation and oxidative stress (191).

Collectively, dietary or pharmacological activation of autophagy seems to protect the vasculature from common structural and functional abnormalities that are common to aging and hypertension. Therefore, spermidine and other autophagy-boosting caloric restriction mimetics may hold promise as therapeutic interventions to preserve or even improve vascular health in the face of aging and related diseases, such as hypertension.

Table 3. List of interventions that induce autophagy and improve vascular health

Intervention	Mechanism of autophagy regulation	Effect on vascular health	Age; Model	vascular effect abolished by	Ref.
Caloric restriction	SIRT1 activation mTOR inhibition AMPK activation	- Attenuated wall thickening, vascular stiffness and restored endothelial function of conduit arteries; neutralized arterial collagen accumulation and elastin remodeling. - Reduced oxidative stress and inflammation; increased eNOS expression and bioavailability	29-31 months; Mice 24-28 months; Rats	Not reported	(188) (189) (190) (191) (161)
Intermittent fasting	SIRT1 activation mTOR inhibition AMPK activation	- Attenuated fibrosis and vascular wall alterations in the aorta - Reduced oxidative stress	24 months; Rats	Not reported	(142 – 144)
Trehalose	AMPK activation by inhibiting glucose transport (192)	- Reduced vascular stiffness and restored vascular endothelial function - Reduced oxidative stress and enhanced eNOS expressing and NO levels; reduced vascular inflammation.	27-28 months; Mice	In endothelial cell culture, autophagy blocker 3-MA abolishes trehalose-induced oxidative stress reduction and NO bioavailability enhancement	(181, 182)
		- Enhanced vascular function in resistance arteries - Increased microvascular NO bioavailability; improving vascular smooth muscles NO sensitivity	Middle-aged to elderly humans		
Resveratrol	SIRT1 and AMPK activation	- Attenuated arterial stiffness and vascular endothelial dysfunction - Enhanced NO-mediated vasorelaxation; reduced vascular oxidative stress, inflammation and endothelial apoptosis	18 months; Mice	Not reported	(44)
SRT1720	SIRT1 activation	- Restored endothelial function - Reduced oxidative stress and inflammatory markers; enhanced COX-2-dependent vasorelaxation	29-32 months; Mice	Not reported	(185)
NMN	SIRT1 activation by replenishing cellular NAD^+	- Restored endothelial function; restored large elastic arteries stiffness; neutralized collagen deposition and partially limited elastin damage - Reduced oxidative stress; restored NO bioavailability	26-28 months; Mice	Not reported	(186)

Abbreviations: AMPK, AMP-activated kinase; Cox-2, cyclooxygenase-2; NMN, Nicotinamide mononucleotide; NAD+, nicotinamide adenine dinucleotide; mTOR, mechanistic target of rapamycin; SIRT1, Sirtuin1; tg, transgenic overexpression. *This table is adapted from Abdellatif et. al. Circulation Research, 2018; Ref.* (70) *with permission from the publisher (Wolters Kluwer).*

5. Spermidine in Humans

(RESULTS & DISCUSSION)

Parts of the results presented in this chapter have been published in Eisenberg and Abdellatif et. al. Nature Medicine, 2016; Ref. (100) *and were reproduced with permission from the publisher (Springer Nature).*

5.1. Introduction to anti-aging interventions in humans

5.1.1. Caloric restriction promotes healthy aging in humans

In line with preclinical evidence, a growing body of clinical data supports the notion that autophagy-inducing interventions delay aging and improve cardiovascular health in humans. For instance, long-term dietary restriction protects aged, otherwise healthy individuals, from multiple characteristics of age-related functional decline in the cardiovascular system, including diastolic dysfunction, cardiac fibrosis, high blood pressure and systemic pro-inflammatory cytokines (162). More importantly, old individuals with heart failure also benefit from caloric restriction. In fact, within a relatively short period of time, precisely 20 weeks, reduced caloric intake improves cardiopulmonary functional capacity in heart failure with preserved ejection fraction patients (193). Interestingly, the effect of caloric restriction in these patients is two-fold stronger than that of exercise (193).

In pursuit of finding beneficial interventions that might be more tolerable than caloric restriction, a few alternative regimens have been proposed and clinically tested. One such regimen is time-restricted feeding, which is a form of intermittent fasting whereby food intake is limited to a defined time interval during the day. Early time-restricted feeding (*i.e.,* food intake within 6 hours before 3 pm) has been shown to improve several parameters of cardiometabolic health, including insulin sensitivity, blood pressure and oxidative stress in prediabetics. Interestingly, these benefits were evident after 5 weeks despite ensuring isocaloric intake throughout this randomized trial, thus, avoiding any potential confounding effects of weight loss (194). An alternative regimen is the fasting-mimicking diet, which is characterized by low intake of sugars, proteins and overall calories, but high amounts of unsaturated fats. Consuming this diet for 5 days per month reportedly improves various aspects of cardiovascular health. In fact, 3 cycles of fasting-mimicking diet ameliorates several cardiovascular risk factors, including blood pressure, body mass index, inflammatory mediators, glucose homeostasis and circulating lipids (150). Nonetheless, some individuals seem to indulge in overfeeding behaviours during their *ad libitum* periods of the day, thus jeopardizing the benefits of these intermittent fasting regimens. In addition, fasting in any of its forms still does not appeal the majority of people and only a few show adherence for extended periods (195). Hence, dietary solutions with better compliance or better so pharmacological

approaches that recapitulate the benefits of fasting without enduring food deprivation are substantially needed.

5.1.2. The Mediterranean diet promotes health and longevity without fasting

There is a general consensus that the Mediterranean diet is a healthy dietary option that does not necessarily involve energy restriction. This diet involves a high consumption of olive oil, nuts, whole-grain cereals, legumes and vegetables, with a moderate intake of dairy products and fish with a trivial amount of sugar and refined carbohydrates. The remarkable health- and longevity-promoting properties of the Mediterranean diet is supported by a substantial amount of clinical evidence (196). Epidemiological proof that adhering to the Mediterranean diet improves longevity was initially provided by a large population-based study in Greece reporting reduced all-cause mortality and death due to coronary heart disease and cancer in those adhering to this diet (197). These observations were then further validated in another study, which enrolled aged individuals (between 70 and 90 years old) from 11 European countries, showing that consuming the Mediterranean diet lowers the risk of total mortality, and also death due to cardiovascular disease (198).

Furthermore, the Lyon Heart study – a randomised trial for the secondary prevention of coronary heart disease – showed that a Mediterranean α-linolenic acid-rich diet reduces both recurrence of myocardial infarction and risk of mortality due to cardiac or other causes (199). Of note, the benefits of this diet lasted for almost 4 years following the first cardiac event (200). Along the same lines, another randomised trial (PRIMIDED study) showed protective effects of the Mediterranean diet against cardiovascular disease in individuals at high risk (201). Supplementation of extra-virgin olive oil or nuts resulted in lower incidence of major cardiovascular events as measured by a composite score incorporating myocardial infarction, stroke, and cardiovascular mortality (201). However, the conclusions of PRIMIDED study are still a matter of debate due to patient randomization issues (202). Regardless, available clinical trials and epidemiological studies collectively vouch for a positive effect of the Mediterranean diet on health and aging. In fact, in PRIMIDED and Lyon Heart trials, non-treated control patients were consuming a relatively healthy diet,

suggesting that the protective effects of the Mediterranean diet might be even stronger, if compared to a standard 'obesogenic' western diet.

Although several mechanisms have been proposed to underlie the beneficence of the Mediterranean diet, its exact mechanisms are still unknown (196). Nonetheless, this diet is known to contain high concentrations of polyamines, including spermidine, and this has been proposed to contribute, at least in part, to its protective cardiovascular effects (203,204). To this end, we decided to examine the clinical relevance and translational potential of our promising preclinical findings (described in Chapters 3 and 4) in humans.
For this purpose, we quantified spermidine levels in non-failing and failing human donor hearts, which are readily available from the Graz Heart Bank. In addition, we studied the correlation between dietary spermidine intake and the incidence of cardiovascular disease in a prospective population-based cohort (Bruneck study).

5.1.3. Bruneck Study: a long-term prospective community-based cohort

The Bruneck study is a prospective community-based cohort on the epidemiology and pathogenesis of atherosclerosis and cardiovascular disease (96). The cohort recruited participants from the Bruneck region (South Tyrol, Italy) taking in consideration equal representation of both genders and different age groups (between 4^{th} and 7^{th} decade). The fact that a single hospital serves the whole community in Bruneck allowed the study to achieve extraordinary participation and long-term follow-up rates for more than 20 years; making this cohort optimal for the study of age-related cardiovascular disorders. In addition, detailed information regarding dietary habits of all participants was made available based on a series of detailed food frequency questionnaires conducted by specialized dietitians (refer to Methods for more details). Combined with thorough medical records on health, disease and survival, these dietary details allowed us to quantify the average intake of spermidine and correlate it to the cardiovascular health status of the participants over the study's duration.

5.2. Results: Cardiac benefits of spermidine in humans

5.2.1. Cardiac spermidine levels progressively decline with age in humans

To provide initial proof that spermidine is involved in preserving human cardiac health, we quantified the absolute concentrations of spermidine in human myocardial biopsies obtained from non-failing and failing donor hearts. The examined samples covered a wide range of ages (26-81 years) and, thus, allowed us to examine – for the first time – whether a correlation exists between person's age and their cardiac spermidine abundance. Indeed, we could detect an inverse linear correlation between age and spermidine levels in the heart (Fig. 32). More importantly, we conducted an additional multi-variate regression analysis, where we found age to be a significant predictor of cardiac spermidine levels independent of potential confounding factors, including heart failure, NT-proBNP and EF (corrected *P=0.003, 0.038, 0.014,* respectively). We concluded that cardiac spermidine levels progressively decline with age, which might, in turn, facilitate the development of heart diseases in the elderly.

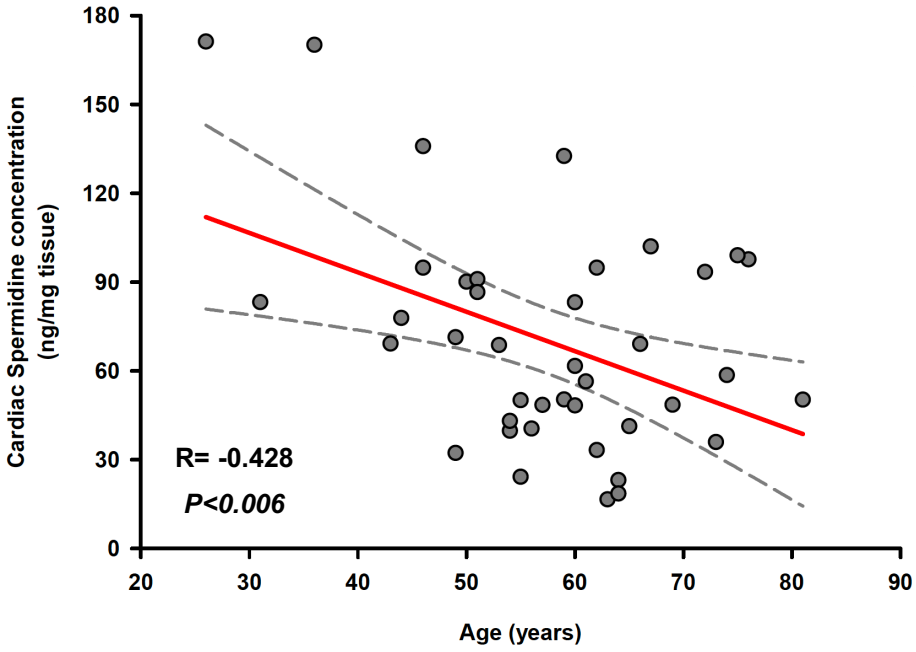

Figure 32. Cardiac spermidine levels progressively decline with age in humans.

Absolute spermidine concentrations were measured in myocardial samples of failing and non-failing heart donors (*n*=40) and correlated to donor's age. Indicated *P* value and correlation coefficient R were derived by Pearson correlation analysis. Additional analyses correcting for EF, NTproBNP or heart failure show consistent results (see text for the respective *P* values of multiple regression analysis).

5.2.2. Human failing hearts exhibit a compensatory increase in spermidine content

To confirm whether spermidine deficiency is implicated in the development of heart failure, we examined the difference in spermidine abundance between failing and non-failing hearts. Specifically, we compared explanted failing hearts from patients of heart failure with reduced or preserved ejection fraction to non-failing donor hearts, which had no history of cardiac abnormalities, and had a comparable age to the heart failure patients. Unexpectedly, both forms of failing hearts, *i.e.*, with preserved or reduced EF, exhibited higher spermidine levels than non-failing hearts (Fig. 33). In light of our experimental results (Chapters 3 and 4), we speculated that higher spermidine levels in heart failure patients are compensatory in nature and might have a rather positive impact. Therefore, we verified this hypothesis as described in the following section.

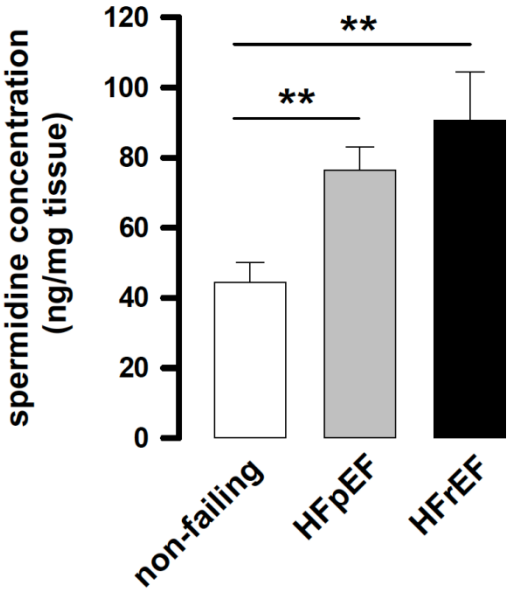

Figure 33. Human failing hearts exhibit a compensatory increase in endogenous spermidine levels.

Cardiac spermidine levels in heart failure with preserved or reduced ejection fraction (HFpEF and HFrEF, respectively) patients compared to non-failing donors. *n*=9-11 hearts/group.

***P*<0.01 *vs.* non-failing by ANOVA followed by Tukey post-hoc test.

5.2.3. Dietary spermidine intake inversely correlates with cardiovascular disease in humans

To substantiate clinical evidence that spermidine plays an active role in determining cardiac health in humans, we examined the correlation between different levels of dietary spermidine intake and cardiovascular disease development in the Bruneck study (a prospective population-based cohort). In line with our hypothesis that spermidine confers cardioprotection in humans, we found that a reported higher

intake of spermidine was associated with a lower general risk of cardiovascular disease, as evaluated by a composite score encompassing acute coronary artery disease, stroke and vascular death (Fig. 34A). More importantly, increased spermidine intake was associated with reduced mortality due to heart failure (Fig. 34B). In fact, dietary spermidine consumption inversely correlated with the clinical biomarker of heart failure, N-terminal pro-B type natriuretic peptide (NT-proBNP; R=-0.115, *P*=0.001), and higher intake of spermidine tended to lower the incidence of overt heart failure (Fig. 34C). Finally, higher consumption of spermidine-rich diet was correlated with lower systolic and diastolic blood pressures (Fig. 34D). Interestingly, spermidine benefits seemed to be more prominent in males (Fig. 34A-D).

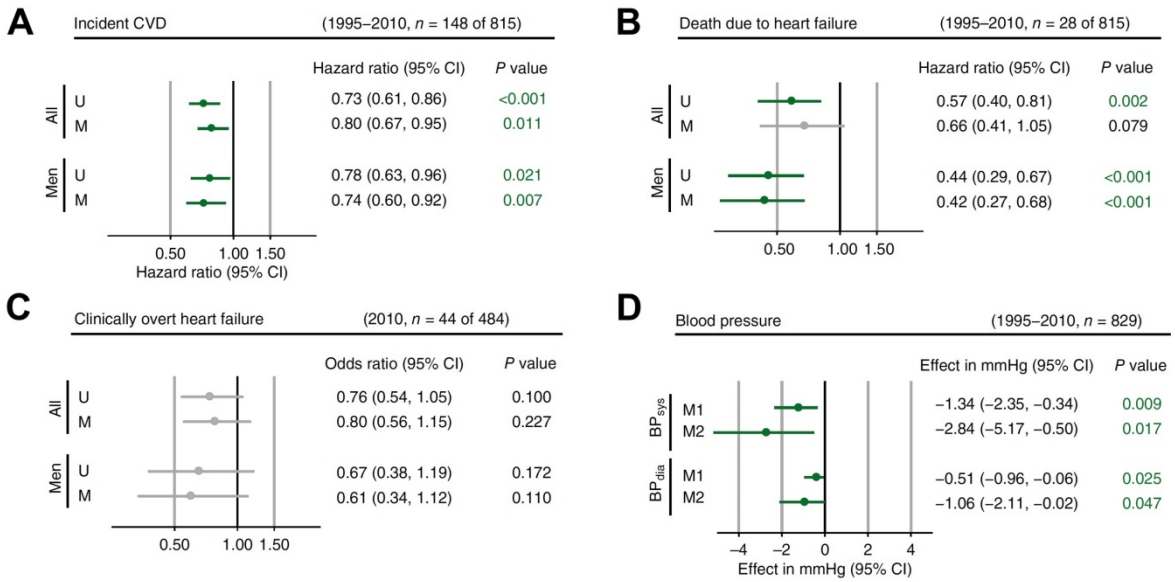

Figure 34. Dietary intake of spermidine inversely correlates with cardiovascular disease in humans

(A) Risk of incident cardiovascular disease (CVD; a composite of acute coronary artery disease, stroke and vascular death) for one standard deviation (SD) higher intake of spermidine (time to event analysis).

(B) Risk of death due to heart failure for one SD higher intake of spermidine (time to event analysis).

(C) Risk of clinically overt heart failure for one SD higher intake of spermidine (cross-sectional analysis).

Models were unadjusted (U) or had multivariable adjustment (M) for age, sex, total caloric intake, smoking, diabetes, alcohol consumption and diastolic blood pressure.

(D) The average difference in systolic (BPsys) and diastolic (BPdia) blood pressures (mm Hg) for one SD higher intake of spermidine (M1) or between the first and third tertile groups (M2) after adjustment for age, sex and total caloric intake. *(These results were generated in collaboration with Dr. Stefan Kiechl, Medical University of Innsbruck)*

5.3. Discussion

In this chapter, we examined the clinical relevance of our preclinical data on spermidine, whereby we took initial steps towards translating our findings to humans. Specifically, we examined human cardiac biopsies, wherein we found spermidine levels to show a progressive decline with age. This is in line with a previous report showing lower spermidine blood levels in the elderly (205), suggesting that inadequate cardiac spermidine might contribute to the pathogenesis of heart disease in late-life stages. Surprisingly, however, patients suffering from heart failure in either of its forms (*i.e.*, reduced or preserved ejection fraction) had higher spermidine levels than those not exhibiting any cardiac abnormalities. That said, such increase in spermidine levels might be an adaptive coping mechanism, one that has a positive impact on disease progression and outcomes. Although this notion might not come as the most intuitive interpretation, such phenomena are not uncommon in medicine or biology. In fact, natriuretic peptides, the most commonly used clinical biomarker for HF, are known to play key beneficial roles in heart failure adaptation. These include, but are not limited to, antagonizing the harmful actions of renin-angiotensin-aldosterone system by inducing natriuresis and vasodilation, as well as sympatho-inhibitory, anti-inflammatory, antioxidative and anti-ischemic effects (206). In fact, exogenous administration of natriuretic peptides is an approved therapy by the FDA (Food and Drug Administration in the United States) for advanced decompensated congestive heart failure patients (206). Therefore, increased cardiac spermidine levels in HF could be, like natriuretic peptides, adaptive and may even be beneficial.

In support of this hypothesis, we found consuming a spermidine-rich diet to be associated with a lower risk of heart failure, hypertension and general cardiovascular disease and related mortality in a prospective cohort. Along similar lines, Kiechl *et al.* have recently shown that a spermidine-rich diet is also associated with reduced all-cause mortality (207). Precisely, one standard deviation higher intake of spermidine was associated with 24% lower risk of overall mortality, after adjusting for several confounding factors, including age, sex, BMI, smoking, diabetes, hypertension, socioeconomic status, physical activity, caloric intake-to-energy expenditure ratio, alcohol consumption, and aspirin medication (207).

Furthermore, cause-specific mortality was reduced upon increased dietary intake of spermidine as exemplified by the lower risk of vascular and cancer mortality (207).

It is important to mention that despite adjusting for a wide array of potential confounding factors, neither nutritional, nor epidemiological evidence *per se* are sufficient to prove the clinical utility of medical interventions. In this regard, randomized clinical trials are pivotal to provide definitive evidence that spermidine can promote health and longevity in humans. That being said, a small pilot trial has been recently conducted to determine the safety and tolerability of spermidine in the elderly (60-80 years old) with subjective cognitive decline (208). Although the applied dose was quite low (1.2 mg spermidine/day for 3 months), the supplementation of spermidine in the form of a plant-rich extract was safe and well-tolerated and also associated with a positive, albeit modest, impact on memory performance (208,209).

Taken together, available clinical evidence supports the notion that spermidine might promote health and longevity in humans as it does in animals. However, the upcoming years will reveal whether spermidine is ready for clinical use by performing large clinical trials and providing sufficient doses of spermidine.

6. CONCLUSIONS

6. Conclusions

Through a series of animal experiments and clinical studies, including human myocardial tissues and a large prospective cohort, we have demonstrated that the polyamine spermidine effectively attenuates cardiac aging and protects from cardiovascular disease. Hence, we can conclude that spermidine holds great promise to reduce the burden of cardiovascular disease in our aging society. Mechanistically, the startling cardioprotective ability of spermidine against aging and other risk factors, like hypertension, seems to pertain to multiple factors:

Firstly, spermidine is a naturally occurring polyamine, whose cellular levels progressively decline with age. This includes, as we demonstrated for the first time here, human myocardial tissue. Therefore, supplementation of spermidine appears necessary to restore its physiological levels. This could be especially relevant in individuals following dietary patterns that are inherently poor in spermidine intake and, thus, would be at a higher risk of experiencing an exaggerated late-life reduction in spermidine concentrations. Similarly, exogenous supplementation might be important for those in high spermidine demand, such as heart failure patients, whom we have found to show a compensatory, yet inadequate, increase in spermidine levels. Taken together, by virtue of restoring adequate levels of spermidine during times of need (reduced production or high demand), spermidine supplementation might restore essential functions of vitally important polyamines, and, thus, promote health and delay aging.

Secondly, spermidine, like caloric restriction, boosts the cellular homeostatic mechanism autophagy, which is responsible for cleaning and recycling cellular waste in different body organs, including the heart. Interestingly, the efficiency of autophagy is also known to progressively decline with aging under the influence of reduced activity of its molecular machinery and increased work demand due to mounting waste accumulation with aging. In fact, diminished autophagy is postulated as one of the driving forces for aging. Contrarily, various autophagy-promoting strategies successfully delay aging and promote longevity. Hence, the protective effects of spermidine could stem, at least in part, from rescuing the cellular ability to eliminate harmful contents by autophagy induction. In fact,

spermidine feeding did not exert any cardio-beneficial effects in transgenic mice lacking essential autophagy genes. In fact, these mice tended to do worse under spermidine supplementation. This does not only strongly suggest that autophagy underlies the cardioprotective effects of spermidine, but also illustrates that intact autophagic machinery is a prerequisite for spermidine use.

Thirdly, spermidine supplementation exerts a negative feedback on *de novo* polyamine biosynthesis from their precursor, the amino acid arginine. Therefore, endogenous polyamine production seems to be spared by exogenous spermidine and, thus, arginine is instead re-routed towards generating the vasodilator NO. Spermidine might further improve NO bioavailability indirectly *via* limiting its breakdown by reactive oxygen species. We attribute this outcome to a newly identified anti-inflammatory effect of spermidine against subclinical sterile inflammation, which also can on its own confer cardioprotection independent of associated NO abundance. These systemic effects on NO and inflammation can contribute to, or possibly underlie the beneficial effects of spermidine not only against aging, but also hypertension, the most common risk factor for cardiovascular disease in the elderly.

In summary, spermidine supplementation improves cardiovascular health through multiple cardiac-specific and systemic effects, which effectively counteract the detrimental effects of aging and related disease and, thus, restore cellular homeostasis and normal function. Of note, many aspects of spermidine-mediated cardioprotection are common to caloric restriction (Fig. 35). Therefore, spermidine is considered a caloric restriction mimetic, which in addition to being natural and safe, might offer wider adherence and compliance than commonly suggested stringent dietary interventions that involve cumbersome food abstinence or radical changes in dietary habits. That being said, future clinical trials only will reveal whether spermidine is suitable for clinical use to counteract age-related cardiovascular disorders in humans.

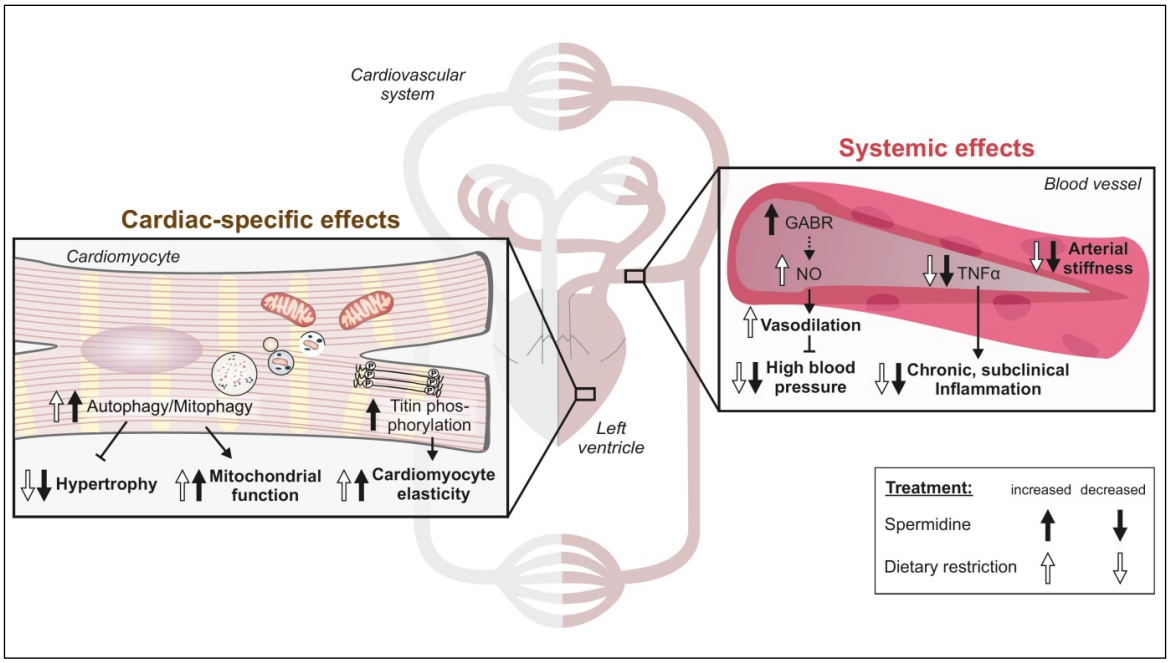

Figure 35. Spermidine improves aspects of cardiovascular health in a similar fashion to caloric restriction.

Cardiac-specific and systemic effects of spermidine, which underlie cardioprotection against aging and hypertension are depicted. In addition, these effects are compared to those of caloric restriction (black arrows in case of spermidine and white ones in case of caloric restriction). Abbreviations: GABR, global arginine bioavailability ratio; NO, nitric oxide; TTN, titin. *This figure is reproduced from Eisenberg and Abdellatif et al., Autophagy, 2017; Ref.* (210) *with permission from the publisher (Taylor & Francis).*

7. REFERENCES

7. References

1. Piraino S, Boero F, Aeschbach B, Schmid V. Reversing the Life Cycle: Medusae Transforming into Polyps and Cell Transdifferentiation in Turritopsis nutricula (Cnidaria, Hydrozoa). Biol Bull. 1996 Jun;190(3):302–12.
2. Keane M, Semeiks J, Webb AE, Li YI, Quesada V, Craig T, et al. Insights into the evolution of longevity from the bowhead whale genome. Cell Rep. 2015 Jan;10(1):112–22.
3. Nielsen J, Hedeholm RB, Heinemeier J, Bushnell PG, Christiansen JS, Olsen J, et al. Eye lens radiocarbon reveals centuries of longevity in the Greenland shark (Somniosus microcephalus). Science. 2016 Aug;353(6300):702–4.
4. Guzman J. Ageing in the Twenty-First Century: A Celebration and A Challenge. 2012.
5. Osborne TB, Mendel LB, Ferry EL. THE EFFECT OF RETARDATION OF GROWTH UPON THE BREEDING PERIOD AND DURATION OF LIFE OF RATS. Science. 1917 Mar;45(1160):294–5.
6. Speakman JR, Hambly C. Starving for life: what animal studies can and cannot tell us about the use of caloric restriction to prolong human lifespan. J Nutr. 2007 Apr;137(4):1078–86.
7. Longo VD, Mattson MP. Fasting: molecular mechanisms and clinical applications. Cell Metab. 2014 Feb;19(2):181–92.
8. Cruzen C, Colman RJ. Effects of caloric restriction on cardiovascular aging in non-human primates and humans. Clin Geriatr Med. 2009 Nov;25(4):733–43, ix–x.
9. Di Francesco A, Di Germanio C, Bernier M, de Cabo R. A time to fast. Science. 2018 Nov;362(6416):770–5.
10. Mitchell SJ, Madrigal-Matute J, Scheibye-Knudsen M, Fang E, Aon M, Gonzalez-Reyes JA, et al. Effects of Sex, Strain, and Energy Intake on Hallmarks of Aging in Mice. Cell Metab. 2016 Jun;23(6):1093–112.
11. Al-Regaiey KA, Masternak MM, Bonkowski M, Sun L, Bartke A. Long-lived growth hormone receptor knockout mice: interaction of reduced insulin-like growth factor i/insulin signaling and caloric restriction. Endocrinology. 2005 Feb;146(2):851–60.

12. Speakman JR, Mitchell SE. Caloric restriction. Mol Aspects Med. 2011 Jun;32(3):159–221.
13. Fontana L, Villareal DT, Das SK, Smith SR, Meydani SN, Pittas AG, et al. Effects of 2-year calorie restriction on circulating levels of IGF-1, IGF-binding proteins and cortisol in nonobese men and women: a randomized clinical trial. Aging Cell. 2016 Feb;15(1):22–7.
14. Rincon M, Muzumdar R, Atzmon G, Barzilai N. The paradox of the insulin/IGF-1 signaling pathway in longevity. Mech Ageing Dev. 2004 Jun;125(6):397–403.
15. Anversa P. Aging and longevity: the IGF-1 enigma. Vol. 97, Circulation research. United States; 2005. p. 411–4.
16. Yuan R, Tsaih S-W, Petkova SB, Marin de Evsikova C, Xing S, Marion MA, et al. Aging in inbred strains of mice: study design and interim report on median lifespans and circulating IGF1 levels. Aging Cell. 2009 Jun;8(3):277–87.
17. Milman S, Atzmon G, Huffman DM, Wan J, Crandall JP, Cohen P, et al. Low insulin-like growth factor-1 level predicts survival in humans with exceptional longevity. Aging Cell. 2014 Aug;13(4):769–71.
18. van der Spoel E, Rozing MP, Houwing-Duistermaat JJ, Slagboom PE, Beekman M, de Craen AJM, et al. Association analysis of insulin-like growth factor-1 axis parameters with survival and functional status in nonagenarians of the Leiden Longevity Study. Aging (Albany NY). 2015 Nov;7(11):956–63.
19. Ben-Avraham D, Govindaraju DR, Budagov T, Fradin D, Durda P, Liu B, et al. The GH receptor exon 3 deletion is a marker of male-specific exceptional longevity associated with increased GH sensitivity and taller stature. Sci Adv. 2017 Jun;3(6):e1602025.
20. Ock S, Lee WS, Ahn J, Kim HM, Kang H, Kim H-S, et al. Deletion of IGF-1 Receptors in Cardiomyocytes Attenuates Cardiac Aging in Male Mice. Endocrinology. 2016 Jan;157(1):336–45.
21. Li Q, Ceylan-Isik AF, Li J, Ren J. Deficiency of insulin-like growth factor 1 reduces sensitivity to aging-associated cardiomyocyte dysfunction. Rejuvenation Res. 2008 Aug;11(4):725–33.
22. Delaughter MC, Taffet GE, Fiorotto ML, Entman ML, Schwartz RJ. Local insulin-like growth factor I expression induces physiologic, then pathologic,

cardiac hypertrophy in transgenic mice. FASEB J Off Publ Fed Am Soc Exp Biol. 1999 Nov;13(14):1923–9.

23. Li Q, Wu S, Li S-Y, Lopez FL, Du M, Kajstura J, et al. Cardiac-specific overexpression of insulin-like growth factor 1 attenuates aging-associated cardiac diastolic contractile dysfunction and protein damage. Am J Physiol Heart Circ Physiol. 2007 Mar;292(3):H1398-403.
24. Csiszar A, Labinskyy N, Perez V, Recchia FA, Podlutsky A, Mukhopadhyay P, et al. Endothelial function and vascular oxidative stress in long-lived GH/IGF-deficient Ames dwarf mice. Am J Physiol Heart Circ Physiol. 2008 Nov;295(5):H1882-94.
25. Reddy AK, Hartley CJ, Pham TT, Darlington G, Entman ML, Taffet GE. Young little mice express a premature cardiovascular aging phenotype. J Gerontol A Biol Sci Med Sci. 2014 Feb;69(2):152–9.
26. Abbas A, Imrie H, Viswambharan H, Sukumar P, Rajwani A, Cubbon RM, et al. The insulin-like growth factor-1 receptor is a negative regulator of nitric oxide bioavailability and insulin sensitivity in the endothelium. Diabetes. 2011 Aug;60(8):2169–78.
27. Yuldasheva NY, Rashid ST, Haywood NJ, Cordell P, Mughal R, Viswambharan H, et al. Haploinsufficiency of the insulin-like growth factor-1 receptor enhances endothelial repair and favorably modifies angiogenic progenitor cell phenotype. Arterioscler Thromb Vasc Biol. 2014 Sep;34(9):2051–8.
28. Shinmura K, Tamaki K, Sano M, Murata M, Yamakawa H, Ishida H, et al. Impact of long-term caloric restriction on cardiac senescence: caloric restriction ameliorates cardiac diastolic dysfunction associated with aging. J Mol Cell Cardiol. 2011 Jan;50(1):117–27.
29. Bjornsti M-A, Houghton PJ. The TOR pathway: a target for cancer therapy. Nat Rev Cancer. 2004 May;4(5):335–48.
30. Hua Y, Zhang Y, Ceylan-Isik AF, Wold LE, Nunn JM, Ren J. Chronic Akt activation accentuates aging-induced cardiac hypertrophy and myocardial contractile dysfunction: role of autophagy. Basic Res Cardiol. 2011 Nov;106(6):1173–91.
31. Johnson SC, Rabinovitch PS, Kaeberlein M. mTOR is a key modulator of ageing and age-related disease. Nature. 2013 Jan;493(7432):338–45.

32. Harrison DE, Strong R, Sharp ZD, Nelson JF, Astle CM, Flurkey K, et al. Rapamycin fed late in life extends lifespan in genetically heterogeneous mice. Nature. 2009 Jul;460(7253):392–5.
33. Miller RA, Harrison DE, Astle CM, Baur JA, Boyd AR, de Cabo R, et al. Rapamycin, but not resveratrol or simvastatin, extends life span of genetically heterogeneous mice. J Gerontol A Biol Sci Med Sci. 2011 Feb;66(2):191–201.
34. Flynn JM, O'Leary MN, Zambataro CA, Academia EC, Presley MP, Garrett BJ, et al. Late-life rapamycin treatment reverses age-related heart dysfunction. Aging Cell. 2013 Oct;12(5):851–62.
35. Lesniewski LA, Seals DR, Walker AE, Henson GD, Blimline MW, Trott DW, et al. Dietary rapamycin supplementation reverses age-related vascular dysfunction and oxidative stress, while modulating nutrient-sensing, cell cycle, and senescence pathways. Aging Cell. 2017 Feb;16(1):17–26.
36. Lamming DW, Ye L, Katajisto P, Goncalves MD, Saitoh M, Stevens DM, et al. Rapamycin-induced insulin resistance is mediated by mTORC2 loss and uncoupled from longevity. Science. 2012 Mar;335(6076):1638–43.
37. Neff F, Flores-Dominguez D, Ryan DP, Horsch M, Schroder S, Adler T, et al. Rapamycin extends murine lifespan but has limited effects on aging. J Clin Invest. 2013 Aug;123(8):3272–91.
38. Houtkooper RH, Pirinen E, Auwerx J. Sirtuins as regulators of metabolism and healthspan. Nat Rev Mol Cell Biol. 2012 Mar;13(4):225–38.
39. Picard F, Kurtev M, Chung N, Topark-Ngarm A, Senawong T, Machado De Oliveira R, et al. Sirt1 promotes fat mobilization in white adipocytes by repressing PPAR-gamma. Nature. 2004 Jun;429(6993):771–6.
40. Li Y, Xu W, McBurney MW, Longo VD. SirT1 inhibition reduces IGF-I/IRS-2/Ras/ERK1/2 signaling and protects neurons. Cell Metab. 2008 Jul;8(1):38–48.
41. Zhang H, Ryu D, Wu Y, Gariani K, Wang X, Luan P, et al. NAD(+) repletion improves mitochondrial and stem cell function and enhances life span in mice. Science. 2016 Jun;352(6292):1436–43.
42. Kanfi Y, Naiman S, Amir G, Peshti V, Zinman G, Nahum L, et al. The sirtuin SIRT6 regulates lifespan in male mice. Nature. 2012 Feb;483(7388):218–21.
43. Herranz D, Munoz-Martin M, Canamero M, Mulero F, Martinez-Pastor B, Fernandez-Capetillo O, et al. Sirt1 improves healthy ageing and protects from

metabolic syndrome-associated cancer. Nat Commun. 2010 Apr;1:3.

44. Pearson KJ, Baur JA, Lewis KN, Peshkin L, Price NL, Labinskyy N, et al. Resveratrol delays age-related deterioration and mimics transcriptional aspects of dietary restriction without extending life span. Cell Metab. 2008 Aug;8(2):157–68.
45. Baur JA, Pearson KJ, Price NL, Jamieson HA, Lerin C, Kalra A, et al. Resveratrol improves health and survival of mice on a high-calorie diet. Nature. 2006 Nov;444(7117):337–42.
46. Minor RK, Baur JA, Gomes AP, Ward TM, Csiszar A, Mercken EM, et al. SRT1720 improves survival and healthspan of obese mice. Sci Rep. 2011;1:70.
47. Alcendor RR, Gao S, Zhai P, Zablocki D, Holle E, Yu X, et al. Sirt1 regulates aging and resistance to oxidative stress in the heart. Circ Res. 2007 May;100(10):1512–21.
48. Hafner A V, Dai J, Gomes AP, Xiao C-Y, Palmeira CM, Rosenzweig A, et al. Regulation of the mPTP by SIRT3-mediated deacetylation of CypD at lysine 166 suppresses age-related cardiac hypertrophy. Aging (Albany NY). 2010 Dec;2(12):914–23.
49. Donato AJ, Magerko KA, Lawson BR, Durrant JR, Lesniewski LA, Seals DR. SIRT-1 and vascular endothelial dysfunction with ageing in mice and humans. J Physiol. 2011 Sep;589(Pt 18):4545–54.
50. Hardie DG, Carling D. The AMP-activated protein kinase--fuel gauge of the mammalian cell? Eur J Biochem. 1997 Jun;246(2):259–73.
51. Miller BF, Robinson MM, Bruss MD, Hellerstein M, Hamilton KL. A comprehensive assessment of mitochondrial protein synthesis and cellular proliferation with age and caloric restriction. Aging Cell. 2012 Feb;11(1):150–61.
52. Edwards AG, Donato AJ, Lesniewski LA, Gioscia RA, Seals DR, Moore RL. Life-long caloric restriction elicits pronounced protection of the aged myocardium: a role for AMPK. Mech Ageing Dev. 2010;131(11–12):739–42.
53. Jager S, Handschin C, St-Pierre J, Spiegelman BM. AMP-activated protein kinase (AMPK) action in skeletal muscle via direct phosphorylation of PGC-1alpha. Proc Natl Acad Sci U S A. 2007 Jul;104(29):12017–22.
54. Turdi S, Fan X, Li J, Zhao J, Huff AF, Du M, et al. AMP-activated protein

kinase deficiency exacerbates aging-induced myocardial contractile dysfunction. Aging Cell. 2010 Aug;9(4):592–606.

55. Lesniewski LA, Zigler MC, Durrant JR, Donato AJ, Seals DR. Sustained activation of AMPK ameliorates age-associated vascular endothelial dysfunction via a nitric oxide-independent mechanism. Mech Ageing Dev. 2012 May;133(5):368–71.
56. Pu Y, Zhang H, Wang P, Zhao Y, Li Q, Wei X, et al. Dietary curcumin ameliorates aging-related cerebrovascular dysfunction through the AMPK/uncoupling protein 2 pathway. Cell Physiol Biochem. 2013;32(5):1167–77.
57. Martin-Montalvo A, Mercken EM, Mitchell SJ, Palacios HH, Mote PL, Scheibye-Knudsen M, et al. Metformin improves healthspan and lifespan in mice. Nat Commun. 2013;4:2192.
58. Anisimov VN, Berstein LM, Egormin PA, Piskunova TS, Popovich IG, Zabezhinski MA, et al. Metformin slows down aging and extends life span of female SHR mice. Cell Cycle. 2008 Sep;7(17):2769–73.
59. Wang C-P, Lorenzo C, Habib SL, Jo B, Espinoza SE. Differential effects of metformin on age related comorbidities in older men with type 2 diabetes. J Diabetes Complications. 2017 Apr;31(4):679–86.
60. Santos-Parker JR, Strahler TR, Bassett CJ, Bispham NZ, Chonchol MB, Seals DR. Curcumin supplementation improves vascular endothelial function in healthy middle-aged and older adults by increasing nitric oxide bioavailability and reducing oxidative stress. Aging (Albany NY). 2017 Jan;9(1):187–208.
61. Wang J, Song Y, Li H, Shen Q, Shen J, An X, et al. Exacerbated cardiac fibrosis induced by beta-adrenergic activation in old mice due to decreased AMPK activity. Clin Exp Pharmacol Physiol. 2016 Nov;43(11):1029–37.
62. Galluzzi L, Pietrocola F, Levine B, Kroemer G. Metabolic control of autophagy. Cell. 2014 Dec;159(6):1263–76.
63. Sica V, Galluzzi L, Bravo-San Pedro JM, Izzo V, Maiuri MC, Kroemer G. Organelle-Specific Initiation of Autophagy. Mol Cell. 2015 Aug;59(4):522–39.
64. Rubinsztein DC, Marino G, Kroemer G. Autophagy and aging. Cell. 2011 Sep;146(5):682–95.
65. Levine B, Kroemer G. Autophagy in the pathogenesis of disease. Cell. 2008

Jan;132(1):27–42.

66. Cuervo AM. Autophagy and aging: keeping that old broom working. Trends Genet. 2008 Dec;24(12):604–12.
67. Melendez A, Talloczy Z, Seaman M, Eskelinen E-L, Hall DH, Levine B. Autophagy genes are essential for dauer development and life-span extension in C. elegans. Science. 2003 Sep;301(5638):1387–91.
68. Morselli E, Maiuri MC, Markaki M, Megalou E, Pasparaki A, Palikaras K, et al. Caloric restriction and resveratrol promote longevity through the Sirtuin-1-dependent induction of autophagy. Cell Death Dis. 2010;1:e10.
69. Yang S, Long L-H, Li D, Zhang J-K, Jin S, Wang F, et al. beta-Guanidinopropionic acid extends the lifespan of Drosophila melanogaster via an AMP-activated protein kinase-dependent increase in autophagy. Aging Cell. 2015 Dec;14(6):1024–33.
70. Abdellatif M, Sedej S, Carmona-Gutierrez D, Madeo F, Kroemer G. Autophagy in cardiovascular aging. Circ Res. 2018;123(7):803–24.
71. Jia K, Levine B. Autophagy is required for dietary restriction-mediated life span extension in C. elegans. Autophagy. 2007;3(6):597–9.
72. Gelino S, Chang JT, Kumsta C, She X, Davis A, Nguyen C, et al. Intestinal Autophagy Improves Healthspan and Longevity in C. elegans during Dietary Restriction. PLoS Genet. 2016 Jul;12(7):e1006135.
73. Madeo F, Tavernarakis N, Kroemer G. Can autophagy promote longevity? Nat Cell Biol. 2010 Sep;12(9):842–6.
74. Madeo F, Zimmermann A, Maiuri MC, Kroemer G. Essential role for autophagy in life span extension. J Clin Invest. 2015 Jan;125(1):85–93.
75. Galluzzi L, Bravo-San Pedro JM, Levine B, Green DR, Kroemer G. Pharmacological modulation of autophagy: therapeutic potential and persisting obstacles. Nat Rev Drug Discov. 2017 Jul;16(7):487–511.
76. Marino G, Pietrocola F, Madeo F, Kroemer G. Caloric restriction mimetics: natural/physiological pharmacological autophagy inducers. Vol. 10, Autophagy. United States; 2014. p. 1879–82.
77. Pegg AE. Functions of Polyamines in Mammals. J Biol Chem. 2016 Jul;291(29):14904–12.
78. Madeo F, Eisenberg T, Pietrocola F, Kroemer G. Spermidine in health and disease. Science. 2018 Jan;359(6374).

79. Scalabrino G, Ferioli ME. Polyamines in mammalian ageing: an oncological problem, too? A review. Mech Ageing Dev. 1984 Aug;26(2–3):149–64.
80. Eisenberg T, Knauer H, Schauer A, Buttner S, Ruckenstuhl C, Carmona-Gutierrez D, et al. Induction of autophagy by spermidine promotes longevity. Nat Cell Biol. 2009 Nov;11(11):1305–14.
81. Gupta VK, Scheunemann L, Eisenberg T, Mertel S, Bhukel A, Koemans TS, et al. Restoring polyamines protects from age-induced memory impairment in an autophagy-dependent manner. Nat Neurosci. 2013 Oct;16(10):1453–60.
82. Taneike M, Yamaguchi O, Nakai A, Hikoso S, Takeda T, Mizote I, et al. Inhibition of autophagy in the heart induces age-related cardiomyopathy. Autophagy. 2010 Jul;6(5):600–6.
83. Doi R, Masuyama T, Yamamoto K, Doi Y, Mano T, Sakata Y, et al. Development of different phenotypes of hypertensive heart failure: systolic versus diastolic failure in Dahl salt-sensitive rats. J Hypertens. 2000 Jan;18(1):111–20.
84. Kilkenny C, Browne WJ, Cuthill IC, Emerson M, Altman DG. Improving bioscience research reporting: the ARRIVE guidelines for reporting animal research. PLoS Biol. 2010 Jun;8(6):e1000412.
85. Troy BL, Pombo J, Rackley CE. Measurement of left ventricular wall thickness and mass by echocardiography. Circulation. 1972 Mar;45(3):602–11.
86. Burkhoff D, Mirsky I, Suga H. Assessment of systolic and diastolic ventricular properties via pressure-volume analysis: a guide for clinical, translational, and basic researchers. Am J Physiol Heart Circ Physiol. 2005 Aug;289(2):H501-12.
87. Wolf D, Hochegger K, Wolf AM, Rumpold HF, Gastl G, Tilg H, et al. CD4+CD25+ regulatory T cells inhibit experimental anti-glomerular basement membrane glomerulonephritis in mice. J Am Soc Nephrol. 2005 May;16(5):1360–70.
88. Magnes C, Fauland A, Gander E, Narath S, Ratzer M, Eisenberg T, et al. Polyamines in biological samples: rapid and robust quantification by solid-phase extraction online-coupled to liquid chromatography-tandem mass spectrometry. J Chromatogr A. 2014 Feb;1331:44–51.
89. Boykins RA, Liu TY. Micro-analysis of amino acids. J Biochem Biophys Methods. 1982 Dec;7(1):55–65.

90. Duicu OM, Mirica SN, Gheorgheosu DE, Privistirescu AI, Fira-Mladinescu O, Muntean DM. Ageing-induced decrease in cardiac mitochondrial function in healthy rats. Can J Physiol Pharmacol. 2013 Aug;91(8):593–600.
91. Hariharan N, Zhai P, Sadoshima J. Oxidative stress stimulates autophagic flux during ischemia/reperfusion. Antioxid Redox Signal. 2011 Jun;14(11):2179–90.
92. Shirakabe A, Fritzky L, Saito T, Zhai P, Miyamoto S, Gustafsson AB, et al. Evaluating mitochondrial autophagy in the mouse heart. J Mol Cell Cardiol. 2016 Mar;92:134–9.
93. Hamdani N, Krysiak J, Kreusser MM, Neef S, Dos Remedios CG, Maier LS, et al. Crucial role for Ca2(+)/calmodulin-dependent protein kinase-II in regulating diastolic stress of normal and failing hearts via titin phosphorylation. Circ Res. 2013 Feb;112(4):664–74.
94. Muhlfeld C, Nyengaard JR, Mayhew TM. A review of state-of-the-art stereology for better quantitative 3D morphology in cardiac research. Cardiovasc Pathol. 2010;19(2):65–82.
95. Mayhew TM. Taking tissue samples from the placenta: an illustration of principles and strategies. Placenta. 2008 Jan;29(1):1–14.
96. Kiechl S, Willeit J. In a Nutshell: Findings from the Bruneck Study. Gerontology. 2019;65(1):9–19.
97. Willett WC, Sampson L, Stampfer MJ, Rosner B, Bain C, Witschi J, et al. Reproducibility and validity of a semiquantitative food frequency questionnaire. Am J Epidemiol. 1985 Jul;122(1):51–65.
98. McKee PA, Castelli WP, McNamara PM, Kannel WB. The natural history of congestive heart failure: the Framingham study. N Engl J Med. 1971 Dec;285(26):1441–6.
99. Willett W, Stampfer MJ. Total energy intake: implications for epidemiologic analyses. Am J Epidemiol. 1986 Jul;124(1):17–27.
100. Eisenberg T, Abdellatif M, Schroeder S, Primessnig U, Stekovic S, Pendl T, et al. Cardioprotection and lifespan extension by the natural polyamine spermidine. Nat Med. 2016 Dec;22(12):1428–38.
101. Horn MA, Trafford AW. Aging and the cardiac collagen matrix: Novel mediators of fibrotic remodelling. J Mol Cell Cardiol. 2016 Apr;93:175–85.
102. de Souza RR. Aging of myocardial collagen. Biogerontology. 2002;3(6):325–

35.

103. Lakatta EG, Levy D. Arterial and cardiac aging: major shareholders in cardiovascular disease enterprises: Part II: the aging heart in health: links to heart disease. Circulation. 2003 Jan;107(2):346–54.
104. Levy D, Anderson KM, Savage DD, Kannel WB, Christiansen JC, Castelli WP. Echocardiographically detected left ventricular hypertrophy: prevalence and risk factors. The Framingham Heart Study. Ann Intern Med. 1988 Jan;108(1):7–13.
105. Antelmi I, de Paula RS, Shinzato AR, Peres CA, Mansur AJ, Grupi CJ. Influence of age, gender, body mass index, and functional capacity on heart rate variability in a cohort of subjects without heart disease. Am J Cardiol. 2004 Feb;93(3):381–5.
106. North BJ, Sinclair DA. The intersection between aging and cardiovascular disease. Circ Res. 2012 Apr;110(8):1097–108.
107. Strait JB, Lakatta EG. Aging-associated cardiovascular changes and their relationship to heart failure. Heart Fail Clin. 2012 Jan;8(1):143–64.
108. Stamford BA. Exercise and the elderly. Exerc Sport Sci Rev. 1988;16:341–79.
109. Nilsson PM, Khalili P, Franklin SS. Blood pressure and pulse wave velocity as metrics for evaluating pathologic ageing of the cardiovascular system. Blood Press. 2014 Feb;23(1):17–30.
110. Sawabe M. Vascular aging: from molecular mechanism to clinical significance. Geriatr Gerontol Int. 2010 Jul;10 Suppl 1:S213-20.
111. Collins C, Tzima E. Hemodynamic forces in endothelial dysfunction and vascular aging. Exp Gerontol. 2011;46(2–3):185–8.
112. Brandes RP, Fleming I, Busse R. Endothelial aging. Cardiovasc Res. 2005 May;66(2):286–94.
113. Dai D-F, Rabinovitch PS, Ungvari Z. Mitochondria and cardiovascular aging. Circ Res. 2012 Apr;110(8):1109–24.
114. Lesnefsky EJ, Chen Q, Hoppel CL. Mitochondrial Metabolism in Aging Heart. Circ Res. 2016 May;118(10):1593–611.
115. Bergmann O, Bhardwaj RD, Bernard S, Zdunek S, Barnabe-Heider F, Walsh S, et al. Evidence for cardiomyocyte renewal in humans. Science. 2009 Apr;324(5923):98–102.

116. Morimoto RI, Cuervo AM. Protein homeostasis and aging: taking care of proteins from the cradle to the grave. J Gerontol A Biol Sci Med Sci. 2009 Feb;64(2):167–70.
117. Martin GM. Cellular aging--postreplicative cells. A review (Part II). Am J Pathol. 1977 Nov;89(2):513–30.
118. Terman A, Brunk UT. Myocyte aging and mitochondrial turnover. Exp Gerontol. 2004 May;39(5):701–5.
119. Herraiz-Martinez A, Alvarez-Garcia J, Llach A, Molina CE, Fernandes J, Ferrero-Gregori A, et al. Ageing is associated with deterioration of calcium homeostasis in isolated human right atrial myocytes. Cardiovasc Res. 2015 Apr;106(1):76–86.
120. Signore S, Sorrentino A, Borghetti G, Cannata A, Meo M, Zhou Y, et al. Late Na(+) current and protracted electrical recovery are critical determinants of the aging myopathy. Nat Commun. 2015 Nov;6:8803.
121. Kajstura J, Cheng W, Sarangarajan R, Li P, Li B, Nitahara JA, et al. Necrotic and apoptotic myocyte cell death in the aging heart of Fischer 344 rats. Am J Physiol. 1996 Sep;271(3 Pt 2):H1215-28.
122. Paulus WJ, Tschope C. A novel paradigm for heart failure with preserved ejection fraction: comorbidities drive myocardial dysfunction and remodeling through coronary microvascular endothelial inflammation. J Am Coll Cardiol. 2013 Jul;62(4):263–71.
123. Csiszar A, Gautam T, Sosnowska D, Tarantini S, Banki E, Tucsek Z, et al. Caloric restriction confers persistent anti-oxidative, pro-angiogenic, and anti-inflammatory effects and promotes anti-aging miRNA expression profile in cerebromicrovascular endothelial cells of aged rats. Am J Physiol Heart Circ Physiol. 2014 Aug;307(3):H292-306.
124. Moslehi J, DePinho RA, Sahin E. Telomeres and mitochondria in the aging heart. Circ Res. 2012 Apr;110(9):1226–37.
125. Csiszar A, Ungvari Z, Edwards JG, Kaminski P, Wolin MS, Koller A, et al. Aging-induced phenotypic changes and oxidative stress impair coronary arteriolar function. Circ Res. 2002 Jun;90(11):1159–66.
126. Radovits T, Seres L, Gero D, Lin L, Beller CJ, Chen S-H, et al. The peroxynitrite decomposition catalyst FP15 improves ageing-associated cardiac and vascular dysfunction. Mech Ageing Dev. 2007 Feb;128(2):173–

81.
127. Martin-Fernandez B, Gredilla R. Mitochondria and oxidative stress in heart aging. Age (Dordr). 2016 Aug;38(4):225–38.
128. Chiao YA, Rabinovitch PS. The Aging Heart. Cold Spring Harb Perspect Med. 2015 Sep;5(9):a025148.
129. LaRocca TJ, Gioscia-Ryan RA, Hearon CMJ, Seals DR. The autophagy enhancer spermidine reverses arterial aging. Mech Ageing Dev. 2013;134(7–8):314–20.
130. Dai D-F, Santana LF, Vermulst M, Tomazela DM, Emond MJ, MacCoss MJ, et al. Overexpression of catalase targeted to mitochondria attenuates murine cardiac aging. Circulation. 2009 Jun;119(21):2789–97.
131. Krysiak J, Unger A, Beckendorf L, Hamdani N, von Frieling-Salewsky M, Redfield MM, et al. Protein phosphatase 5 regulates titin phosphorylation and function at a sarcomere-associated mechanosensor complex in cardiomyocytes. Nat Commun. 2018 Jan;9(1):262.
132. Shirakabe A, Ikeda Y, Sciarretta S, Zablocki DK, Sadoshima J. Aging and Autophagy in the Heart. Circ Res. 2016 May;118(10):1563–76.
133. Omodei D, Fontana L. Calorie restriction and prevention of age-associated chronic disease. FEBS Lett. 2011 Jun;585(11):1537–42.
134. Postnikoff SDL, Johnson JE, Tyler JK. The integrated stress response in budding yeast lifespan extension. Microb cell (Graz, Austria). 2017 Oct;4(11):368–75.
135. Sheng Y, Lv S, Huang M, Lv Y, Yu J, Liu J, et al. Opposing effects on cardiac function by calorie restriction in different-aged mice. Aging Cell. 2017 Oct;16(5):1155–67.
136. Barger JL, Kayo T, Vann JM, Arias EB, Wang J, Hacker TA, et al. A low dose of dietary resveratrol partially mimics caloric restriction and retards aging parameters in mice. PLoS One. 2008 Jun;3(6):e2264.
137. Yan L, Gao S, Ho D, Park M, Ge H, Wang C, et al. Calorie restriction can reverse, as well as prevent, aging cardiomyopathy. Age (Dordr). 2013 Dec;35(6):2177–82.
138. Dai D-F, Karunadharma PP, Chiao YA, Basisty N, Crispin D, Hsieh EJ, et al. Altered proteome turnover and remodeling by short-term caloric restriction or rapamycin rejuvenate the aging heart. Aging Cell. 2014 Jun;13(3):529–39.

139. Chen K, Kobayashi S, Xu X, Viollet B, Liang Q. AMP activated protein kinase is indispensable for myocardial adaptation to caloric restriction in mice. PLoS One. 2013;8(3):e59682.
140. Zheng Q, Zhao K, Han X, Huff AF, Cui Q, Babcock SA, et al. Inhibition of AMPK accentuates prolonged caloric restriction-induced change in cardiac contractile function through disruption of compensatory autophagy. Biochim Biophys Acta. 2015 Feb;1852(2):332–42.
141. Gill S, Le HD, Melkani GC, Panda S. Time-restricted feeding attenuates age-related cardiac decline in Drosophila. Science. 2015 Mar;347(6227):1265–9.
142. Castello L, Maina M, Testa G, Cavallini G, Biasi F, Donati A, et al. Alternate-day fasting reverses the age-associated hypertrophy phenotype in rat heart by influencing the ERK and PI3K signaling pathways. Mech Ageing Dev. 2011;132(6–7):305–14.
143. Castello L, Froio T, Maina M, Cavallini G, Biasi F, Leonarduzzi G, et al. Alternate-day fasting protects the rat heart against age-induced inflammation and fibrosis by inhibiting oxidative damage and NF-kB activation. Free Radic Biol Med. 2010 Jan;48(1):47–54.
144. Goodrick CL, Ingram DK, Reynolds MA, Freeman JR, Cider NL. Effects of intermittent feeding upon growth and life span in rats. Gerontology. 1982;28(4):233–41.
145. Inuzuka Y, Okuda J, Kawashima T, Kato T, Niizuma S, Tamaki Y, et al. Suppression of phosphoinositide 3-kinase prevents cardiac aging in mice. Circulation. 2009 Oct;120(17):1695–703.
146. Liu H, Javaheri A, Godar RJ, Murphy J, Ma X, Rohatgi N, et al. Intermittent fasting preserves beta-cell mass in obesity-induced diabetes via the autophagy-lysosome pathway. Autophagy. 2017;13(11):1952–68.
147. Newman JC, Covarrubias AJ, Zhao M, Yu X, Gut P, Ng C-P, et al. Ketogenic Diet Reduces Midlife Mortality and Improves Memory in Aging Mice. Cell Metab. 2017 Sep;26(3):547-557.e8.
148. Roberts MN, Wallace MA, Tomilov AA, Zhou Z, Marcotte GR, Tran D, et al. A Ketogenic Diet Extends Longevity and Healthspan in Adult Mice. Cell Metab. 2017 Sep;26(3):539-546.e5.
149. Brandhorst S, Choi IY, Wei M, Cheng CW, Sedrakyan S, Navarrete G, et al. A Periodic Diet that Mimics Fasting Promotes Multi-System Regeneration,

Enhanced Cognitive Performance, and Healthspan. Cell Metab. 2015 Jul;22(1):86–99.

150. Wei M, Brandhorst S, Shelehchi M, Mirzaei H, Cheng CW, Budniak J, et al. Fasting-mimicking diet and markers/risk factors for aging, diabetes, cancer, and cardiovascular disease. Sci Transl Med. 2017 Feb;9(377).
151. Ren J, Yang L, Zhu L, Xu X, Ceylan AF, Guo W, et al. Akt2 ablation prolongs life span and improves myocardial contractile function with adaptive cardiac remodeling: role of Sirt1-mediated autophagy regulation. Aging Cell. 2017 Oct;16(5):976–87.
152. Hoshino A, Mita Y, Okawa Y, Ariyoshi M, Iwai-Kanai E, Ueyama T, et al. Cytosolic p53 inhibits Parkin-mediated mitophagy and promotes mitochondrial dysfunction in the mouse heart. Nat Commun. 2013;4:2308.
153. Hariharan N, Maejima Y, Nakae J, Paik J, Depinho RA, Sadoshima J. Deacetylation of FoxO by Sirt1 Plays an Essential Role in Mediating Starvation-Induced Autophagy in Cardiac Myocytes. Circ Res. 2010 Dec;107(12):1470–82.
154. Chiao YA, Kolwicz SC, Basisty N, Gagnidze A, Zhang J, Gu H, et al. Rapamycin transiently induces mitochondrial remodeling to reprogram energy metabolism in old hearts. Aging (Albany NY). 2016 Feb;8(2):314–27.
155. Teng ACT, Miyake T, Yokoe S, Zhang L, Rezende LMJ, Sharma P, et al. Metformin increases degradation of phospholamban via autophagy in cardiomyocytes. Proc Natl Acad Sci U S A. 2015 Jun;112(23):7165–70.
156. Pietrocola F, Malik SA, Marino G, Vacchelli E, Senovilla L, Chaba K, et al. Coffee induces autophagy in vivo. Cell Cycle. 2014;13(12):1987–94.
157. Sinha RA, Farah BL, Singh BK, Siddique MM, Li Y, Wu Y, et al. Caffeine stimulates hepatic lipid metabolism by the autophagy-lysosomal pathway in mice. Hepatology. 2014 Apr;59(4):1366–80.
158. El Agaty SMT, Seif AA. Cardiovascular effects of long-term caffeine administration in aged rats. Ir J Med Sci. 2015 Jun;184(2):265–72.
159. Furman D, Chang J, Lartigue L, Bolen CR, Haddad F, Gaudilliere B, et al. Expression of specific inflammasome gene modules stratifies older individuals into two extreme clinical and immunological states. Nat Med. 2017 Feb;23(2):174–84.
160. Levine B, Packer M, Codogno P. Development of autophagy inducers in

clinical medicine. J Clin Invest. 2015 Jan;125(1):14–24.
161. Ahmet I, Tae H-J, de Cabo R, Lakatta EG, Talan MI. Effects of calorie restriction on cardioprotection and cardiovascular health. J Mol Cell Cardiol. 2011 Aug;51(2):263–71.
162. Meyer TE, Kovacs SJ, Ehsani AA, Klein S, Holloszy JO, Fontana L. Long-term caloric restriction ameliorates the decline in diastolic function in humans. J Am Coll Cardiol. 2006 Jan;47(2):398–402.
163. Lakatta EG, Levy D. Arterial and cardiac aging: major shareholders in cardiovascular disease enterprises: Part I: aging arteries: a “set up” for vascular disease. Circulation. 2003 Jan;107(1):139–46.
164. Pursnani S, Diener-West M, Sharrett AR. The effect of aging on the association between coronary heart disease risk factors and carotid intima media thickness: an analysis of the Atherosclerosis Risk in Communities (ARIC) cohort. Atherosclerosis. 2014 Apr;233(2):441–6.
165. Odden MC, Coxson PG, Moran A, Lightwood JM, Goldman L, Bibbins-Domingo K. The impact of the aging population on coronary heart disease in the United States. Am J Med. 2011 Sep;124(9):827-33.e5.
166. Sharma K, Kass DA. Heart failure with preserved ejection fraction: mechanisms, clinical features, and therapies. Circ Res. 2014 Jun;115(1):79–96.
167. Katz AM, Rolett EL. Heart failure: when form fails to follow function. Eur Heart J. 2016 Feb;37(5):449–54.
168. Dickstein K, Cohen-Solal A, Filippatos G, McMurray JJ V, Ponikowski P, Poole-Wilson PA, et al. ESC guidelines for the diagnosis and treatment of acute and chronic heart failure 2008: the Task Force for the diagnosis and treatment of acute and chronic heart failure 2008 of the European Society of Cardiology. Developed in collaboration with the Heart. Eur J Heart Fail. 2008 Oct;10(10):933–89.
169. Lam CSP, Rienstra M, Tay WT, Liu LCY, Hummel YM, van der Meer P, et al. Atrial Fibrillation in Heart Failure With Preserved Ejection Fraction: Association With Exercise Capacity, Left Ventricular Filling Pressures, Natriuretic Peptides, and Left Atrial Volume. JACC Heart Fail. 2017 Feb;5(2):92–8.
170. Forouzanfar MH, Liu P, Roth GA, Ng M, Biryukov S, Marczak L, et al. Global

Burden of Hypertension and Systolic Blood Pressure of at Least 110 to 115 mm Hg, 1990-2015. JAMA. 2017 Jan;317(2):165–82.

171. Global, regional, and national comparative risk assessment of 79 behavioural, environmental and occupational, and metabolic risks or clusters of risks, 1990-2015: a systematic analysis for the Global Burden of Disease Study 2015. Lancet (London, England). 2016 Oct;388(10053):1659–724.
172. Kannel WB. Blood pressure as a cardiovascular risk factor: prevention and treatment. JAMA. 1996 May;275(20):1571–6.
173. Turnbull F, Neal B, Ninomiya T, Algert C, Arima H, Barzi F, et al. Effects of different regimens to lower blood pressure on major cardiovascular events in older and younger adults: meta-analysis of randomised trials. BMJ. 2008 May;336(7653):1121–3.
174. Rahimi K, Emdin CA, MacMahon S. The epidemiology of blood pressure and its worldwide management. Circ Res. 2015 Mar;116(6):925–36.
175. Kirkland EB, Heincelman M, Bishu KG, Schumann SO, Schreiner A, Axon RN, et al. Trends in Healthcare Expenditures Among US Adults With Hypertension: National Estimates, 2003-2014. J Am Heart Assoc. 2018 May;7(11).
176. Chow CK, Teo KK, Rangarajan S, Islam S, Gupta R, Avezum A, et al. Prevalence, awareness, treatment, and control of hypertension in rural and urban communities in high-, middle-, and low-income countries. JAMA. 2013 Sep;310(9):959–68.
177. Rapp JP, Wang SM, Dene H. A genetic polymorphism in the renin gene of Dahl rats cosegregates with blood pressure. Science. 1989 Jan;243(4890):542–4.
178. von Lutterotti N, Camargo MJ, Campbell WGJ, Mueller FB, Timmermans PB, Sealey JE, et al. Angiotensin II receptor antagonist delays renal damage and stroke in salt-loaded Dahl salt-sensitive rats. J Hypertens. 1992 Sep;10(9):949–57.
179. Health effects of dietary risks in 195 countries, 1990-2017: a systematic analysis for the Global Burden of Disease Study 2017. Lancet (London, England). 2019 May;393(10184):1958–72.
180. Chen PY, Sanders PW. L-arginine abrogates salt-sensitive hypertension in Dahl/Rapp rats. J Clin Invest. 1991 Nov;88(5):1559–67.

181. LaRocca TJ, Henson GD, Thorburn A, Sindler AL, Pierce GL, Seals DR. Translational evidence that impaired autophagy contributes to arterial ageing. J Physiol. 2012 Jul;590(14):3305–16.
182. Kaplon RE, Hill SD, Bispham NZ, Santos-Parker JR, Nowlan MJ, Snyder LL, et al. Oral trehalose supplementation improves resistance artery endothelial function in healthy middle-aged and older adults. Aging (Albany NY). 2016 Jun;8(6):1167–83.
183. Mattison JA, Wang M, Bernier M, Zhang J, Park S-S, Maudsley S, et al. Resveratrol prevents high fat/sucrose diet-induced central arterial wall inflammation and stiffening in nonhuman primates. Cell Metab. 2014 Jul;20(1):183–90.
184. Wong RHX, Berry NM, Coates AM, Buckley JD, Bryan J, Kunz I, et al. Chronic resveratrol consumption improves brachial flow-mediated dilatation in healthy obese adults. J Hypertens. 2013 Sep;31(9):1819–27.
185. Gano LB, Donato AJ, Pasha HM, Hearon CMJ, Sindler AL, Seals DR. The SIRT1 activator SRT1720 reverses vascular endothelial dysfunction, excessive superoxide production, and inflammation with aging in mice. Am J Physiol Heart Circ Physiol. 2014 Dec;307(12):H1754-63.
186. de Picciotto NE, Gano LB, Johnson LC, Martens CR, Sindler AL, Mills KF, et al. Nicotinamide mononucleotide supplementation reverses vascular dysfunction and oxidative stress with aging in mice. Aging Cell. 2016 Jun;15(3):522–30.
187. Ou X, Lee MR, Huang X, Messina-Graham S, Broxmeyer HE. SIRT1 positively regulates autophagy and mitochondria function in embryonic stem cells under oxidative stress. Stem Cells. 2014 May;32(5):1183–94.
188. Donato AJ, Walker AE, Magerko KA, Bramwell RC, Black AD, Henson GD, et al. Life-long caloric restriction reduces oxidative stress and preserves nitric oxide bioavailability and function in arteries of old mice. Aging Cell. 2013 Oct;12(5):772–83.
189. Rippe C, Lesniewski L, Connell M, LaRocca T, Donato A, Seals D. Short-term calorie restriction reverses vascular endothelial dysfunction in old mice by increasing nitric oxide and reducing oxidative stress. Aging Cell. 2010 Jun;9(3):304–12.
190. Zanetti M, Gortan Cappellari G, Burekovic I, Barazzoni R, Stebel M, Guarnieri

G. Caloric restriction improves endothelial dysfunction during vascular aging: Effects on nitric oxide synthase isoforms and oxidative stress in rat aorta. Exp Gerontol. 2010 Nov;45(11):848–55.

191. Csiszar A, Labinskyy N, Jimenez R, Pinto JT, Ballabh P, Losonczy G, et al. Anti-oxidative and anti-inflammatory vasoprotective effects of caloric restriction in aging: role of circulating factors and SIRT1. Mech Ageing Dev. 2009 Aug;130(8):518–27.
192. DeBosch BJ, Heitmeier MR, Mayer AL, Higgins CB, Crowley JR, Kraft TE, et al. Trehalose inhibits solute carrier 2A (SLC2A) proteins to induce autophagy and prevent hepatic steatosis. Sci Signal. 2016 Feb;9(416):ra21.
193. Kitzman DW, Brubaker P, Morgan T, Haykowsky M, Hundley G, Kraus WE, et al. Effect of Caloric Restriction or Aerobic Exercise Training on Peak Oxygen Consumption and Quality of Life in Obese Older Patients With Heart Failure With Preserved Ejection Fraction: A Randomized Clinical Trial. JAMA. 2016 Jan;315(1):36–46.
194. Sutton EF, Beyl R, Early KS, Cefalu WT, Ravussin E, Peterson CM. Early Time-Restricted Feeding Improves Insulin Sensitivity, Blood Pressure, and Oxidative Stress Even without Weight Loss in Men with Prediabetes. Cell Metab. 2018 Jun;27(6):1212-1221.e3.
195. Trepanowski JF, Kroeger CM, Barnosky A, Klempel MC, Bhutani S, Hoddy KK, et al. Effect of Alternate-Day Fasting on Weight Loss, Weight Maintenance, and Cardioprotection Among Metabolically Healthy Obese Adults: A Randomized Clinical Trial. JAMA Intern Med. 2017 Jul;177(7):930–8.
196. Tosti V, Bertozzi B, Fontana L. Health Benefits of the Mediterranean Diet: Metabolic and Molecular Mechanisms. J Gerontol A Biol Sci Med Sci. 2018 Mar;73(3):318–26.
197. Trichopoulou A, Costacou T, Bamia C, Trichopoulos D. Adherence to a Mediterranean diet and survival in a Greek population. N Engl J Med. 2003 Jun;348(26):2599–608.
198. Knoops KTB, de Groot LCPGM, Kromhout D, Perrin A-E, Moreiras-Varela O, Menotti A, et al. Mediterranean diet, lifestyle factors, and 10-year mortality in elderly European men and women: the HALE project. JAMA. 2004 Sep;292(12):1433–9.

199. de Lorgeril M, Renaud S, Mamelle N, Salen P, Martin JL, Monjaud I, et al. Mediterranean alpha-linolenic acid-rich diet in secondary prevention of coronary heart disease. Lancet (London, England). 1994 Jun;343(8911):1454–9.
200. de Lorgeril M, Salen P, Martin JL, Monjaud I, Delaye J, Mamelle N. Mediterranean diet, traditional risk factors, and the rate of cardiovascular complications after myocardial infarction: final report of the Lyon Diet Heart Study. Circulation. 1999 Feb;99(6):779–85.
201. Estruch R, Ros E, Salas-Salvado J, Covas M-I, Corella D, Aros F, et al. Primary Prevention of Cardiovascular Disease with a Mediterranean Diet Supplemented with Extra-Virgin Olive Oil or Nuts. N Engl J Med. 2018 Jun;378(25):e34.
202. Agarwal A, Ioannidis JPA. PREDIMED trial of Mediterranean diet: retracted, republished, still trusted? BMJ. 2019 Feb;364:l341.
203. Soda K, Nguyen Thanh Binh P, Kawakami M. Mediterranean diet and polyamine intake: Possible contribution of increased polyamine intake to inhibition of age-associated disease. Vol. 3, Nutrition and Dietary Supplements. 2010. 1 p.
204. Soda K. Polyamine intake, dietary pattern, and cardiovascular disease. Med Hypotheses. 2010 Sep;75(3):299–301.
205. Pucciarelli S, Moreschini B, Micozzi D, De Fronzo GS, Carpi FM, Polzonetti V, et al. Spermidine and spermine are enriched in whole blood of nona/centenarians. Rejuvenation Res. 2012 Dec;15(6):590–5.
206. de Sa DDC, Chen HH. The role of natriuretic peptides in heart failure. Curr Cardiol Rep. 2008 May;10(3):182–9.
207. Kiechl S, Pechlaner R, Willeit P, Notdurfter M, Paulweber B, Willeit K, et al. Higher spermidine intake is linked to lower mortality: a prospective population-based study. Am J Clin Nutr. 2018 Aug;108(2):371–80.
208. Schwarz C, Stekovic S, Wirth M, Benson G, Royer P, Sigrist SJ, et al. Safety and tolerability of spermidine supplementation in mice and older adults with subjective cognitive decline. Aging (Albany NY). 2018 Jan;10(1):19–33.
209. Wirth M, Benson G, Schwarz C, Kobe T, Grittner U, Schmitz D, et al. The effect of spermidine on memory performance in older adults at risk for dementia: A randomized controlled trial. Cortex. 2018 Dec;109:181–8.

210. Eisenberg T, Abdellatif M, Zimmermann A, Schroeder S, Pendl T, Harger A, et al. Dietary spermidine for lowering high blood pressure. Autophagy. 2017 Apr;13(4):767–9.

8. APPENDIX

(Supplementary Tables)

The Tables included in this appendix have been published in Eisenberg and Abdellatif et. al. Nature Medicine, 2016; Ref. (100) *and were reproduced with permission from the publisher (Springer Nature).*

Supplementary Tables

Supplementary Table 1. Left ventricular echocardiography of C57BL/6J aging mice.

Young (4M), middle-aged (18M) and aged (23M) controls were compared with aged late-in-life spermidine-treated (23M+S) C57BL/6J male mice (see Fig. 1 for the feeding scheme). Abbreviations: EF, ejection fraction; FS, fractional shortening; HR, heart rate; IVS, interventricular septum thickness during diastole; LV, left ventricular; LVEDD, left ventricular end-diastolic diameter; LVESD, left ventricular end-systolic diameter; PW, posterior wall thickness during diastole; RWT, relative wall thickness; TL, tibia length. Data show means ± s.e.m. of indicated number of mice analyzed per group.

	Young	Aged		
	(4M) N=10	(18M) N=14	(23M) N=20	(23M+S) N=20
Body weight (g)	25.1±0.5***	33.9±0.8***	30±0.6	30.2±0.6
HR (bpm)	572±18	545±16	538±13	519±17
LV mass (mg)	92±3***	152±6	153±6	137±4§
LV mass/TL (mg/mm)	5.17±0.17***	8.48±0.35	8.73±0.37	7.52±0.22*
IVS (mm)	0.80±0.02***	1.04±0.03	1.05±0.03	0.99±0.03
IVS/TL	0.045±0.001***	0.058±0.001	0.06±0.002	0.055±0.002
PW (mm)	0.73±0.02***	0.89±0.02	0.94±0.03	0.86±0.02§
PW/TL	0.041±0.001***	0.05±0.001	0.054±0.002	0.047±0.001**
LVEDD (mm)	3.57±0.05**	3.99±0.06	3.88±0.06	3.88±0.05
LVESD (mm)	2.00±0.10*	2.52±0.07	2.33±0.08	2.26±0.07
RWT	0.43±0.01**	0.48±0.01	0.52±0.02	0.48±0.01
FS (%)	44±2	37±1	40±1	42±1
EF (%)	76±2	67±2	71±2	73±1

***p<0.001, **p<0.01, *p<0.05 vs. 23M (ANOVA with post-hoc Tukey or Welch's test with post-hoc Games-Howell according to equality of variances)

§p<0.05 vs. 23M (unpaired Student's t-test comparing 23M+S vs. 23M)

This table is reproduced from Eisenberg and Abdellatif et. al. Nature Medicine, 2016; Ref. (100) *with permission from the publisher (Springer Nature).*

Supplementary Table 2. Left ventricular hemodynamics of C57BL/6J aging mice.

Young (4M), middle-aged (18M) and aged (24M) controls were compared with aged late-in-life spermidine-treated (24M+S) C57BL/6J male mice (see Fig. 1 for the feeding schemes). Abbreviations: CO, cardiac output; dP/dt_{max}, peak rate of pressure rise; dP/dt_{min}, peak rate of pressure decay; Ea, arterial elastance; EF, ejection fraction; ESP, end-systolic pressure; EDP, end-diastolic pressure; ESV, end-systolic volume; EDV, end-diastolic volume; HR, heart rate; P_{max}, maximum ventricular pressure; SV, stroke volume; τ, left ventricular pressure decay time constant (according to Weiss' Method); VVC, ventricular-vascular coupling; EDPVR β, Exponential end-diastolic pressure-volume relationship chamber stiffness constant; ESPVR Ees, Linear end-systolic pressure-volume relationship slope. Data show means ± s.e.m. or median [IQR] (according to normality) of indicated number of mice analyzed per group.

	Young	**Aged**		
	(4M) N=10	**(18M) N=8**	**(24M) N=10**	**(24M+S) N=10**
HR (bpm)	505±10*	502±20	457±12	476±26
EF (%)	76±3	66±2	70±1	71±2
CO (ml/min)	20.8 [20.4-21]	23 [20.8-26.1]	20.2 [19.6-23.4]	23.9 [20.6-25]
SV (µl)	40.4±0.9**	45.2±1.7	47±1.1	48.1±1.5
ESV (µl)	12.9±1.6**	24.1±2.2	20.9±1.5	20.1±1.6
EDV (µl)	53.3±1.6***	69.3±2.8	67.8±2.3	68.2±2.1
P_{max} (mmHg)	68±2*	69±3	56±3	59±5
ESP (mmHg)	56±2	61±2	50±3	50±4
EDP (mmHg)	3.3±0.4#	4.6±0.3	5.2±0.7	3.3±0.5#
Ea (mmHg/µl)	1.39±0.06**	1.37±0.06*	1.06±0.06	1.06±0.09
dP/dt_{max} (mmHg/s)	3298±130	3825±332*	2580±261	3131±381
dP/dt_{min} (mmHg/s)	-3445±177#	-3528±291*	-2396±255	-2803±372
τ (ms)	6.9±0.3*	7.7±0.7	10.6±1.3	8.1±0.8§
VVC	1.45±0.18	1.07±0.17	1.02±0.1	1.63±0.19*
ESPVR Ees (mmHg/µl)	2.05±0.31*	1.51±0.26	1.06±0.1	1.76±0.28
EDPVR β (µl)	0.023±0.004*	0.025±0.004	0.049±0.009	0.031±0.003**

***p<0.001, **p<0.01, *p<0.05, #p<0.055 vs. 24M (ANOVA with post-hoc Tukey, Welch's test with post-hoc Games-Howell or Kruskal-Wallis followed by corrected multiple comparisons by Mann-Whitney U-test according to normality and equality of variances. §p<0.05 vs. 24M (unpaired Student's t-test comparing 24M+S vs. 24M)

Note: for ESPVR Ees and EDPVR β, other parameters in the fitting equation (V0 and α, respectively) were included as covariates using ANCOVA and post-hocs were Bonferroni-corrected. *This table is reproduced from Eisenberg and Abdellatif et. al. Nature Medicine, 2016; Ref.* (100) *with permission from the publisher (Springer Nature).*

Supplementary Table 3. Gravimetric analysis of C57BL/6J aging mice.

Young (4M), middle-aged (18M) and aged (24M) controls were compared with aged late-in-life spermidine-treated (24M+S) C57BL/6J male mice (see Fig. 1 for the feeding scheme). Abbreviations: BAT, brown adipose tissue; WAT, white adipose tissue; TL, tibia length. Data show means ± s.e.m. of indicated number of mice analyzed per group.

	Young	**Aged**		
	(4M) N=10	**(18M) N=8**	**(24M) N=10**	**(24M+S) N=10**
Body weight (g)	28.2±0.6	35.1±1**	30.6±1	29.3±0.7
Heart weight (HW, mg)	136±6***	194±10	200±12	191±9
HW/TL (mg/mm)	7.7±0.4***	10.9±0.6	11.2±0.7	10.8±0.5
Lung weight (mg)	157±4**	168±8	187±3	166±6*
Lung weight/TL (mg/mm)	8.8±0.3**	9.4±0.5	10.5±0.2	9.4±0.3§
Kidney weight (mg)	336±11	433±5***	279±21	295±25
Kidney weight/TL (mg/mm)	18.9±0.8	24.3±0.4***	15.7±1.3	16.8±1.5
Liver weight (mg)	1376±82*	1606±114	1688±82	1651±65
Liver weight/TL (mg/mm)	77.7±5.1	90.4±6.9	94.3±4.2	93.5±3.4
Spleen weight (mg)	80±8***	102±8	156±19	159±16
WAT (mg)	347±33**	1057±185**	165±16	177±14
BAT (mg)	64±2	85±11	59±7	50±5

***p<0.001, **p<0.01, *p<0.05 *vs.* 24M (ANOVA with post-hoc Tukey or Welch's test with post-hoc Games-Howell according to equality of variances)

§p<0.05 *vs.* 24M (unpaired Student's *t*-test comparing 24M+S *vs.* 24M)

This table is reproduced from Eisenberg and Abdellatif et. al. Nature Medicine, 2016; Ref. (100) *with permission from the publisher (Springer Nature).*

Supplementary Table 4. Left ventricular echocardiography of Atg5-transgenic mice.

Control and spermidine-treated *Atg5$^{flox/flox}$/MLC2a-Cre^{-} (Atg5$^{+/+}$)* and *Atg5$^{flox/flox}$/MLC2a-Cre^{+} (Atg5$^{-/-}$)* male mice at the age of 13-14 weeks were used (see Fig. 5 for the feeding scheme). Abbreviations: EF, ejection fraction; FS, fractional shortening; HR, heart rate; IVS, interventricular septum thickness during diastole; LV, left ventricular; LVEDD, left ventricular end-diastolic diameter; LVESD, left ventricular end-systolic diameter; PW, posterior wall thickness during diastole; RWT, relative wall thickness; TL, tibia length. Data show means ± s.e.m. of indicated number of mice analyzed per group.

	Atg5$^{+/+}$		***Atg5$^{-/-}$***		**Two-way ANOVA** (p-values)		
	Control (N=16)	Spermidine (N=15)	Control (N=12)	Spermidine (N=14)	Geno-type	Treat-ment	Inter-action
Body weight (g)	26.8±0.6	26.8±0.5	25.4±0.7	27.7±0.6*	n.s.	0.052	n.s.
HR (bpm)	558±14	567±13	535±9	559±16	n.s.	n.s.	n.s.
LV mass (mg)	116±5	104±3	121±5	139±8$^{+++, *}$	0.001	n.s.	0.008
LV mass/ TL (mg/mm)	6.65±0.29	5.84±0.17*	6.86±0.3	7.94±0.43$^{+++, *}$	<0.001	n.s.	0.004
IVS (mm)	0.87±0.02	0.86±0.02	0.86±0.03	0.97±0.03$^{++, **}$	0.055	n.s.	0.016
IVS/TL	0.05±0.001	0.05±0.001	0.05±0.002	0.06±0.002$^{++, *}$	0.03	n.s.	0.007
PW (mm)	0.81±0.02	0.76±0.02	0.83±0.02	0.89±0.02^{+++}	<0.001	n.s.	0.013
PW/TL	0.05±0.001	0.04±0.001*	0.05±0.001	0.05±0.002$^{+++, *}$	<0.001	n.s.	0.002
LVEDD (mm)	3.8±0.05	3.67±0.04	3.87±0.08	3.84±0.06^{+}	0.004	n.s.	n.s.
LVESD (mm)	2.22±0.09	2.08±0.06	2.34±0.08	2.43±0.08^{++}	0.005	n.s.	n.s.
RWT	0.78±0.04	0.79±0.03	0.74±0.03	0.78±0.03	n.s.	n.s.	n.s.
FS (%)	41.7±1.7	43.5±1.2	39.6±1.2	37±1.1^{++}	0.003	n.s.	n.s.
EF (%)	73±2	75±2	71±1	67±2^{++}	0.005	n.s.	n.s.

***p<0.001, **p<0.01, *p<0.05 *vs.* respective genotype-matched control (Simple main effects following significant two-way ANOVA)

$^{+++}$p<0.001, $^{++}$p<0.01, $^{+}$p<0.05 *vs.* respective treatment-matched *Atg5$^{+/+}$* (Simple main effects following significant two-way ANOVA)

This table is reproduced from Eisenberg and Abdellatif et. al. Nature Medicine, 2016; Ref. (100) *with permission from the publisher (Springer Nature).*

Supplementary Table 5. Left ventricular hemodynamics of Atg5-transgenic mice.

Control and spermidine-treated *Atg5*$^{flox/flox}$/*MLC2a-Cre*$^{-}$ (*Atg5*$^{+/+}$) and *Atg5*$^{flox/flox}$/*MLC2a-Cre*$^{+}$ (*Atg5*$^{-/-}$) male mice at the age of 16 weeks were used (see Fig. 5 for the feeding scheme). Abbreviations: CO, cardiac output; dP/dt_{max}, peak rate of pressure rise; dP/dt_{min}, peak rate of pressure decay; Ea, arterial elastance; EF, ejection fraction; ESP, end-systolic pressure; EDP, end-diastolic pressure; ESV, end-systolic volume; EDV, end-diastolic volume; HR, heart rate; P_{max}, maximum ventricular pressure; SV, stroke volume; τ, left ventricular pressure decay time constant (according to Weiss' Method); VVC, ventricular-vascular coupling; EDPVR β, Exponential end-diastolic pressure-volume relationship chamber stiffness constant; ESPVR Ees, Linear end-systolic pressure-volume relationship slope. Data show means ± s.e.m. of indicated number of mice analyzed per group.

	***Atg5*$^{+/+}$**		***Atg5*$^{-/-}$**		**Two-way ANOVA** (p-values)		
	Control (N=10)	Spermidine (N=10)	Control (N=9)	Spermidine (N=11)	Geno-type	Treat-ment	Inter-action
HR (bpm)	477±12	472±16	464±7	464±12	n.s.	n.s.	n.s.
EF (%)	76±2	76±1	74±1	70±1$^{+++,\,*}$	0.002	n.s.	0.051
CO (ml/min)	21±0.7	20.2±1.1	20.5±0.7	19.4±0.6	n.s.	n.s.	n.s.
SV (µl)	44.1±1.1	42.8±1.3	44.3±1.7	41.8±0.6	n.s.	n.s.	n.s.
ESV (µl)	14.3±1.4	13.2±0.4	15.3±0.8	18.4±1$^{+++,\,*}$	0.004	n.s.	0.045
EDV (µl)	58.4±2	56±1.5	59.7±1.6	60.2±1.2	n.s.	n.s.	n.s.
P_{max}	73±3	74±4	74±6	81±1	n.s.	n.s.	n.s.
ESP (mmHg)	60±3	64±4	65±6	70±2	n.s.	n.s.	n.s.
EDP (mmHg)	4.4±0.7	4.3±0.5	4.6±1.1	5.1±0.5	n.s.	n.s.	n.s.
Ea (mm Hg/µl)	1.38±0.07	1.51±0.11	1.46±0.13	1.68±0.05	n.s.	n.s.	n.s.
dP/dt_{max} (mmHg/s)	4048±398	4331±450	4371±688	4798±462	n.s.	n.s.	n.s.
dP/dt_{min} (mmHg/s)	-3787±308	-4085±417	-3913±554	-4445±309	n.s.	n.s.	n.s.
τ (ms)	6.8±0.3	7.4±0.4	8.1±0.8	6.9±0.4	n.s.	n.s.	n.s.
VVC	1.18±0.23	1.63±0.23*	0.83±0.1	0.81±0.05^{+++}	0.002	n.s.	n.s.
ESPVR Ees (mmHg/µl)	1.63±0.30	2.33±0.27†	1.24±0.20	1.35±0.09^{+}	0.048	n.s.	n.s.
EDPVR β (µl)	0.020±0.002	0.020±0.002	0.021±0.003	0.039±0.005*	n.s.	n.s.	0.045

***p<0.001, **p<0.01, *p<0.05 and †p = 0.054 *vs.* respective genotype-matched control (Simple main effects following significant two-way ANOVA)

†††p<0.001, ††p<0.01, †p<0.05 *vs.* respective treatment-matched *Atg5*$^{+/+}$ (Simple main effects following significant two-way ANOVA)

Note: for ESPVR Ees and EDPVR β, other parameters in the fitting equation (V_0 and α, respectively) were included as covariates using ANCOVA.

This table is reproduced from Eisenberg and Abdellatif et. al. Nature Medicine, 2016; Ref. (100) *with permission from the publisher (Springer Nature).*

Supplementary Table 6. Left ventricular echocardiography of *Dahl* salt-sensitive rats.

Control and spermidine-treated *Dahl* salt-sensitive rats fed a high-salt diet (8% NaCl) starting from the age of 7 weeks (see Fig. 3 for the feeding scheme) were used at the indicated ages. Abbreviations: E/E', peak early filling Doppler velocity of transmitral flow (E) to the corresponding myocardial tissue Doppler velocity (E') ratio; EF, ejection fraction; FS, fractional shortening; HR, heart rate; IVS, interventricular septum thickness during diastole; RWT, relative wall thickness; LA, left atrium; LV, left ventricular; LVEDD, left ventricular end-diastolic diameter; LVESD, left ventricular end-systolic diameter; PW, left ventricular posterior wall thickness during diastole. Data show means ± s.e.m. of indicated number of rats analyzed per group.

	9-week-old (2 weeks high-salt)		**14-week-old** (7 weeks high-salt)		**19-week-old** (12 weeks high-salt)		**Two-way ANOVA (p-values[§])**		
	Control (N=10)	Spermidine (N=10)	Control (N=10)	Spermidine (N=10)	Control (N=10)	Spermidine (N=10)	Age	Treatment	Interaction
Body weight (g)	300±4	268±3***	371±5^{+++}	341±5$^{***, +++}$	360±11^{+++}	389±11	<0.001	n.s.	<0.001
HR (bpm)	377±6	387±6	375±5	378±6	371±5	376±4	n.s.	n.s.	n.s.
LV mass (mg)	1304±29	1231±36	1762±66^{+++}	1404±44$^{***, +}$	2053±85^{+++}	1719±55$^{**, +++}$	<0.001	<0.001	0.02
LV mass/body weight (mg/g)	4.36±0.13	4.60±0.16	4.75±0.17	4.11±0.1$^{**, +}$	5.70±0.15^{+++}	4.43±0.14***	<0.001	<0.001	<0.001
LA area (mm^2)	22.3±1	21.8±0.9	27.9±0.8^{+++}	26.8±0.6^{+}	27.7±1.3^{++}	24.2±0.7*	<0.001	0.01	n.s.
IVS (mm)	2.20±0.04	2.09±0.04	2.74±0.07^{+++}	2.36±0.07$^{**, +}$	2.99±0.05^{+++}	2.69±0.09$^{*, +++}$	<0.001	<0.001	0.043
PW (mm)	2.38±0.06	2.25±0.07	2.73±0.08^{+++}	2.42±0.08*	3.12±0.13^{+++}	2.65±0.07$^{**, ++}$	<0.001	0.003	0.048
LVEDD (mm)	7.10±0.1	7.14±0.1	7.30±0.15	7.33±0.11	7.26±0.19	7.39±0.13	0.035	n.s.	n.s.
LVESD (mm)	3.08±0.09	3.33±0.14	3.51±0.11^{+++}	3.60±0.13^{+}	4.26±0.16^{+++}	4.11±0.21^{+++}	<0.001	n.s.	n.s.
RWT	2.88±0.06	2.79±0.08	3.30±0.08^{+++}	3.02±0.07$^{*, +}$	3.41±0.07^{+++}	3.05±0.03$^{***, ++}$	<0.001	0.002	n.s.
FS (%)	57±1	54±2	52±1^{++}	51±1	42±1^{+++}	45±2^{+++}	<0.001	n.s.	0.028
EF (%)	84±1	83±1	81±1	79±1^{+}	73±1^{+++}	76±1^{+++}	<0.001	n.s.	0.017
E/E'	22.4±1.4	24.4±1.2	35.2±1.6^{+++}	28.2±1.1$^{**, +++}$	43.9±1.4^{+++}	32.9±1.1$^{***, +++}$	<0.001	0.001	<0.001

[§]p-values of two-way ANOVA (mixed-design) including two factors: (i) age (9, 14 and 19 weeks, as repeated measurements) and (ii) treatment (high-salt control *vs.* high-salt + spermidine, as independent observations).

***p<0.001, **p<0.01, *p<0.05 *vs.* age-matched control (Simple main effects following significant two-way ANOVA)

[+++]p<0.001, [++]p<0.01, [+]p<0.05 *vs.* 9-week-old treatment-matched group (Simple main effects [Bonferroni-corrected] following significant two-way ANOVA)

This table is reproduced from Eisenberg and Abdellatif et. al. Nature Medicine, 2016; Ref. (100) *with permission from the publisher (Springer Nature).*

Supplementary Table 7. Gravimetric analysis of *Dahl* salt-sensitive rats.

Control and spermidine-treated *Dahl* salt-sensitive rats fed a high-salt (8% NaCl) diet starting from the age of 7 weeks (see Fig. 3 for the feeding scheme) were used at the indicated ages. Abbreviations: TL, tibia length. Data show means ± s.e.m. of indicated number of rats analyzed per group.

	7-week-old (no high-salt)	**14-week-old (7 weeks high-salt)**		**19-week-old (12 weeks high-salt)**		**Two-way ANOVA** (p-values[§])		
	Control (N=10)	Control (N=9)	Spermidine (N=9)	Control (N=10)	Spermidine (N=10)	Age	Treatment	Interaction
Body weight (g)	202±3†,‡	370±6	351±7	365±12	383±9^{+}	n.s.	n.s.	0.54
Heart weight (HW, mg)	889±18†,‡	1596±32	1412±53**	1757±27^{++}	1599±29**$^{,+++}$	<0.001	<0.001	n.s.
HW/TL (mg/mm)	24.1±0.5†,‡	39.7±0.9	35.2±1.3**	42.3±0.7^{+}	38.1±0.6**$^{,+}$	0.004	<0.001	n.s.
Lung weight (mg)	1104±19†,‡	2146±91	1896±116*	1973±59	1781±71	n.s.	0.014	n.s.
Lung weight/TL (mg/mm)	29.9±0.6†,‡	53.3±2.3	47.3±3	47.5±1.5	42.4±1.7	0.018	0.014	n.s.
Kidney weight (mg)	1779±40†,‡	3626±142	3195±69*	4386±172^{+++}	3692±143***$^{,+}$	<0.001	<0.001	n.s.
Kidney weight/TL (mg/mm)	48.1±1†,‡	90.1±3.7	79.5±1.6*	105.6±4.3^{++}	87.9±3.4**	0.002	<0.001	n.s.
Liver weight (g)	8.27±0.36†,‡	13.85±0.32	12.61±0.74	15.89±0.82^{+}	14.11±0.45*	n.s.	0.021	n.s.
Liver weight/TL (mg/mm)	223.7±9.4†,‡	343.9±8.3	313.9±17.9	383.4±21.6	336.2±10.9	n.s.	0.021	n.s.
Spleen weight (mg)	632±14†,‡	1046±51	900±37	1354±98^{++}	1009±60***	0.004	0.001	n.s.
Spleen weight/TL (mg/mm)	17.1±0.4†,‡	26±1.3	22.4±0.9	32.6±2.4^{++}	24±1.4**	0.007	0.013	0.05

[§]p-values of two-way ANOVA including two factors: (i) age (14 *vs.* 19 weeks) and (ii) treatment (high-salt control *vs.* high-salt + spermidine).

***p<0.001, **p<0.01, *p<0.05 *vs.* age-matched control (simple main effects following significant two-way ANOVA)

$^{+++}$p<0.001, $^{++}$p<0.01, $^{+\#}$p<0.05 *vs.* 14-week-old treatment-matched group (simple main effect following significant two-way ANOVA)

†p<0.001 and ‡p<0.001 *vs.* 14-week-old and 19-week-old controls, respectively (one-way ANOVA comparing all controls with post-hoc Tukey or Welch's test with post-hoc Games-Howell according to equality of variances). *This table is reproduced from Ref.* (100) *with permission from the publisher (Springer Nature).*

Supplementary Table 8. Left ventricular hemodynamics of *Dahl* salt-sensitive rats.

Control and spermidine-treated *Dahl* salt-sensitive rats fed a high-salt (8% NaCl) diet starting from the age of 7 weeks (see Fig. 3 for the feeding scheme) were used at the indicated ages. Abbreviations: BSA, body surface area; CI, cardiac index; dP/dt_{max}, peak rate of pressure rise; dP/dt_{min}, peak rate of pressure decay; Ea_i, arterial elastance for indexed volumes, EF, ejection fraction; ESP, end-systolic pressure; EDP, end-diastolic pressure; ESV_i, indexed end-systolic volume; EDV_i, indexed end-diastolic volume; P_{max}, maximum ventricular pressure; SV_i, indexed stroke volume; VVC, ventricular-vascular coupling; τ, Left-ventricular pressure decay time constant (according to Weiss' method); EDPVR β_i, exponential end-diastolic pressure-volume relationship chamber stiffness constant for indexed volumes; ESPVR Ees_i, linear end-systolic pressure-volume relationship slope for indexed volumes. Data show means ± s.e.m. of indicated number of rats analyzed per group.

	7-week-old (no high-salt)	**14-week-old (7 weeks high-salt)**		**19-week-old (12 weeks high-salt)**		**Two-way ANOVA§**		
	Control (N=10)	Control (N=9)	Spermidine (N=9)	Control (N=10)	Spermidine (N=10)	Age	Treatment	Interaction
BSA (cm^2)	314±3$^{\dagger\dagger\dagger, \ddagger\ddagger\ddagger}$	469±5	453±6	464±11	480±7^{+}	n.s.	n.s.	0.052
HR (bpm)	429±8	419±12	421±11	410±8	403±10	n.s.	n.s.	n.s.
EF (%)	85±1$^{\dagger, \ddagger\ddagger\ddagger}$	81±1	80±2	70±1^{+++}	72±2^{++}	<0.001	n.s.	n.s.
CI (µl/min.cm^2)	298±16$^{\dagger\dagger\dagger, \ddagger\ddagger\ddagger}$	207±8	211±4	167±8^{+++}	178±7^{++}	<0.001	n.s.	n.s.
SV_i (µl/cm^2)	0.70±0.04$^{\dagger\dagger\dagger, \ddagger\ddagger\ddagger}$	0.49±0.02	0.5±0.01	0.41±0.02^{+++}	0.44±0.02^{+}	<0.001	n.s.	n.s.
ESV_i (µl/cm^2)	0.12±0.01‡‡	0.11±0.01	0.13±0.01	0.18±0.01^{++}	0.17±0.02^{+}	<0.001	n.s.	n.s.
EDV_i (µl/cm^2)	0.82±0.05$^{\dagger\dagger\dagger, \ddagger\ddagger\ddagger}$	0.61±0.03	0.63±0.02	0.59±0.03	0.62±0.02	n.s.	n.s.	n.s.
P_{max} (mmHg)	112±4$^{\dagger\dagger\dagger, \ddagger\ddagger\ddagger}$	136±4	123±4*	151±5^{++}	145±3^{+++}	<0.001	0.012	n.s.
ESP (mmHg)	99±5‡‡‡	116±5	106±4	132±6^{+}	130±3^{+++}	<0.001	n.s.	n.s.
EDP (mmHg)	7±0.7$^{\dagger, \ddagger\ddagger}$	10±0.4	8.7±0.3	10.6±1	7.8±0.5**	n.s.	0.005	n.s.
Ea_i (mmHg*cm^2/µl)	147±11$^{\dagger\dagger\dagger, \ddagger\ddagger\ddagger}$	236±9	212±8	331±21^{+++}	298±15^{+++}	<0.001	0.042	n.s.
dP/dt_{max} (mmHg/s)	6840±358	6711±282	6409±169	7475±234^{+}	7314±260^{+}	0.001	n.s.	n.s.
dP/dt_{min} (mmHg/s)	-6966±377†	-5960±393	-5560±319	-6948±306^{++}	-6703±208^{++}	<0.001	n.s.	n.s.
τ (ms)	7.7±0.2$^{\dagger\dagger, \ddagger}$	9±0.3	8.7±0.3	8.7±0.3	8.3±0.3	n.s.	n.s.	n.s.
VVC	1.15±0.18	1.07±0.08	1.28±0.14	0.99±0.15	1.35±0.14	n.s.	0.043	n.s.
ESPVR Ees_i (mmHg*cm^2/µl)	162±22$^{\dagger\dagger, \ddagger\ddagger}$	254±24	269±31	317±48	393±33^{+}	0.016	n.s.	n.s.
EDPVR β_i (µl/cm^2)	1.31±0.16$^{\dagger\dagger\dagger, \ddagger\ddagger\ddagger}$	1.83±0.24	1.45±0.14*	2.85±0.42	1.93±0.26***	n.s.	<0.001	n.s.

§p-values of two-way ANOVA including two factors: (i) age (14 *vs.* 19 weeks) and (ii) treatment (high-salt *vs.* high-salt + spermidine).

***p<0.001, **p<0.01, *p<0.05 *vs.* age-matched control (simple main effects following significant two-way ANOVA)

⁺⁺⁺p<0.001, ⁺⁺p<0.01, ⁺p<0.05 *vs.* 14-week-old treatment-matched group (simple main effect following significant two-way ANOVA)

†††p<0.001, ††p<0.01, †p<0.05 *vs.* 14-week-old control and ‡‡‡p<0.001, ‡‡p<0.01, ‡p<0.05 *vs.* 19-week-old control (one-way ANOVA comparing all controls with post-hoc Tukey or Welch's test with post-hoc Games-Howell according to equality of variances)

Note: for ESPVR Ees_i and EDPVR β_i, other parameters in the fitting equation (V_0 and α, respectively) were included as covariates using ANCOVA.

This table is reproduced from Eisenberg and Abdellatif et. al. Nature Medicine, 2016; Ref. (100) *with permission from the publisher (Springer Nature).*